





This is to certify that the  
dissertation entitled

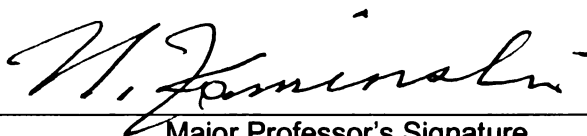
CHARACTERIZATION OF DELTA-9-  
TETRAHYDROCANNABINOL-MEDIATED  
ALTERATIONS IN LEUKOCYTE AND PULMONARY  
AIRWAY EPITHELIAL CELL RESPONSES TO A  
PRIMARY CHALLENGE WITH INFLUENZA A/PR/8/34  
IN C57BL/6 WILD-TYPE AND CB1/CB2 RECEPTOR-  
NULL MICE

presented by

JOHN PHILIP BUCHWEITZ

has been accepted towards fulfillment  
of the requirements for the

Ph.D. degree in Pharmacology and Toxicology



Major Professor's Signature

8/2/07

Date

**PLACE IN RETURN BOX** to remove this checkout from your record.  
**TO AVOID FINES** return on or before date due.  
**MAY BE RECALLED** with earlier due date if requested.

DATE DUE	DATE DUE	DATE DUE
		111108
	NOV 10 2008	

CHARACTERIZATION OF DELTA-9-TETRAHYDROCANNABINOL-MEDIATED  
ALTERATIONS IN LEUKOCYTE AND PULMONARY AIRWAY EPITHELIAL  
CELL RESPONSES TO A PRIMARY CHALLENGE WITH INFLUENZA A/PR/8/34  
IN C57BL/6 WILD-TYPE AND CB1/CB2 RECEPTOR-NULL MICE

By

John Philip Buchweitz

A DISSERTATION

Submitted to  
Michigan State University  
In partial fulfillment of the requirements  
for the degree of

DOCTOR OF PHILOSOPHY

Department of Pharmacology and Toxicology

2007

## ABSTRACT

### CHARACTERIZATION OF DELTA-9-TETRAHYDROCANNABINOL-MEDIATED ALTERATIONS IN LEUKOCYTE AND PULMONARY AIRWAY EPITHELIAL CELL RESPONSES TO A PRIMARY CHALLENGE WITH INFLUENZA A/PR/8/34 IN C57BL/6 WILD-TYPE AND CB1/CB2 RECEPTOR-NULL MICE

By

John Philip Buchweitz

Delta-9-tetrahydrocannabinol ( $\Delta^9$ -THC) is a well-established immunosuppressive agent derived from the plant *Cannabis Sativa*. The biological activity of  $\Delta^9$ -THC is presumed to result from interactions of  $\Delta^9$ -THC with the cannabinoid receptors CB<sub>1</sub> and CB<sub>2</sub>.  $\Delta^9$ -THC has been demonstrated to effect innate, cell-mediated, and humoral immune responses. Accordingly,  $\Delta^9$ -THC has been implicated as both a therapeutic agent toward unwarranted humoral immune responses and as a determinant of susceptibility toward infectious disease. Influenza is a common respiratory pathogen that affects millions of people world-wide each year. Viral clearance from the respiratory tract occurs through a combination of innate, cell-mediated, and humoral immune responses in the immunocompetent host. Therefore, it was hypothesized that the intrinsic immunosuppressive properties of  $\Delta^9$ -THC could lead to decreased host resistance in mice resulting in a greater viral burden when compared with uninfected mice. It was further hypothesized that decreased host resistance to influenza would enhance morphologic features consistent with cellular injury and repair along the bronchiolar epithelium lining the airways of mouse lungs. Moreover, since clonal expansion of T cell populations critical to viral clearance are dependent on IL-2, and IL-2 expression is modulated by cannabinoids through a mechanism that is independent of CB<sub>1</sub>/CB<sub>2</sub> receptors, the proposed increased susceptibility to influenza in the current studies might also arise from

CB<sub>1</sub> and CB<sub>2</sub> receptor-independent mechanisms. In the current studies, challenging mice with influenza alone resulted in robust inflammatory responses that were comprised of a diverse array of transient immune cells and their secretory chemical mediators in the airways. In addition to the inflammatory response, there were concomitant alterations in epithelial morphology that included cellular apoptosis and influenza virus-induced mucous cell metaplasia (MCM). Treatment of influenza infected mice with Δ<sup>9</sup>-THC led to a dose-dependent increase in viral burden as compared to mice infected with influenza alone. More importantly, Δ<sup>9</sup>-THC treated mice exhibited decreased recruitment of critical populations of CD4<sup>+</sup> and CD8<sup>+</sup> T cells and macrophages necessary for the clearance of influenza as compared to mice infected with influenza alone. Lastly, there were identifiable CB<sub>1</sub> and CB<sub>2</sub> receptor-dependent and -independent mechanisms involved in host immune responses to influenza infection. More specifically, the profile of viral burden included an increase in H1 mRNA amongst mice treated with Δ<sup>9</sup>-THC that was similar between CB<sub>1</sub><sup>-/-</sup>/CB<sub>2</sub><sup>-/-</sup> and wild type mice suggesting a CB<sub>1</sub> and CB<sub>2</sub> receptor-independent finding. Conversely, the magnitude of viral burden was strikingly less in CB<sub>1</sub><sup>-/-</sup>/CB<sub>2</sub><sup>-/-</sup> mice than in wild type mice which suggested the involvement of CB<sub>1</sub> and/or CB<sub>2</sub> receptors in mediating immune homeostasis. In addition to viral burden, there were other unique findings exhibited by CB<sub>1</sub><sup>-/-</sup>/CB<sub>2</sub><sup>-/-</sup> mice in response to Δ<sup>9</sup>-THC treatment alone as compared to Δ<sup>9</sup>-THC treated wild type mice. Most notably, Δ<sup>9</sup>-THC induced MCM of the bronchiolar epithelium independent of PR8 challenge in CB<sub>1</sub><sup>-/-</sup>/CB<sub>2</sub><sup>-/-</sup> mice. In conclusion, these findings suggest that Δ<sup>9</sup>-THC is a determinant of susceptibility to increased viral burden and that alternative receptors for Δ<sup>9</sup>-THC are, in part, responsible.

This dissertation is dedicated to the men and women of our armed services who have fought so bravely in the defense of my family's freedoms. God Bless all of you.

## ACKNOWLEDGMENTS

First, I would like to extend my gratitude to my mentor, Norbert E. Kaminski, whose guidance and encouragement has not gone unnoticed in my tireless pursuit of the doctorate degree. In addition, I would like to thank my committee members, Dr. Alex Chen, Dr. Jane Maddox, and Dr. Jack Harkema for their support and assistance.

My research was made all the more enjoyable by the camaraderie of my fellow colleagues including Dr. Courtney Sulentic, Dr. Cheryl Rockwell, Dr. gautham Rao, Dr. Jim Wagner, Dr. Aimen Farraj, Dr. Ammie Bachman, Dr. Barb Faubert Kaplan, Dr. Steve Carey, Dina Schneider, Colin North, and Peer Karmaus. The research was also made possible by the valuable assistance and skills of Lori Bramble, Bob Crawford, Kimberly Hambleton and the histology group (Amy, Joselyn, Kathy, and Rick)... you have all been a blessing.

Lastly, I would like to thank my family, Cynthia, Nathan, Olivia, for being supportive and making each day more fulfilling.

## TABLE OF CONTENTS

LIST OF TABLES .....	x
LIST OF FIGURES .....	xi
LIST OF ABBREVIATIONS .....	xiv
INTRODUCTION .....	1
I. Respiratory toxicology .....	1
A) Basic anatomy and physiology .....	1
B) Respiratory clearance of inhaled particles and pathogens .....	4
1. Mucociliary clearance .....	4
2. Alveolar clearance .....	5
C) Epithelial cell death and regeneration .....	6
1. Clara cells .....	7
2. Type II cells .....	8
II. Influenza Virus .....	8
A) Classification .....	8
B) Viral Entry .....	9
C) Viral Clearance .....	9
D) Chemokine and cytokine responses to influenza virus.....	11
E) Models of susceptibility.....	13
III. Cannabinoids .....	15
A) Chemistry of delta-(9)-tetrahydrocannabinol .....	15
B) Pharmacokinetics .....	15
1. Absorption .....	16
2. Distribution .....	16
3. Metabolism .....	18
C) Biological receptors and activity .....	18
1. CB1 and CB2 receptors .....	18
2. Alternative receptors .....	19
D) Effects of cannabinoids on the immune system .....	20
1. Effects on macrophage function .....	20
2. Effects on neutrophil function .....	21
3. Effects on natural killer cell function .....	22
4. Effects on T <sub>H</sub> 1 cells .....	23
5. Effects on CD8 <sup>+</sup> T cells .....	24
6. Effects on immune cell-derived chemokines and cytokines.....	24
E) Models of host-resistance .....	25
1. Model of Δ <sup>9</sup> -THC and <i>Listeria monocytogenes</i> .....	25

2. Model of $\Delta^9$ -THC and Herpes Simplex Virus .....	26
3. Model of $\Delta^9$ -THC and <i>Legionella pneumophila</i> .....	27
IV. Objectives .....	29
 MATERIALS AND METHODS .....	 30
I. Cannabinoid compounds .....	30
II. Animals .....	30
III. Experimental designs .....	30
IV. Influenza A/PR/8/34 instillation .....	31
V. Steady state blood serum levels of $\Delta^9$ -THC and its metabolites.....	31
VI. Necropsy, lavage collection, and tissue preparation.....	31
VII. Immunocytochemistry .....	34
VIII. Total and PCNA positive epithelial numeric cell density and labeling index .....	34
IX. CAS-3 and alcian blue numeric cell densities.....	34
X. Morphometry of stored intraepithelial mucosubstances .....	35
XI. Bronchoalveolar lavage cellularity .....	36
XII. Histopathology scores for inflammation .....	36
XIII. Total protein .....	37
XIV. Neutrophil elastase .....	37
XV. Inflammatory and TH1/TH2 cytokines .....	38
XVI. T-lymphocyte flow cytometry.....	39
XVII. RNA isolation .....	39
XVIII. Statistical Analysis .....	40
 EXPERIMENTAL RESULTS.....	 41
I. Model development:Establishing the dose .....	41
A) Concentration-dependent inflammatory responses to PR8 in pulmonary airways .....	41
B) Steady state blood serum levels of $\Delta^9$ -THC and its metabolites .....	41
II. Time-dependent airway epithelial and inflammatory cell responses induced by influenza virus A/PR/8/34 in C57BL/6 mice .....	45
A) PR8 induces time-dependent alterations in epithelial morphology.....	45
B) Temporal analysis of stored intraepithelial mucosubstances following PR8 challenge.....	49
C) Expression levels of whole lung MUC5AC mRNA at 7 days post infection.....	49
D) Time-dependent differences in total and PCNA immunopositive epithelial numeric cell densities.....	49
E) Bronchoalveolar lavage fluid analysis .....	54

1. Protein .....	54
2. Total and differential inflammatory cell counts .....	54
3. inflammatory chemokines and cytokines .....	54
4. TH2 cytokines IL-4, IL-5, IL-9 and IL-13 .....	58
5. Elastase .....	58
III. Modulation of airway responses to influenza A/PR/8/34 by $\Delta^9$ -tetrahydrocannabinol in C57BL/6 mice.....	62
A) $\Delta^9$ -THC increases whole lung H1 mRNA following PR8 challenge.....	62
B) $\Delta^9$ -THC does not affect total protein levels in BALF .....	62
C) $\Delta^9$ -THC decreases leukocyte populations retrieved in BALF .....	62
D) $\Delta^9$ -THC decreases CD4 <sup>+</sup> and CD8 <sup>+</sup> T cells in BALF .....	66
E) $\Delta^9$ -THC modestly affects chemokines and cytokines in retrieved in BALF .....	66
F) $\Delta^9$ -THC treatment reduces inflammation scores for mouse lung sections.....	70
G) Effect of $\Delta^9$ -THC on the observed pulmonary histopathology to PR8....	70
H) Caspase-3 mRNA expression levels and G5 numeric cell densities .....	75
I) MUC5AC mRNA expression levels and G5 numeric cell densities .....	76
J) $\Delta^9$ -THC modestly enhances neutrophil-derived elastase levels in BALF.....	81
IV. Pulmonary airway responses to influenza A/PR/8/34 in CB <sub>1</sub> <sup>-/-</sup> /CB <sub>2</sub> <sup>-/-</sup> mice exposed to $\Delta^9$ -tetrahydrocannabinol: An examination for the role of cannabinoid receptors.....	81
A) Qualitative health assessment .....	81
B) The viral load of PR8 in the pulmonary airways of CB <sub>1</sub> <sup>-/-</sup> /CB <sub>2</sub> <sup>-/-</sup> and wild type mice measured 7 days after challenge.....	83
C) $\Delta^9$ -THC affects vascular permeability induced by Pr8 infection of the airways in CB <sub>1</sub> <sup>-/-</sup> /CB <sub>2</sub> <sup>-/-</sup> and wild type mice.....	83
D) CB <sub>1</sub> <sup>-/-</sup> /CB <sub>2</sub> <sup>-/-</sup> mice treated with $\Delta^9$ -THC exhibit a distinctly different composition of leukocytes recruited to the airways in response to PR8 infection when compared to wild type mice.....	85
E) BALF-associated CD4 <sup>+</sup> and CD8 <sup>+</sup> T cell levels following PR8 challenge in CB <sub>1</sub> <sup>-/-</sup> /CB <sub>2</sub> <sup>-/-</sup> and wild type mice.....	90
F) Cannabinoid receptor deficient mice exhibit unique differences in epithelial and leukocytic chemokine and cytokine secretion in the pulmonary airways.....	93
G) Cytokines and chemokines detected in blood serum .....	98
H) The absence of cannabinoid receptors CB <sub>1</sub> and CB <sub>2</sub> enhances the observed pulmonary histopathology .....	101
I) $\Delta^9$ -THC affects the magnitude of the inflammatory response to PR8 in wild type and CB <sub>1</sub> and CB <sub>2</sub> deficient mice.....	104
J) Effects of CB <sub>1</sub> and CB <sub>2</sub> deficiency on the numeric cell densities of apoptotic cells and metaplastic goblet cells.....	104

DISCUSSION .....	109
I. Animals utilized in these studies .....	109
II. The method of delivery and the dose of PR8 utilized .....	109
III. The method of delivery and dose of $\Delta^9$ -THC utilized in these studies .....	109
IV. Effect of $\Delta^9$ -THC on viral H1 mRNA levels in wild type and $CB_1^{-/-}$ / $CB_2^{-/-}$ mice.....	111
V. Effect of PR8 on inflammatory cell recruitment to the pulmonary airways in the presence or absence of $\Delta^9$ -THC in wild type and $CB_1^{-/-}$ / $CB_2^{-/-}$ mice.....	113
VI. Effect of PR8 on the release of soluble mediators into the pulmonary airways in the presence or absence of $\Delta^9$ -THC in wild type and $CB_1^{-/-}$ / $CB_2^{-/-}$ mice.....	115
VII. Effect of a single PR8 instillation on pulmonary histopathology in the presence or absence of $\Delta^9$ -THC in wild type and $CB_1^{-/-}$ / $CB_2^{-/-}$ mice.....	119
VIII. Effect of a single PR8 instillation on epithelial cell apoptosis and MCM in the presence or absence of $\Delta^9$ -THC in wild type and $CB_1^{-/-}$ / $CB_2^{-/-}$ mice..	121
IX. Significance and relevance .....	123
X.	
LITERATURE CITED .....	128
APPENDIX .....	140

## LIST OF TABLES

1. Analysis of $\Delta^9$ -THC, 9-COOH- $\Delta^9$ -THC, and 11-OH- $\Delta^9$ -THC concentrations in mouse blood serum.....	44
2. Total and differential cell counts from BALF.....	67
3. CD4 <sup>+</sup> and CD8 <sup>+</sup> T cell populations observed in BALF by flow cytometry.....	68
4. Inflammatory cytokines quantified in BALF by cytometric bead array.....	69
5. Summary of the effects of corn oil and $\Delta^9$ -THC on BALF and histochemistry measurements taken for epithelial and inflammatory cells in wild type and CB <sub>1</sub> <sup>-/-</sup> /CB <sub>2</sub> <sup>-/-</sup> mice.....	110

## LIST OF FIGURES

1.	Diagram of human (A) and mouse (B) lungs.....	3
2.	Structure of $\Delta^9$ -tetrahydrocannabinol.....	17
3.	Diagram of the microdissection of mouse right lung lobes (R1, R2, R3, R4) and left lung lobe at generations 5 (G5) and 11 (G11).....	33
4.	Increasing concentrations of influenza virus result in increasing inflammatory responses in the hilar region of the left lung lobe at generation 5 of the main axial airway.....	43
5.	Bronchiolar epithelial morphometry following influenza infection..	47
6.	Time-to-onset of mucous cell metaplasia following influenza infection.....	50
7.	MUC5AC gene induction by influenza at 7 days post infection.....	51
8.	Time-dependent proliferation of epithelial cells lining the main axial airway following influenza infection.....	53
9.	Time-dependent detection of total protein in bronchoalveolar lavage fluid following influenza infection.....	55
10.	Time-dependent recruitment of leukocytes to the pulmonary airways following influenza infection.....	57
11.	Secretion of chemokines and cytokines into the airways in response to influenza infection.....	60
12.	Detection of $T_H2$ cytokines secreted into the airways in response to influenza infection.....	61
13.	Secretion of neutrophil-derived elastase into the airways in response to influenza infection.....	63
14.	$\Delta^9$ -THC treatment enhances hemagglutinin 1 mRNA levels.....	64
15.	$\Delta^9$ -THC does not alter total protein levels in BALF.....	65
16.	$\Delta^9$ -THC decreases inflammation scores in a time-dependent manner.....	72

17.	Examination of the effects of $\Delta^9$ -THC on the inflammatory response to influenza challenge by histopathology.....	74
18.	$\Delta^9$ -THC has no effect on Caspase-3 mRNA levels and epithelial numeric cell densities.....	78
19.	$\Delta^9$ -THC increases MUC5AC mRNA levels and decreases epithelial numeric cell densities for acidic mucosubstances.....	80
20.	$\Delta^9$ -THC modestly increases neutrophil-derived elastase levels secreted in the pulmonary airways.....	82
21.	Effects of $\Delta^9$ -THC treatment on the expression levels of H1 mRNA in $CB_1^{-}/CB_2^{-}$ and wild type mice.....	84
22.	Effects of $\Delta^9$ -THC treatment on total protein in BALF in $CB_1^{-}/CB_2^{-}$ and wild type mice.....	86
23.	Effects of $\Delta^9$ -THC treatment on total and differential leukocyte counts in BALF in $CB_1^{-}/CB_2^{-}$ and wild type mice.....	89
24.	Effects of $\Delta^9$ -THC treatment on $CD4^+$ and $CD8^+$ T cells retrieved in BALF in $CB_1^{-}/CB_2^{-}$ and wild type mice.....	92
25.	Effects of $\Delta^9$ -THC treatment on inflammatory chemokines and cytokines in secreted into the pulmonary airways in $CB_1^{-}/CB_2^{-}$ and wild type mice.....	95
26.	Effects of $\Delta^9$ -THC treatment on $T_H2$ cytokines secreted into the pulmonary airways in $CB_1^{-}/CB_2^{-}$ and wild type mice.....	97
27.	Effects of $\Delta^9$ -THC treatment on inflammatory chemokines and cytokines released into blood serum in $CB_1^{-}/CB_2^{-}$ and wild type mice.....	100
28.	Inflammatory response to PR8 in the proximal section of the left lung lobe in $CB_1^{-}/CB_2^{-}$ and wild type mice.....	103
29.	Effects of $\Delta^9$ -THC treatment on histopathology-based inflammation scores in $CB_1^{-}/CB_2^{-}$ and wild type mice .....	105
30.	Effects of $\Delta^9$ -THC treatment on the numeric cell density of caspase-3 positive epithelial cells in $CB_1^{-}/CB_2^{-}$ and wild type mice.....	106

31. Effects of  $\Delta^9$ -THC treatment on the numeric cell density of mucosubstances in airway epithelial cells in  $CB_1^{-/-}/CB_2^{-/-}$  and wild type mice..... 108

## LIST OF ABBREVIATIONS

AB/H	Alcian blue/hematoxylin
AB/PAS	Alcian blue/periodic acid schiff
ABS	Automation buffer solution
AIDS	Acquired Immune Deficiency Syndrome
ANOVA	Analysis of variance
AP-1	Activating protein-1
B-1	Non-antigen stimulated B cell
B-2	Antigen stimulated B cell
BALF	Bronchoalveolar lavage fluid
BCA	Bicinchoninic acid
CAS-3	Caspase-3
CB <sub>1</sub>	Cannabinoid receptor type 1
CB <sub>1</sub> <sup>-/-</sup>	Cannabinoid receptor type 1 null
CB <sub>2</sub>	Cannabinoid receptor type 2
CB <sub>2</sub> <sup>-/-</sup>	Cannabinoid receptor type 2 null
CB <sub>1</sub> <sup>-/-</sup> /CB <sub>2</sub> <sup>-/-</sup>	Cannabinoid receptors type 1 and 2 null
CD	Cluster of differentiation
cDNA	copy-deoxynucleic acid
C/EBPβ	Nuclear factor-IL-6
CNS	Central nervous system
CO	Corn oil
CTL	Cytotoxic T lymphocytes

$\Delta^9$ -THC	Delta-9-tetrahydrocannabinol
DNA	Deoxynucleic acid
dpi	Days post-infection
FACS	Flourescence assisted cell sorting
FasL	Fas ligand
FCM	Flow cytometer
G5	Airway generation 5
G11	Airway generation 11
H	Hemagglutinin
H&E	Hematoxylin and eosin
HSV1	Herpes simplex virus type 1
HSV2	Herpes simplex virus type 2
icv	intracerebroventricularly
IFN $\alpha/\beta$	Interferons -alpha and -beta
IFN- $\gamma$	Interferon-gamma
IL	Interleukin
IP-10	Interferon-gamma-inducible protein
IRF	Interferon regulatory factors
KO	Knockout
LAK	Lymphocyte activated killer cells
LD50	Lethal dose to 50 percent of the population
M1	Matrix protein 1
MCM	Mucous cell metaplasia

MCP-1	Monocyte chemoattractant protein-1
MCP-3	Monocyte chemoattractant protein-3
MDCK	Madin-Darby Canine Kidney cell
MHC	Major histocompatibility complex
MIP1- $\alpha$	Macrophage inflammatory protein 1-alpha
MIP1- $\beta$	Macrophage inflammatory protein 1-beta
MIP-2	Macrophage inflammatory protein 2
MIP3- $\alpha$	Macrophage inflammatory protein 3-alpha
mRNA	Messenger ribonucleic acid
N	neuraminidase
NFAT	Nuclear factor of activated T cells
NF- $\kappa$ B	Nuclear factor kappa B
NIH	National Institutes of Health
NK	Natural killer cells
NP	nucleoprotein
NS	nonstructural protein
PA	Polymerase type A
PB1	Polymerase type B1
PB2	Polymerase type B2
PAS	Periodic acid schiff
PCNA	Proliferating cell nuclear antigen
pfu	Plaque forming units
PMA	Phorbol myristate acetate

PMN	Polymorphonuclear leukocyte
PR8	Influenza A/PR/8/34
RANTES	Regulated on activation, normal T expressed and secreted
RNA	Ribonucleic acid
RT-PCR	Reverse transcriptase-polymerase chain reaction
SAL	Saline
SEM	Standard error of the mean
STAT	Signal transducers and activators of transcription
T <sub>H</sub> 1	T-helper 1 lymphocyte
T <sub>H</sub> 2	T-helper 2 lymphocyte
TNF- $\alpha$	Tumor necrosis factor-alpha
TGF- $\beta$	Transforming growth factor-beta
V <sub>s</sub>	Volume density

## **INTRODUCTION**

### **I. Respiratory toxicology**

The primary function of the respiratory system is the exchange of gases (e.g., oxygen and carbon dioxide) across the alveolar and capillary beds. Gas exchange is so important to the function of all other systems in the body that merely minutes without oxygen will lead to the death of the host. Therefore, noxious gases, particulates and pathogens that perturb normal lung function have life threatening potential. To better understand the responses of the lung to toxicant or pathogen insult, a basic background on the anatomy and physiology of the respiratory tract is provided.

#### **A) Basic anatomy and physiology**

The respiratory tract can be divided into two parts: 1) the upper respiratory tract, and 2) the lower respiratory tract. The upper respiratory tract consists of the nasal airways, larynx, and trachea. While the lower airways consist of the trachea and right and left lung lobes which contain bronchi, bronchioles, terminal bronchioles, alveolar ducts and alveoli.

In the nasal cavity of the upper respiratory tract, incoming air is filtered, for the removal of large particulate matter, and conditioned (humidified) for passage into the lower respiratory tract. In addition, chemical odors are processed by the olfactory epithelium and olfactory sensory neurons to provide a sense of smell. From a comparative standpoint, humans breathe nasally and orally (through the mouth), whereas mice are obligatory nose breathers. Developmentally, the nasal cavity in man is relatively simple in comparison to that of the rodent. Increased specialization in the nasal cavity of

mice that includes increased numbers of olfactory epithelial cells which emphasizes a primary function of the nose for olfaction in mice (1).

From the upper respiratory tract, the trachea bifurcates into the right and left lung lobes. In humans, the left lung lobe is divided by an interlobular fissure into two lobes (superior and inferior), and the right lung lobe is also divided by interlobular fissures into three lobes (superior, middle and inferior) (Figure 1A). Comparatively, the mouse right lung is divided into four structurally distinct lobes (apical, middle, caudal, and accessory), and the mouse has a single left lung lobe (Figure 1B). Structurally, the lower respiratory tract can be further divided into the conducting airways and the respiratory airways. The conducting airways consist of the trachea, bronchus, secondary and tertiary bronchi and non-respiratory bronchioles. The respiratory bronchioles consist of alveolar ducts and alveoli.

The epithelium lining the larger conducting airways is predominantly pseudostratified and columnar whereas smaller conducting airways are primarily comprised of cuboidal epithelial cells. The cellular makeup includes clara cells, basal cells, ciliated epithelial cells and mucin-producing, goblet cells. Together, these cells provide an important defense mechanism for the lung, termed the mucocilliary escalator. The mucociliary escalator is regulated by the production of mucous by goblet cells and the beating of cilia. The movement of cilia is under the control of the autonomic nervous system.

The alveoli are composed of type I and type II cells. The Type I cell is a thin cell stretched over a very large area. Type I cells cannot replicate and are susceptible to a large number of toxic insults. Type I cells are responsible for gas exchanges occurring in

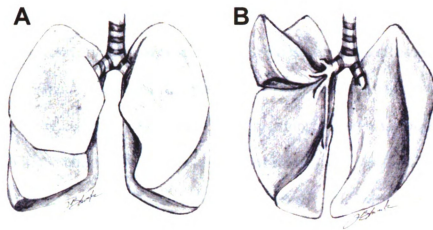


**Figure 1.** Diagram of human (A) and mouse (B) lungs. (Not drawn to scale).

the alveoli. The Type II cell is a smaller, roughly cuboidal cell that is usually found at the alveolar septal junction. Type II cells are spherical cells which comprise only 4% of the alveolar surface area, yet they constitute 60% of alveolar epithelial cells and 10-15% of all lung cells. Four major functions have been attributed to alveolar type II cells: 1) synthesis and secretion of surfactant; 2) xenobiotic metabolism; 3) transepithelial movement of water; and 4) regeneration of the alveolar epithelium following lung injury (2, 3).

### **B) Respiratory clearance of inhaled particles and pathogens**

A variety of different particles, such as bacterial or viral agents and environmental pollutants are deposited in the lungs while breathing. Three main clearance mechanisms operate in the lungs of humans to remove the inhaled and deposited materials as well as cellular debris in order to keep the airways relatively clean. Mucociliary clearance clears the conducting airways of its own secreted mucus, together with substances trapped in it, by means of the mucociliary escalator. Coughing serves as a backup system if mucociliary clearance fails. Lastly, alveolar clearance removes insoluble particles deposited on the respiratory surface of the lungs (4). In contrast to humans, mice do not possess a cough reflex.

#### **1) Mucociliary clearance**

Mucus behaves as a viscoelastic gel, consisting of water and high molecular mass cross-linked glycoproteins mixed with serum and cellular protein, including albumin, enzymes, immunoglobulins, and lipids (4). Ciliary movement in the conducting airways

propels mucus in a cephalic direction to be swallowed or expectorated. If levels of mucus exceed the threshold by which normal ciliary movement cannot propel the mucus in a cephalic direction, then the potential for mucus plugging exists (5).

## **2) Alveolar clearance.**

Small particles from 2 to 0.2 microns in diameter can escape the defense mechanisms of the upper respiratory tract and the mucociliary escalator to reach the alveoli. Pathogens such as bacteria and viruses are generally less than 2 microns in diameter. Once these microorganisms arrive in the alveoli they are handled in different ways.

Bacteria can be opsonized by immunoglobulins present in the fluid lining the alveoli. The opsonized bacterium is readily phagocytosed by resident alveolar macrophages. If the organism bypasses opsonization then the macrophage may still be able to phagocytose the bacterium, however, at a much slower rate. Once the microorganism is phagocytosed by the macrophage, the organism is destroyed within an endosome and small microbial protein fragments are presented on the surface of the macrophage in the context of type II major histocompatibility complexes (MHC II) to awaiting T cells. Once activated, T cells can signal B cells to produce more antibody and/or activate macrophages to increase phagocytic activity and release soluble chemical mediators that help recruit polymorphonuclear neutrophils (PMN) from the blood stream. PMNs are also phagocytic cells that work optimally in conditions where antibody and complement are present.

Viruses, unlike bacteria, are obligate intracellular parasites that replicate inside

the epithelial cells lining the airways of the lung. Viral clearance is accomplished by cell-mediated immunity. Cell-mediated immunity involves the activation of T cell subsets into effector T cell populations that include cytotoxic T cells, and T helper cells of the  $T_{H1}$  and  $T_{H2}$  subtypes. During a cell-mediated immune response to viral infection, antigens are presented to  $CD8^+$  T cells in the context of a major histocompatibility complex I (MHC I), that is present on all nucleated cells. Conversely,  $CD4^+$   $T_{H1}$  and  $T_{H2}$  cells detect antigens in the context of MHC II presented by macrophages, dendritic cells and B cells. Once  $CD8^+$  T cells recognize host cells bearing new antigens in the context of MHC I, the cytotoxic T cell releases cytolytic proteins (perforin) that form holes in the membrane through which granzyme is delivered to induce apoptosis of the target cell. The process is continued until all infected cells have been cleared. There is growing support for the role of  $CD4^+$  T cells as contributing immune effectors in the protection against influenza (6-8).  $CD4^+$  T cells carry out a supportive role through the promotion of long-lasting  $CD8^+$  T memory cells, mediating the clearance of virus by an interferon-gamma ( $IFN-\gamma$ )-dependent mechanism, or through direct cytolytic effects on infected cells, or by a combination of these functions (7). The direct cytolytic activity of  $CD4^+$  cytolytic T cells (CTL's) through Fas-Fas ligand (Fas-FasL) interactions has been previously established (9, 10). These findings illustrate the redundancies found within the acquired immune response that collectively defend the host against infectious pathogens.

### **C) Epithelial cell death and regeneration.**

The cells of the lung are under constant insult by airborne chemicals or pathogens. Typically these insults are dealt with by the inherent functional properties of the lung

(e.g. mucociliary escalator, resident alveolar macrophages, and the cough reflex). However, when chemical agents or viral pathogens target cells directly for death, mechanisms to replace the dying cells must be in place. Specialized cells like the Clara cell and the type II cell are responsible for replicating and differentiating to fill the void.

### **1) Clara cells**

In the conducting airways, Clara cells with enhanced epidermal growth factor receptor expression can be activated by multiple stimuli to differentiate into goblet cells. Differentiating into increased numbers of goblet cells, also known as mucous cell metaplasia, (MCM) has the potential to lead to a state of hypersecretion of mucus that contributes to airway plugging.

MCM has been well characterized in rodent models that exhibit airway remodeling after allergen exposure (11-13) as well as after toxicant exposure (13-15). The pathogenesis of MCM in these models appears to be intimately linked with soluble mediators derived from pro-inflammatory neutrophils and macrophages as well as T<sub>H</sub>2 cells during the acquired immune response. For instance, neutrophil-derived elastase (16), tumor necrosis factor – alpha (TNF- $\alpha$ ) (17) and the T<sub>H</sub>2 cytokines IL-4 (18), IL-5 (19), IL-9 (20), and IL-13 (21) have been implicated in the etiology of MCM. More recently, there has been an increasing body of evidence that MCM also occurs as a component of the progressive changes in respiratory pathology in models of viral infections (22) including adenovirus (23), respiratory syncytial virus (RSV) (24) and influenza virus (25).

## **2) Type II cells.**

In the alveoli, type II cells replace dying type I and type II cells. The type II cell is a pluripotent cell that can divide and differentiate into type I cells. Efforts to further characterize type II cell proliferation and differentiation *in vitro* utilizing freshly isolated type II cells, however, has been met with difficulty. In particular, the isolation procedure has been suggested to result in the blockage of cell cycling as a cell stress response (26).

## **II. Influenza Virus**

### **A) Classification**

Influenza viruses are enveloped, negative-stranded RNA viruses belonging to the family of *Orthomyxoviridae*. Influenza A virus RNA is composed of eight segmented genes, which encode for ten different proteins (27). These proteins include: the envelope glycoproteins hemagglutinin (H) and neuraminidase (N), matrix protein (M1), nucleoprotein (NP), three polymerases (PB1, PB2 and PA), ion channel protein M2, and nonstructural proteins NS1 and NS2. Influenza A viruses are classified according to their H (H1–H15) and N (N1–N9) genes. Viruses with hemagglutinin types H1, H2 and H3 and neuraminidase types N1 and N2 are pathogenic in humans. The nomenclature of influenza viruses provides detailed information regarding virus type and origin. For example, the nomenclature for influenza virus A/PR/8/34 (H1N1) indicates that the virus type is influenza virus type A, originating from Puerto Rico, as the 8<sup>th</sup> isolated strain, in the year 1934. Additionally, the surface proteins H and N subtype the virus as an influenza virus that belongs to the group of influenza viruses designated H1N1.

## **B) Viral Entry**

Influenza viruses preferentially replicate in the epithelial cell layers of the upper respiratory tract; however, macrophages and other leukocytes may also be infected (28). Most cell types carrying the influenza A virus receptor, sialic acid containing cell surface glycoproteins, are susceptible to the virus (29). Recent work by Chu and Whittaker (2004) (30) has provided evidence that a cell line deficient in terminal N-linked glycosylation, caused by a mutation in the N-acetylglucosaminyltransferase I gene, could not be infected by influenza virus. The cells were not deficient for total cell-surface sialic acid and, accordingly, were able to bind the virus. However, viral binding to sialic acid was not sufficient for infection, suggesting that virus binding to the sialic acid moiety merely brought the virus into close proximity of a secondary receptor that triggered internalization of the virus.

## **C) Viral Clearance**

Myeloid cells such as neutrophils and macrophages, and acquired immune cells like cytolytic and helper T cells mediate the clearance of virally infected epithelial cells within the pulmonary airways. In addition, B cells provide support against subsequent re-infection through the secretion of antigen-specific antibodies.

The contributions of phagocytic cells like the neutrophil and macrophage to the complex process of viral clearance have been previously studied. Tsuru and coworkers (1987) (31) examined phagocyte-depleted mice challenged intravenously with a sublethal inoculate of influenza virus. Phagocyte depletion was accomplished by either carrageenan treatment or gamma-irradiation. Neutrophils are sensitive to gamma-

irradiation and resistant to carrageenan treatment, whereas macrophages and natural killer cells are gamma-insensitive and carrageenan-sensitive. Mice treated by gamma-irradiation and challenged with influenza exhibited increased viral titres and death by 8 days. Conversely, mice treated with carrageenan cleared the virus by day 7. In addition, the adoptive transfer of syngeneic neutrophils into gamma-irradiated mice was not accompanied by increased viral titres. Hence, the neutrophil, and not the macrophage, was suggested to play an important role in early phase responses to influenza.

CD8<sup>+</sup> T cells are cytolytic T cells that induce the apoptotic cell death of virus-infected cells upon antigen recognition and coordinated co-stimulation. Allan et al., (1990) (32) demonstrated that CD8<sup>+</sup> T cells mediated the clearance of influenza virus from the lung. Specifically, the authors depleted mice of CD4<sup>+</sup> T cells and subsequently challenged mice with influenza virus A (H3N2). An increase in the mediastinal lymph node size during influenza infection was not observed with CD4<sup>+</sup> T cell depletion. In addition, elimination of CD4<sup>+</sup> T cells did not influence the severity of the inflammatory response in the lung. Moreover, mice deficient of CD4<sup>+</sup> T cells were capable of clearing the virus infection, suggesting that CD8<sup>+</sup> T cells were the most important of the two T cell types for developing an effective cell-mediated immune response against influenza.

Although CD4<sup>+</sup> T cells were not required for viral clearance, the role for CD4<sup>+</sup> T cells in the immune response to influenza was unclear. Graham et al., (1994) (33) examined the contribution of CD4<sup>+</sup> T cell subsets. Influenza virus-specific T<sub>H1</sub> and T<sub>H2</sub> clones were generated from influenza-primed BALB/c mice. T<sub>H1</sub> clones were shown to have cytolytic properties *in vitro* and were protective against a lethal challenge of virus *in vivo*. T<sub>H2</sub> clones were nonprotective and mice exhibited an exacerbation of the

pulmonary pathology associated with influenza infection. The results suggested that T<sub>H</sub>1 cells provided support against primary influenza infections. Likely, T<sub>H</sub>1 cells through the release of IFN- $\gamma$  elicited a cell-mediated immune response against influenza-infected cells.

Moran et al (1999) (34) recognized that immunization with live virus expanded T<sub>H</sub>1 memory cells and provided protection against a heterosubtypic (different viral surface marker subtype) viral challenge and that immunization with inactivated virus expanded T<sub>H</sub>2 memory cells without affording the host protection. Hence, the authors created a T<sub>H</sub>1 priming environment with the inclusion of IL-12 and antibodies to IL-4 along with the inactivated virus to yield a T<sub>H</sub>1 memory cell population that facilitated the generation of cytotoxic T cells upon challenge with a heterosubtypic virus.

Antibodies play an important role in targeting specific viral surface proteins like hemagglutinin and neuraminidase to neutralize and more importantly opsonize the virus for clearance by phagocytic cells. Therefore, the humoral immune response is beneficial to the host with subsequent re-infection. Baumgarth et al., (2000) (35), studied the contribution of B cells and secretory immunoglobulin M in protection against influenza virus. The authors found that 129/Sv mice deficient in secretory IgM but capable of expressing surface IgM had reduced viral clearance and survival rates. More importantly, both B-1 (non-antigen stimulated) and B-2 (antigen stimulated) cell-derived IgM antibodies were deemed necessary for the survival of the host. These findings support the role of antibodies in neutralizing and opsonizing viruses for clearance by phagocytes.

#### **D) Chemokine and cytokine responses to influenza virus**

The antiviral state created by influenza infection of the respiratory epithelium and alveolar macrophages of the lung results in the production of chemotactic [regulated on activation, normal T expressed and secreted (RANTES), macrophage inflammatory protein 1-alpha (MIP-1 $\alpha$ ), monocyte chemoattractant protein-1 (MCP-1), monocyte chemoattractant protein-3 (MCP-3), and interferon-gamma-inducible protein-10 (IP-10)], pro-inflammatory (IL-1 $\beta$ , IL-6, IL-18, and TNF- $\alpha$ ) and anti-viral [interferons -alpha and -beta (IFN- $\alpha/\beta$ )] cytokines (36). The production of specific chemokines and cytokines provide a feedback loop that supports T<sub>H</sub>1 cell-mediated immunity against influenza-infected epithelium.

Chemokines are produced by a variety of cells constitutively or in response to microbial infections. Chemokines bind to their specific cell surface receptors on leukocytes, enabling them to migrate from blood vessels through the vascular endothelium into the site of inflammation (37). Influenza virus infected macrophages secrete MIP-1a, MIP-1b, RANTES, MCP-1, MCP-3, MIP-3 $\alpha$  and IP-10 (38-40) whereas epithelial cells produce RANTES, MCP-1 and IL-8 (41, 42). Antiviral (IFN- $\alpha/\beta$ ) and immune-stimulatory cytokines (IL-1 $\beta$ , IL-6, IL-18, and TNF- $\alpha$ ) are largely produced by influenza-infected macrophages (28, 43-45) and to a lesser extent by influenza infected epithelial cells (28, 43, 46). Dendritic cells are the primary source of IL-12 production (47). IFN- $\alpha/\beta$  is important in the recruitment of monocytes/macrophages and T<sub>H</sub>1 cells through the upregulation of MCP-1, MCP-3, and IP-10 (37, 48). In addition, IFN- $\alpha/\beta$  enhances antigen presentation by upregulating MHC gene expression (49). Moreover, IFN- $\alpha/\beta$  is involved in T cell survival (50) and enhancement of IFN- $\gamma$  production in natural killer cells (NK) and T cells. Conversely, the pro-inflammatory

cytokines IL-1 $\beta$ , IL-6, and TNF- $\alpha$  do not directly contribute to the anti-viral activity of leukocytes (49). IL-1 $\beta$  and TNF- $\alpha$  enhance MCP-1 gene expression and maturation of tissue macrophages. NK and T cell derived IFN- $\gamma$  primes macrophages for increased cytokine production, thereby leading to a positive feedback loop between macrophages and NK and T cells (36).

The induction of chemokines and cytokines by influenza infection involves the activation of transcription factors. Nuclear factor kappa B (NF- $\kappa$ B), activating protein (AP-1), interferon regulatory factors (IRFs), signal transducers and activators of transcription (STATs) and nuclear factor-IL-6 (C/EBP $\beta$ ) have all been shown to be activated during influenza infection (40, 46) (51-54). NF- $\kappa$ B activation occurs during viral replication and protein synthesis (46). Virus replication has also been shown to activate the transcription factor AP-1 (54). The activation of STAT, on the other hand, is indirectly mediated by virus-induced IFN- $\alpha/\beta$  (40, 46).

#### **E) Models of susceptibility**

Increased susceptibility to influenza virus infection following exposure to respirable chemicals or particulates has been a human health concern for people whose occupations include increased risk to inhaled particulate matter. In particular, research has been conducted to address the concern with environmental chemicals and particulates such as coal particulates, diesel exhaust, and ozone.

Coal miners working underground are chronically exposed to respirable particulates of coal and emissions from diesel engines. Studies have been conducted in mice to determine whether coal miners are at increased risk for developing respiratory

infections like influenza virus. Hahon et al. (1985) (55) examined the susceptibility to influenza infection in CD-1 white Swiss mice exposed to coal dust, diesel emissions, or a combination of both for 1, 3, and 6 months. The course of influenza infection in mice did not differ among treatment groups with respect to mortality and duration of exposure to particulates. However, there was an increased severity of reaction to influenza in mice treated with diesel emissions when compared to filtered air controls and mice receiving coal dust.

To elucidate why the severity of the response to influenza was greater with exposure to diesel emissions, Jaspers et al., (2005) (56) utilized an *in vitro* model of human respiratory epithelial cells to determine the effects of aqueous trapped diesel exhaust on influenza A/Bangkok/1/79 infection. Exposure of the respiratory epithelial cells to diesel exhaust resulted in increased influenza infection. Increased infection, however, was not attributed to the suppression of antiviral mediators. Alternatively, the authors suggested that increased oxidative stress generated during exposure to diesel exhaust enhanced viral attachment and infection of the epithelial cells. The role of oxidative stress has been supported by more recent work in which the addition of glutathione *in vitro* and *in vivo* resulted in decreased viral titres with increasing concentrations of glutathione and an inhibition of influenza-induced activation of apoptotic caspases and Fas as compared to controls (57).

Human exposure to ozone, the primary oxidant gas in photochemical smog, has been associated with altered pulmonary function and airway reactivity (58) and airway inflammation (59). Therefore, exposure to ozone might also render individuals more susceptible to respiratory infections. Wolcott et al., (1982) (60) exposed Swiss-Webster

mice to ambient levels (0.5ppm) of ozone during an infection with influenza virus (WSN strain) and demonstrated that infected mice exposed to ozone exhibited a reduced severity of disease, as measured by a decrease in the mortality and delayed time to death. In addition, the infected mice exposed to ozone exhibited differential distribution of the virus with respect to filtered air controls. In particular, mice that were exposed to ozone had no airway epithelial viral-antigen staining; rather the viral-antigen staining was distributed to focal regions of infection in alveolar fields. In contrast, the virus infected the respiratory epithelium in air-filtered controls and dispersed with time to the alveolar parenchyma with relatively even distribution. Since ozone exposure has been shown to induce extensive desquamation of the respiratory epithelium and result in a regenerative epithelium that consists of cells that morphologically represent squamous epithelium (61-63), the pulmonary changes observed might result from an airway lining that is more resistant to infection by influenza virus (60).

### **III. Cannabinoids**

#### **A) Chemistry of delta-(9)-tetrahydrocannabinol**

Marijuana, a crude preparation of *Cannabis sativa*, is comprised of over 426 chemical entities. More than 60 of these compounds are known collectively as cannabinoids (64). Mechoulam and Gaoni first described the isolation of cannabinoid compounds from marijuana extracts in 1965 (65). Turk and coworkers (1971) (66) were the first to isolate and identify delta-9-tetrahydrocannabinol ( $\Delta^9$ -THC) (Figure 2).

#### **B) Pharmacokinetics**

## **1) Absorption**

Cannabinoids are more readily absorbed following inhalation as compared to oral consumption. Moreover, it has been shown that the vehicle in which  $\Delta^9$ -THC is administered has an influence on the pharmacokinetics and, hence the effectivity of the drug (67). For example, in a study conducted by Coper et al, (1971)(68) utilizing the same dose of  $\Delta^9$ -THC administered in either polyethylene glycol or rape oil (canola oil), rats exhibited decreased body temperature with  $\Delta^9$ -THC in polyethylene glycol and no change in body temperature with  $\Delta^9$ -THC in rape oil. Likewise, a study conducted by Perez-Reyes et al., (1973) (69) in humans demonstrated that radiolabeled  $^3\text{H}$ - $\Delta^9$ -THC, when administered orally, was absorbed at different rates depending on the vehicle utilized. However, there were no apparent differences in the overall psychotropic effects, metabolism or excretion of the drug.

## **2) Distribution**

The distribution of cannabinoids and their metabolites occurs based on the physical and chemical properties of the drug. Cannabinoids are highly lipophilic compounds. Therefore, their distribution among tissues, once they are absorbed, is dependent on blood circulation and the hepatic and extrahepatic metabolism of the parent compound.

Klausner and Dingell (1971) (70) quantified the tissue distribution of intravenously administered  $^{14}\text{C}$ - $\Delta^9$ -THC in rats. The highest concentration of radioactivity was measured in the lung and the lowest concentration in the brain. Further studies conducted by Ho et al., (1970) (71) utilized  $^3\text{H}$ - $\Delta^9$ -THC administered by

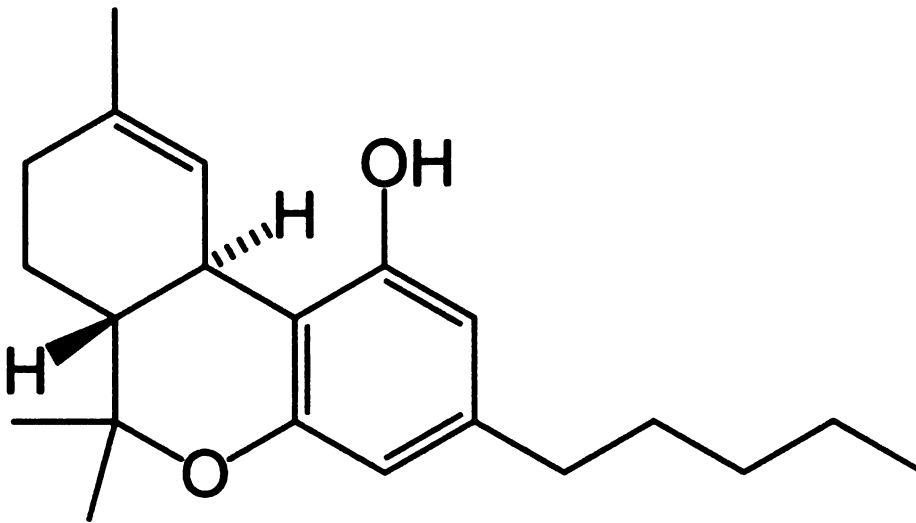


**Figure 2.** Structure of  $\Delta^9$ -tetrahydrocannabinol

inhalation. The tissue distribution was similar to the findings by Klausner and Dingell.

### **3) Metabolism**

The metabolism of  $\Delta^9$ -THC results in a number of metabolites that include 11-hydroxy- $\Delta^9$ -THC, 9-carboxy- $\Delta^9$ -THC, and 8,11-dihydroxy- $\Delta^9$ -THC. Since human exposure to  $\Delta^9$ -THC commonly occurs via inhalation or oral ingestion, likely sites of metabolism might be the alveolar type II cells of the lung, the microflora of the gut, and hepatocytes of the liver.

## **C) Biological receptors and activity**

### **1) CB1 and CB2 receptors**

Cannabinoid compounds produce a myriad of biological effects in animals and humans including effects on the central nervous system (CNS), cardiovascular, endocrine, immune, and reproductive systems (64). The most widely studied of these are the CNS and immune systems.

The putative mechanism by which cannabinoids have been proposed to mediate their biological effects, at least in part, is through the cannabinoid receptors (CB<sub>1</sub> and CB<sub>2</sub>). The CB<sub>1</sub> receptor (brain receptor) was first cloned and characterized for expression by Matsuda and coworkers (72). Likewise, the CB<sub>2</sub> receptor (peripheral receptor) was first cloned and characterized for expression by Munro and coworkers (73). The CB<sub>2</sub> receptor is predominantly expressed in cells of the immune system (74, 75) and has been thought to mediate many of the immune suppressive effects of cannabinoids. In particular, the CB<sub>2</sub> receptor has been shown to mediate the cannabinoid-induced

inhibition of antigen processing and presentation in macrophage (76, 77), and antitumor activity in a murine model of lung cancer (78). These studies illustrate different aspects of host immunity that are cannabinoid receptor (CB<sub>1</sub> and CB<sub>2</sub>)-dependent

## **2) Alternative receptors**

In addition to CB<sub>1</sub>/CB<sub>2</sub> receptor-dependent interactions, cannabinoids have also been reported to induce CB<sub>1</sub>/CB<sub>2</sub> receptor-independent effects. Independence of the CB<sub>1</sub>/CB<sub>2</sub> receptors has been evidenced in many different cells of the body (79-81). Of particular interest to this dissertation are the CB<sub>1</sub>/CB<sub>2</sub> receptor-independent effects exhibited by immune cells. There is emerging evidence for cannabinoid-mediated effects on cytokine production pertinent to T-dependent humoral and cell mediated immune responses that occur independently of CB<sub>1</sub>/CB<sub>2</sub> receptors. Specifically, the suppression of IL-2 production by cannabinoid treated mouse splenocytes stimulated with phorbol myristate acetate/ionomycin (PMA/Io) could not be attenuated by the cannabinoid receptor antagonists, SR141716A and SR144528 (82). Moreover, it has been demonstrated that the endocannabinoid, 2-arachidonyl glycerol, suppressed PMA/Io elicited IFN- $\gamma$  expression similarly in splenocytes attained from cannabinoid receptor-null mice (CB<sub>1</sub><sup>-/-</sup>/CB<sub>2</sub><sup>-/-</sup>) as compared to splenocytes from wild type mice (83). Additional evidence for cannabinoid receptor-independent effects of cannabinoids are illustrated by the plant-derived cannabinoid, cannabidiol. Cannabidiol possesses little to no affinity for the cannabinoid receptors CB<sub>1</sub> and CB<sub>2</sub>, yet it exhibits potent anti-inflammatory activity including the reduced production of prostaglandin E<sub>2</sub>, nitric oxide and other oxygen-derived free radicals to carrageenan-induced inflammation (84), inhibition of the release

of IL-1, TNF- $\alpha$ , and IFN- $\gamma$  by peripheral blood mononuclear cells (85), and suppressed MIP-1a, MIP-1B, and IL-8 in the HTLV-1 B cell line (86). To rigorously examine the combined functional contribution of the CB<sub>1</sub>/CB<sub>2</sub> receptors to biological responses elicited by cannabinoids, mice were developed with specific mutations in the CB<sub>1</sub> and/or CB<sub>2</sub> receptor (77, 87).

Zimmer et al., (1999) (87) generated CB<sub>1</sub><sup>-/-</sup> mice by replacing the coding region in the mouse CB<sub>1</sub> receptor gene, between amino acids 32 and 448, with a PGK-neo cassette, thereby creating embryonic stem cells with a mutant CB<sub>1</sub> gene. These cells were used to create chimeric mice, which were bred with C57BL/6J mice. The resulting heterozygous CB<sub>1</sub><sup>+/-</sup> mice were then inbred to produce CB<sub>1</sub><sup>-/-</sup> and CB<sub>1</sub><sup>+/+</sup> mice. In a similar fashion, the CB<sub>2</sub><sup>-/-</sup> mouse was generated (77) and subsequently CB<sub>1</sub><sup>-/-</sup> / CB<sub>2</sub><sup>-/-</sup> mice were generated by breeding both receptor-null mutants.

#### **D) Effects of cannabinoids on the immune system**

Cannabinoid receptors CB<sub>1</sub> and CB<sub>2</sub> and their transcripts have been identified on cells involved in immune responses, including: B cells, T cells, monocytes, PMNs, and NK cells (75, 88). Hence, through interactions with CB<sub>1</sub> and CB<sub>2</sub> receptors on immune cells, cannabinoids have the potential to alter both innate and acquired immunity toward invasive pathogens.

##### **1) Effects on macrophage function**

Macrophages are components of innate, cell-mediated, and humoral immunity. Macrophages can circulate as blood monocytes or take residence in the liver as Kupffer

cells or the lung as alveolar macrophages. Their phagocytic properties allow for effective removal of circulating debris or xenobiotics. In addition, macrophages release an arsenal of chemical mediators including nitric oxide that are toxic to bacteria and other human pathogens.

Although the mechanism has not been fully defined, cannabinoids alter macrophage function *in vitro* and *in vivo*. Macrophages treated *in vitro* to graded doses of  $\Delta^9$ -THC have been shown to suppress the ability of these cells to spread and to phagocytose particles (89). In addition, exposure of mouse macrophage and human peripheral blood monocyte preparations to  $\Delta^9$ -THC led to decreases in TNF- $\alpha$  production in response to lipopolysaccharide and IFN- $\gamma$  (90). Likewise,  $\Delta^9$ -THC has been shown to inhibit nitric oxide production by mouse macrophages in a concentration and time-dependent manner (91), and the release, but not synthesis, of IL-1 from peritoneal macrophage cultures stimulated with endotoxin (92).

Macrophages are also antigen-presenting cells of the humoral arm of immunity. In brief, antigen-presenting cells internalize antigen, proteolytically cleave the antigen and present the antigen in the form of a complex with MHC class II molecules at the cell surface. Recognition of MHC class II molecules by CD4<sup>+</sup> T cells in the presence of co-stimulatory signals leads to activation and clonal expansion of T cells. Cannabinoids, in particular  $\Delta^9$ -THC, have been shown to interfere with the ability of macrophages to process antigen (93).

## ***2) Effects on neutrophil function***

Once the macrophage has encountered an invading pathogen such as bacteria it

can release cytokines to enhance vascular permeability and chemokines to direct the migration of leukocytes. Neutrophils, or white blood cells, circulating in the blood are one of the first cells recruited during an infection. Neutrophils roll along endothelium that expresses cellular adhesion molecules, and then by diapedesis make their way into the tissue where they can either phagocytose xenobiotic particulates or secrete proteases or reactive oxygen species directed at killing the invading pathogen.

Smith and coworkers (94) examined cannabinoid receptor ligands for their effects on the development of peritoneal inflammation elicited in mice with either thioglycollate broth or staphylococcus enterotoxin A. The synthetic cannabinoid receptor agonists, HU-210 and WIN 55212-2, blocked the migration of neutrophils into the peritoneal cavity in response to these inflammatory stimuli. The authors attributed the effects to a delay in the production of the neutrophil chemoattractant, kuppfer cell and macrophage inflammatory protein-2 (MIP-2).

### ***3) Effect on natural killer (NK) cell function***

NK cells are large granular lymphocytes important in host resistance to tumor cells and virally infected cells. NK cells target host cells with decreased expression of MHC class I surface molecules in the presence of an activating co-stimulatory ligand. When activated, NK cells release perforin and granzyme, which puncture holes into target cells and initiate apoptotic cell death. NK cell activity can be augmented by cytokines such as IL-2.

Lymphokine activated killer cells (LAK), generated by preincubation of NK cells with IL-2, exposed to  $\Delta^9$ -THC at various concentrations exhibit decreased cytolytic

activity toward erythroleukemia (EL-4) target tumor cells, which are highly susceptible to LAK cell killing. Conversely, the killing of YAC-1 cells, a non-IL-2-dependent NK cell target, was less affected by treatment with  $\Delta^9$ -THC (95).

#### **4) Effects on $T_{H1}$ cells**

A T cell-dependent cell-mediated immune response involves the destruction of intracellular pathogens by macrophages activated by  $T_{H1}$  cells, or through the killing of infected cells by cytotoxic  $CD8^+$  T cells. Regardless, both mechanisms target cells infected with intracellular pathogens.

Clonal expansion and differentiation is a critical step for T cell responses to an activating signal. The expansion of T cells in response to mitogens or other ligands requires the synthesis of IL-2 and the expression of IL-2 receptors on T cells.  $\Delta^9$ -THC and 11-hydroxy- $\Delta^9$ -THC inhibit the lymphoproliferative response to T cell mitogens (96). Accordingly,  $\Delta^9$ -THC has been shown to inhibit IL-2-driven proliferation of T cells in a dose-dependent manner (97). In addition,  $\Delta^9$ -THC has been shown to decrease the surface expression of high and intermediate-affinity IL-2 receptors, while increasing the expression of low-affinity IL-2 receptors on the surface of T cells (98).

Differentiation of  $T_{H0}$  into  $T_{H1}$  or  $T_{H2}$  cell types is dependent on IL-12 or IL-4, respectively. In a mouse model for cell-mediated immunity utilizing the bacterial pathogen *Legionella pneumophila*, Klein and coworkers (2000)(99) reported that  $\Delta^9$ -THC suppressed  $T_{H1}$  immunity by attenuating the induction of  $T_{H1}$ -promoting cytokines such as IFN- $\gamma$ , IL-12, and the receptor IL-12R $\beta$ 2. Therefore, the host could not develop an appropriate  $T_{H1}$  cell-mediated response to deal with the infecting pathogen.

### **5) Effects on CD8<sup>+</sup> T cells**

Cytotoxic T lymphocytes (CTL) are CD8<sup>+</sup> T cells that provide protective immunity against viral infection and intracellular pathogens. CTL's mediate protective immunity by inducing the apoptotic cell death of the infected target cell. Apoptosis is induced either by Fas-mediated cell death or perforin and granzyme-mediated target-cell killing.

Fischer-Stenger (100) examined the effect of  $\Delta^9$ -THC on T cell functional competence against Herpes Simplex Virus type 1 (HSV1) infection. Cytotoxicity assays demonstrated that CTL from mice exposed to  $\Delta^9$ -THC were deficient in anti-HSV1 cytolytic activity.  $\Delta^9$ -THC *in vivo* exposure affected CTL cytoplasmic polarization toward the virus-infected target cell resulting in a lower frequency of CTL granule reorientations toward the effector cell-target cell interface following cell conjugation. Hence, there was decreased cell-mediated immunity through CTL activation.

### **6) Effects on immune cell-derived chemokines and cytokines**

Chemokines and cytokines produced by leukocytes in response to inflammatory stimuli provide the necessary signaling to support leukocyte function in the defense against an invading pathogen. Cannabinoids have been shown to suppress the production of chemokines including IL-8, MIP-1 $\alpha$ , MIP-1 $\beta$ , RANTES and MCP-1 (86, 94). In addition, cannabinoids have been shown to modulate the expression of a wide range of cytokines including IFN- $\gamma$ , transforming growth factor-beta (TGF- $\beta$ ), TNF- $\alpha$ , IL-2, IL-4, IL-6, IL-10, IL-12, IL-13, and IL-15 in human and murine cell models (101). The

implication of these findings in the context of pathogen challenge is that cannabinoid treatment would suppress the recruitment of leukocytes and further suppress the ability of T cells and macrophages to communicate effectively when mounting cell-mediated or humoral immune responses.

Regulation of the production of these cytokines by cannabinoids has been linked with the suppression of DNA-binding activity of transcription factors. In particular, AP-1, NF- $\kappa$ B, STATs, and the nuclear factor of activated T cells (NF-AT).  $\Delta^9$ -THC has been shown to inhibit PMA/ionomycin-induced AP-1 DNA-binding activity (102), the activation and binding of NF- $\kappa$ B/Rel proteins to their DNA binding site (103), and the tyrosine phosphorylation of STAT-1 alpha protein (104). More recently, the endocannabinoid 2-arachidonoyl-glycerol has also been shown to disrupt nuclear translocation of NF-AT protein (83).

### **E) Models of host-resistance**

Animal models of host resistance are important for elucidating whether exposure to specific chemicals recognized for their effects on host-immunity, like  $\Delta^9$ -THC, render the host more susceptible to pathogenic challenge.  $\Delta^9$ -THC has been demonstrated to have an effect on host-resistance to a variety of pathogens including Herpes simplex virus (100) and *Legionella pneumophila* (105). In these models, it has been shown that  $\Delta^9$ -THC modulates T cell functionality, thereby suppressing normal pathogen clearance mechanisms.

#### **1) Model of $\Delta^9$ -THC and *Listeria Monocytogenes***

*Listeria Monocytogenes* is a gram-positive bacterium that causes the foodborne illness listeriosis. Listeriosis is associated with septicemia and meningitis in humans. Morahan et al. (1979) (106) examined bacterial infection in BALB/c mice at a 50% lethal dose alone and in combination with  $\Delta^9$ -THC treatment.  $\Delta^9$ -THC was dissolved in a mixture of Emulphor and ethanol and administered intraperitoneally at a dose of 200 mg/kg on the first 2 days of infection. The bacterium was delivered by intravenous inoculation. Mortality of the mice was used as an endpoint and the lethal dose to 50% of the population (LD50) was calculated.  $\Delta^9$ -THC treatment decreased host-resistance to infection as calculated by the arithmetic difference between LD50 values of the untreated and treated groups. The authors concluded that  $\Delta^9$ -THC suppressed cell-mediated immunity, and suggested that the suppression of cell-mediated immunity was likely the result of an effect on T cells by  $\Delta^9$ -THC.

## **2) Model of $\Delta^9$ -THC and Herpes Simplex Virus**

Herpes Simplex Virus type 2 (HSV-2) is an infection that leads to the formation of blisters in the skin or mucous membranes. It is typically transmitted via the lips or genitals. When the virus is asymptomatic it lies dormant in nerve cells. In an experiment of similar design to that of the bacterium *Listeria Monocytogenes*, Morahan et al (1979) (106) infected BALB/c mice with an LD50 dose of HSV-2 by intravenous inoculation. Again,  $\Delta^9$ -THC was dissolved in a mixture of Emulphor and ethanol and administered intraperitoneally at a dose of 200 mg/kg on the first 2 days of infection. Mortality of the mice was used as an endpoint.  $\Delta^9$ -THC decreased host-resistance to infection as calculated by the arithmetic difference between LD50 values of the untreated and treated

groups. The collective conclusion offered by the authors was that  $\Delta^9$ -THC treatment decreased cell-mediated immunity.

Mishkin and coworkers (1985) (107) examined the effects of  $\Delta^9$ -THC treatment on vaginal infections in B6C3F1 mice.  $\Delta^9$ -THC was dissolved in Emulphor and ethanol and administered by intraperitoneal injection at doses ranging from 15 to 100 mg/kg for 4 consecutive days starting on the day before intravaginal infection with HSV-2. The authors concluded that  $\Delta^9$ -THC decreased resistance to HSV-2 in a dose-related manner with an increased trend toward cumulative mortalities and acceleration of the time-to-onset of death.

In 1992, Fischer-Stenger and coworkers (100) examined the effect of  $\Delta^9$ -THC on cytolytic T cell function against HSV-1 infection. Specifically, C3H/HeJ mice were treated with  $\Delta^9$ -THC at doses 15 or 100 mg/kg in a mixture of Emulphor and ethanol intraperitoneally on days 1-4, 8-11, and 15-18. Mice received an intraperitoneal injection of  $1 \times 10^7$  plaque forming units (pfu) of HSV1 on day 21. Spleens were removed 7 days later and T cells were examined by flow cytometry and Nomarski Microscopy. The authors concluded that  $\Delta^9$ -THC treatment decreased cytolytic activity by altering the polarization of the T cells. The inability to polarize rendered the T cells incapable of mounting an efficient release of granules containing the pore-forming protein perforin to the infected cells.

### **3) Model of $\Delta^9$ -THC and *Legionella pneumophila***

*Legionella pneumophila* is a gram-negative bacterium that causes Legionnaires' disease. The primary site of infection is the respiratory tract where it causes pneumonia.

*Legionella pneumophila* is an intracellular parasite that infects macrophages after it has been phagocytosed. Therefore, the macrophage is not capable of destroying the pathogen.

Klein et al. (1993) (105) treated BALB/c mice with  $\Delta^9$ -THC dissolved in dimethyl sulphoxide and heat inactivated mouse serum. Mice were injected intravenously with 8 mg/kg  $\Delta^9$ -THC 24 hours prior to infection and again 24 hours post infection. The bacterium was delivered at a sublethal concentration by intravenous inoculation. Mortality of the mice occurred within 30 minutes of the second injection of  $\Delta^9$ -THC. Treatment of mice with an antibody to IL-6 or TNF- $\alpha$  had a protective effect against mortality. Hence, the authors concluded that the mice died from shock.

In a subsequent study by Klein and coworkers (2000) (99), the effects of  $\Delta^9$ -THC in modulating cytokines involved in the development of T<sub>H</sub>1 cells were examined. The study employed a single injection of  $\Delta^9$ -THC intravenously at a dose of 8 mg/kg, 18 hours prior to infection with *Legionella pneumophila*. The study revealed that treatment of mice with  $\Delta^9$ -THC increased the production of the cytokine IL-4, but suppressed IL-12 and IFN- $\gamma$  serum levels. By implementing cannabinoid receptor (CB<sub>1</sub> and CB<sub>2</sub>) antagonists into the study, it was demonstrated that both the CB<sub>1</sub> and CB<sub>2</sub> receptors might be involved.

In a more recent study, Lu et al., (2006) (108) demonstrated that IL-12 suppression by  $\Delta^9$ -THC was, in part, independent of the CB<sub>1</sub> and CB<sub>2</sub> receptor.  $\Delta^9$ -THC suppression of IL-12 production in dendritic cells obtained from receptor knockout mice was only partially attenuated in the absence of receptors. Moreover, Lu et al (2006b) (109) demonstrated that  $\Delta^9$ -THC inhibits T<sub>H</sub>1 activation by targeting dendritic cell maturation and expression of co-stimulatory and polarizing molecules.

#### IV. Objectives

The objective for the studies outlined in this dissertation project was to examine the hypothesis that the airways of mice treated with  $\Delta^9$ -THC are more susceptible to the adverse sequelae of influenza virus in a CB<sub>1</sub>/CB<sub>2</sub>-receptor-independent manner. First, the magnitude and severity of inflammation associated with the dose of influenza virus alone was established. Second, two different doses of  $\Delta^9$ -THC were administered to mice for five days by oral gavage and blood serum was collected to establish the steady state blood serum concentration of  $\Delta^9$ -THC and its metabolites. Third, the time-dependent effects of influenza on immune and epithelial cell responses to pulmonary infection with influenza were assessed to provide the kinetic basis for monitoring critical time points for  $\Delta^9$ -THC-related effects. Fourth, the dose-dependent effect of  $\Delta^9$ -THC on immune and epithelial cell responses was evaluated. Fifth, the immune and epithelial cell effects of  $\Delta^9$ -THC were examined in the context of mice deficient in the cannabinoid receptors CB<sub>1</sub> and CB<sub>2</sub>. The results of these studies demonstrated that there was a classical pattern of inflammation induced by influenza challenge with concurrent time-dependent changes in epithelial cell death, regeneration, and mucous cell metaplasia.  $\Delta^9$ -THC increased viral H1 mRNA levels in the lung with a concomitant decrease in macrophages and lymphocytes that are essential for the effective cell-mediated clearance of virus infected epithelial cells. Treatment of CB<sub>1</sub><sup>-/-</sup>/CB<sub>2</sub><sup>-/-</sup> mice with  $\Delta^9$ -THC led to alterations in viral H1 mRNA levels, immune cell function, and concomitant morphologic changes of the airway epithelium that were both similar for and unique to CB<sub>1</sub><sup>-/-</sup>/CB<sub>2</sub><sup>-/-</sup> mice as compared to wild type mice.

## MATERIALS AND METHODS

### I. Cannabinoid compounds

$\Delta^9$ -THC was provided by the National Institute on Drug Abuse (Bethesda, MD) as a resin. The resin was solubilized in corn oil for administration to mice by oral gavage.

### II. Animals

C57BL/6 mice (8-10 weeks old), free of pathogens and respiratory disease, were purchased from Charles River (Portage, MI). On arrival, mice were randomly assigned to their experimental groups, transferred to plastic cages containing sawdust bedding, given food (Purina Certified Laboratory Chow) and water *ad libitum*, and quarantined for 1 week until their body weight was 17–20 g. Mice were used in accordance with guidelines set forth by the Institutional Animal Care and Use Committee at Michigan State University. Animal holding rooms were maintained at 21–24°C and 40–60% relative humidity with a 12-h light/dark cycle.

### III. Experimental designs

Five different study designs were employed. The first study was conducted to identify a concentration of PR8 to be administered intranasally to mice that would produce a mild inflammatory response in the lungs by 13 days post infection (dpi) without mortality of the mice (Appendix 1). The second study examined the blood levels of  $\Delta^9$ -THC and its metabolites following five consecutive days of dosing with  $\Delta^9$ -THC by oral gavage (Appendix 2). The third study addressed time-dependent changes in the pulmonary response to PR 8 challenge (Appendix 3). The fourth study evaluated the

effects of varying concentrations of  $\Delta^9$ -THC on the previously characterized time-dependent changes in immune and epithelial cell responses to PR8 (Appendix 4). Finally, the fifth study examined the role of the cannabinoid receptors (CB<sub>1</sub> and CB<sub>2</sub>) in mediating the effects of  $\Delta^9$ -THC on immune and epithelial cell responses following PR8 challenge (Appendix 5).

#### **IV. Influenza A/PR/8/34 instillation**

Influenza A/PR/8/34 (PR8) was generously supplied by the laboratory of Dr. Alan Harmsen (Montana State University, MT). Mice were anesthetized with 4% isoflurane in oxygen, and 50  $\mu$ l of PR8 in pyrogen-free SAL (SAL) was instilled as 25  $\mu$ l per nare at a total dose of 50 plaque forming units (pfu).

#### **V. Steady state blood serum levels of $\Delta^9$ -THC and its metabolites.**

The  $\Delta^9$ -THC utilized in these studies came from a resin that was first weighed and then solubilized in corn oil at different dilutions to give final concentrations of either 25 mg/kg, 50 mg/kg, or 75 mg/kg.  $\Delta^9$ -THC was administered by oral gavage to C57BL/6 mice for five consecutive days. On the fifth day, blood was taken by cardiac puncture 4 h after the final dose of  $\Delta^9$ -THC. Blood was stored in red vacutainers on ice and shipped to the laboratory of Dr. Jim Klaunig for the determination of blood serum levels of  $\Delta^9$ -THC and the primary metabolites, 9-COOH- $\Delta^9$ -THC, and 11-OH- $\Delta^9$ -THC.

#### **VI. Necropsy, lavage collection, and tissue preparation**

On the day sacrifice, mice were anesthetized by an ip injection of 0.1 ml of 12%

pentobarbital solution, a midline laparotomy was performed, and Mice exsanguinated by cutting the abdominal aorta. Immediately after death, the trachea was exposed and cannulated, the heart and lung were excised *en bloc*. One milliliter of sterile SAL was instilled through the tracheal cannula and withdrawn to recover bronchoalveolar lavage fluid (BALF). A second SAL lavage was performed and combined with the first.

After lavage, the lung was processed for histological analysis. The left and right lung lobes were inflated under constant pressure (30 cm H<sub>2</sub>O) with 10% neutral buffered formalin (Sigma Chemical Co., St. Louis, MO) for 1 h. The tracheal airway was ligated and the inflated lobes were stored in a large volume of the same fixative for at least 24 h until further processing.

The intrapulmonary airways of the fixed left or right lung lobes from each rodent were microdissected according to a modified version of the technique of Plopper *et al.*(1983) (110) and fully described in a previous publication (111). Beginning at the lobar bronchus, airways are split down the long axis of the largest daughter branches (i.e., main axial airway; large diameter conducting airway) through the twelfth airway generation. Two transverse tissue blocks were excised at the level of the fifth (proximal) and eleventh (distal) airway generation (Figure 3). Transverse tissue blocks were also excised from the middle of the four right lung lobes perpendicular to the largest airway branch entering each lobe (Figure 3). Tissue blocks from the left and right lung lobes were embedded in paraffin, sectioned at a thickness of 5  $\mu$ m, and then stained with hematoxylin and eosin (H&E) for light microscopic examination. Other paraffin sections were stained with either alcian blue/ periodic acid Schiff (AB/PAS) to detect neutral and acidic mucosubstances or alcian blue (pH 2.5)/Hematoxylin (AB/H) to identify acidic

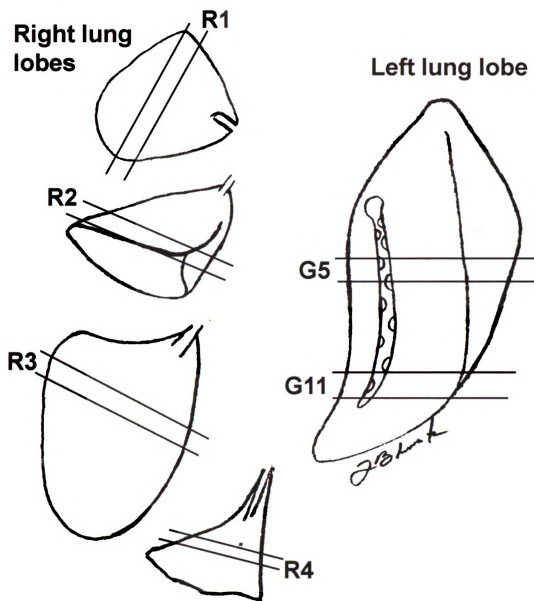


**Figure 3.** Diagram of the microdissection of mouse right lung lobes (R1, R2, R3, R4) and left lung lobes at generations 5 (G5) and 11 (G11).

intraepithelial mucosubstances.

## **VII. Immunocytochemistry.**

Hydrated paraffin sections (5–6  $\mu\text{m}$  thick) from formalin-fixed lung tissues were treated with 0.05% proteinase K for 2 min and washed with 1 N HCl for 1 h. Sections were then treated with 3%  $\text{H}_2\text{O}_2$  (in methanol) to block endogenous peroxide and were incubated with a monoclonal antibody (PC10) cocktail to PCNA (Biogenex, San Ramon, CA) consisting of the primary antibody to PCNA 1:50, a secondary antibody to Immunoglobulin 1:500 and mouse serum 1:50 for 1 h. Immunoreactive PCNA was visualized with the Vectastain Elite ABC kit (Vectastain Laboratories Inc., Burlingame, CA) using 3',3'-diaminobenzidine (DAB) tetrahydrochloride (Sigma Chemical Co., St. Louis, MO) as a chromagen.

## **VIII. Total and PCNA positive epithelial numeric cell density and labeling index.**

The total number of epithelia lining the luminal surface of the main axial airway at generation 5 was enumerated per length of basal lamina. Likewise, cells with nuclei staining positive for PCNA were also enumerated per length of basal lamina. A labeling index for PCNA was determined by dividing the number of PCNA positive cells per unit length of basal lamina by the total number of epithelial cells per unit length of basal lamina.

**IX. CAS-3 and alcian blue numeric cell densities.** Slides of lung sections either stained immunohistochemically for CAS-3 or stained for alcian blue (acidic mucosubstances) were examined. Numeric cell densities were determined for epithelial cells

immunohistochemically reactive to CAS-3 via light microscopy by counting the number of nuclear profiles of these immunoreactive epithelial cells lining the bronchiolar epithelium at generation 5 and dividing by the length of the underlying basal lamina. Numeric cell densities for CAS-3 were expressed as the number of immunoreactive cells per mm basal lamina. In a similar manner, numeric cell densities were determined for epithelial cells staining with alcian blue (acidic mucosubstances). The numeric cell density of epithelial cells staining for alcian blue (acidic mucosubstances) was expressed as the number of alcian blue reactive epithelial cells per mm basal lamina.

#### **X. Morphometry of stored intraepithelial mucosubstances.**

The volume density ( $V_s$ ) of AB/PAS-stained mucosubstances in the respiratory epithelium lining the main axial airway at 3, 7, 10, 15, and 21 dpi was quantified using computerized image analysis and standard morphometric techniques. The area of AB/PAS stained mucosubstance was calculated from the automatically circumscribed perimeter of stained material using a Power Macintosh 7100/66 computer and the public domain NIH Image program (written by Wayne Rasband, U.S. National Institutes of Health and available on the Internet at <http://rsb.info.nih.gov/nih-image/>). The length of the basal lamina underlying the surface epithelium was calculated from the contour length of the digitized image of the basal lamina. The volume of stored mucosubstances per unit of surface area of epithelial basal lamina was estimated using the method described in detail by Harkema *et al.*, (1987) (112). The  $V_s$  of intraepithelial mucosubstances was expressed as nanoliters of intraepithelial mucosubstances per  $\text{mm}^2$  of basal lamina.

## **XI. Bronchoalveolar lavage cellularity.**

The total number of leukocytes in BALF was counted with a hemacytometer. In brief, 10  $\mu$ l of BALF was added to a hemacytometer and the number of leukocytes in the four etched corner quadrants were counted and multiplied by 2500 to yield the number of leukocytes per ml of sample. The percent of total leukocytes consisting of eosinophils, lymphocytes, macrophages, and neutrophils were determined from counts of 200 cells in a cytospin sample stained with Diff-Quick (Dade Behring, Newark, DE). The percentage of eosinophils, lymphocytes, macrophages, and neutrophils were multiplied by the total number of leukocytes determined from the hemacytometer to yield the respective number of each cell type per ml of sample.

## **XII. Histopathology scores for inflammation.**

A histopathologic score was established based upon the numbers and distribution of inflammatory cells within the tissues, as well as non-inflammatory changes such as evidence of bronchiolar epithelial injury and repair. The scores assigned were: 0 = no inflammation, 1 = mild, inflammatory cell infiltrate of the perivascular/peribronchiolar compartment, 2 = moderate, inflammatory cell infiltrate of the perivascular/peribronchiolar space with modest extension into the alveolar parenchyma, and 3 = severe, inflammatory cell infiltrate of the perivascular/peribronchiolar space with a greater magnitude of inflammatory foci found in the alveolar parenchyma. A certified pathologist scored each lung section independently and a mean score with the standard error of the mean was calculated for each treatment group.

### **XIII. Total protein.**

Total protein was quantified in BALF using the bicinchoninic acid (BCA) method as provided by the manufacturer (Pierce, Rockford, IL). In brief, BALF samples were centrifuged at 600 rpm for 5 min to pellet cellular debris. Supernatants were removed and stored at -20°C until testing was performed. 25  $\mu$ l of BALF supernatant or bovine serum albumin protein standard (25-2000  $\mu$ g/ml) was incubated in a 96-well microplate with 200  $\mu$ l of a 50:1 mixture of reagents A (sodium carbonate, sodium bicarbonate, bicinchoninic acid and sodium tartrate in 0.1M sodium hydroxide) and B (4% cupric sulfate) for 30 minutes at 37°C. Samples were read on a Biotek microplate reader at 562 nm.

### **XIV. Neutrophil elastase.**

Airway elastase recovered in BALF was determined by an ELISA for elastase using a rabbit monoclonal antibody to the human elastase (Calbiochem, La Jolla, CA). 50  $\mu$ l aliquots of BALF were applied to a 96-well microtiter plate (Microfluor 2 Black, Dynex Technologies, Chantilly, VA) and dried overnight at 40°C. Plates were blocked with a solution of 1.5% goat serum in automation buffer solution (ABS, pH 7.5; Biomedica Corp., Foster City, CA) for 30 min at 37°C. Plates were then incubated with anti-elastase antibody (1:400 in ABS containing 1.5% goat serum) for 1 h at 37°C and then washed three times with ABS. Bound primary antibody was detected with a biotinylated goat anti-rabbit secondary antibody and quantitated using horseradish-peroxidase-conjugated avidin/biotin complex (ABC Reagent; Vector Laboratories, Burlingame, CA) and a fluorescent substrate (QuantaBlue; Pierce Chemical, Rockford, IL) using a fluorescence

microplate reader (SpectraMax Gemini; Molecular Devices; 318 nm excitation/410 nm emission). Readings were taken at 3 min intervals for 24 min. Duplicate samples were averaged and the group data is represented as mean Vmax units/s.

**XV. Inflammatory and T<sub>H</sub>1/T<sub>H</sub>2 cytokines.** BALF samples were centrifuged at 600 rpm for 5 min to pellet cellular debris. Supernatants were removed and stored at -20°C until testing was performed. The cytokines IL-6, IL-10, MCP-1, IFN- $\gamma$ , TNF- $\alpha$ , and IL-12p70 were detected simultaneously by using the cytometric bead array (CBA) mouse inflammation kit (BD Pharmingen, San Diego, CA) and the T<sub>H</sub>1/T<sub>H</sub>2 cytokines IL-2, IL-4, IL-5, IFN- $\gamma$ , and TNF- $\alpha$  were detected simultaneously by using the mouse T<sub>H</sub>1/T<sub>H</sub>2 kit. In brief, 50  $\mu$ l of BALF or serum from each sample was incubated individually with a mixture of capture beads and 50  $\mu$ l of PE detection reagent consisting of PE-conjugated anti-mouse IL-6, IL-10, MCP-1, IFN- $\gamma$ , TNF- $\alpha$ , and IL-12p70 or 50  $\mu$ l of PE detection reagent consisting of PE-conjugated anti-mouse IL-2, IL-4, IL-5, IFN- $\gamma$ , and TNF- $\alpha$ . The samples were incubated at room temperature for 2 h in the dark. After incubation, samples were washed once and resuspended in 300  $\mu$ l of wash buffer before acquisition on a BD FACSCalibur flow cytometer. Data were analyzed using CBA software (BD Pharmingen, San Diego, CA). Standard curves were generated for each cytokine using the mixed cytokine standard provided with the respective kits. The concentration of each cytokine was determined by interpolation from the corresponding standard curve. The range of detection was 20 – 5000 pg/ml for each cytokine measured. Serum was analyzed for inflammatory cytokines only.

In a similar manner, the cytokines IL-9 and IL-13 were analyzed using BD flex-

sets. Samples and standards were analyzed according to manufacturer-based instructions.

**XVI. T-lymphocyte flow cytometry.** After enumerating the retrieved cells in BALF, the cells were pelleted by centrifugation and reconstituted in 150  $\mu$ l flow cytometer (FCM) buffer (PBS supplemented with 2% (w/v) bovine serum albumin and 0.09% (w/v) sodium azide) with purified anti-mouse CD16/CD32 (Fc $\gamma$  III/II Receptor) antibody (BD Biosciences, San Jose, CA) to block for 30 min. The samples were then split into two groups of equal volume, washed and reconstituted in FCM buffer. One group received antibodies for CD3 (APC anti-mouse CD3 $\epsilon$ ), CD4 [PE anti-mouse CD4(L3T4)] and CD8 [FITC anti-mouse CD8a(Ly-2)], while the other group received the cognate isotype control antibodies. Samples were allowed to incubate 1 h at 4°C, washed twice and then fixed for 10 min. with Cytotfix. Samples were then washed again and reconstituted to a volume of 300  $\mu$ l for analysis on the BD FACSCalibur flow cytometer. The total number of events taken per each sample was 10,000.

**XVII. RNA isolation.**

Total RNA was isolated from the lung lobes by using the TRI-reagent method (Sigma Chemical, St Louis, MO). The evaluation of the relative expression levels of H1, Caspase-3 and MUC5AC messenger ribonucleic acid (mRNA) were determined using the TaqMan real-time multiplex reverse transcriptase-polymerase chain reaction (RT-PCR) with custom designed TaqMan primers and probe to the target gene and the manufacturer's pre-developed primers and probe to 18S (Applied Biosystems, Foster

City, CA). The primers and probe to both the target gene and endogenous reference gene were specifically designed to exclude detection of genomic deoxyribonucleic acid (DNA). Aliquots of isolated tissue RNA (1 µg total RNA) were converted to copy DNA (cDNA) using random primers. The resultant cDNA (2 µl) was added to a reaction mixture that consisted of the target gene primers and probe, endogenous reference primers and probe (18S ribosomal RNA), and Taqman universal master mix to a final volume of 30 µl. Following PCR, amplification plots (change in dye fluorescence versus cycle number) were examined and a dye fluorescence threshold within the exponential phase of the reaction was set separately for the target gene and the endogenous reference (18S). The cycle number at which each amplified product crosses the set threshold represents the  $C_T$  value. The amount of target gene normalized to its endogenous reference was calculated by subtracting the endogenous reference  $C_T$  from the target gene  $C_T$  ( $\Delta C_T$ ). Relative mRNA expression was calculated by subtracting the mean  $\Delta C_T$  of the control samples from the  $\Delta C_T$  of the treated samples ( $\Delta \Delta C_T$ ). The amount of target mRNA, normalized to the endogenous reference and relative to the calibrator (i.e., RNA from control) is calculated by using the formula  $2^{-\Delta \Delta C_T}$ .

### **XVIII. Statistical Analysis.**

Data are expressed as mean  $\pm$  standard error of the mean (SEM). The differences between treatment groups were determined by either a Student's t-test, one-way or two-way analysis of variance (ANOVA) with multiple comparisons made by the Student-Newman-Keuls *post hoc* test using SigmaStat software from Jandel Scientific (San Rafael, CA). The criterion for significance was taken to be  $p < 0.05$ .

## EXPERIMENTAL RESULTS

### I. Model development: Establishing the dose.

#### A) Concentration-dependent inflammatory responses to PR8 in pulmonary airways

The inflammatory response to PR8 was confined to the hilar region of the transverse left lung lobe sections (Figure 4). The inflammatory response was most notable at generation 5 with occasional evidence of inflammation observed at generation 11. The magnitude and severity of the inflammatory response was concentration-dependent, increasing with increasing concentrations of PR8. The inflammatory response consisted primarily of mononuclear cells that included lymphocytes, monocytes/macrophages, and neutrophils.

#### B) Steady state blood serum levels of $\Delta^9$ -THC and its metabolites.

The steady state blood serum levels for  $\Delta^9$ -THC and its primary metabolites, 9-COOH- $\Delta^9$ -THC, and 11-OH- $\Delta^9$ -THC were determined on the fifth day of treatment, 4 h after the final dose of  $\Delta^9$ -THC (Table 1). At a dose of 5 mg/kg  $\Delta^9$ -THC, blood serum levels reached a mean concentration of 84.6 ng/ml  $\Delta^9$ -THC. In addition, there was evidence of modest levels of the 9-COOH- $\Delta^9$ -THC metabolite present in blood serum with no detectable levels of the 11-OH- $\Delta^9$ -THC metabolite. At a dose of 75 mg/kg  $\Delta^9$ -THC, the mean blood serum levels for the parent compound were similar to those observed with the 5 mg/kg  $\Delta^9$ -THC dose. However, levels of the 9-COOH- $\Delta^9$ -THC metabolite in blood serum were augmented when compared to the blood serum levels for mice receiving 5 mg/kg  $\Delta^9$ -THC with concentrations reaching 446 ng/ml 9-COOH- $\Delta^9$ -

**Figure 4. Increasing concentrations of influenza virus result in increasing inflammatory responses in the hilar region of the left lung lobe at generation 5 of the main axial airway.** Light photomicrographs of the respiratory epithelium lining the luminal surface of the main axial airway (MAA) (generation 5) from mice intranasally instilled with PR8 at concentrations of 50 pfu (A), 300 pfu (B), and 500 pfu (C) at 13 days post infection. There was marked inflammatory cell infiltration of the perivascular/peribronchiolar submucosa (sm) extending into the alveolar parenchyma (p) in all of the sections representing each concentration of virus. There was a concentration-dependent increase in the magnitude and severity of the inflammatory response observed. Artery = (a). bar = 100 microns. Images in this dissertation are presented in color.

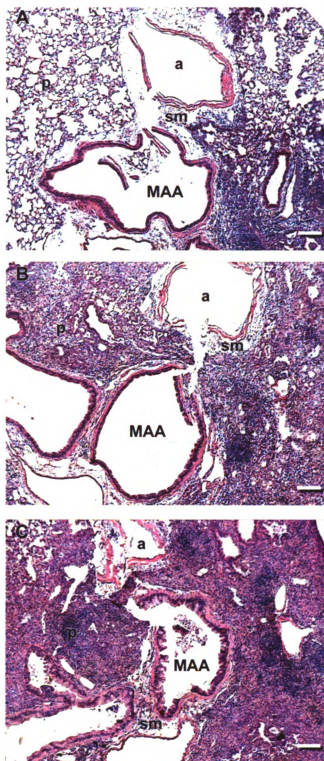


**Figure 4. Increasing concentrations of influenza virus result in increasing inflammatory responses in the hilar region of the left lung lobe at generation 5 of the main axial airway.**

Sample # Vehicle	$\Delta^9$ -THC (ng/ml)	9-COOH- $\Delta^9$ - THC (ng/ml)	11-OH- $\Delta^9$ -THC (ng/ml)
1	3.6	ND	ND
2	2.5	ND	ND
3	3.1	ND	ND
4	4.2	ND	ND
mean	3.4		

Sample # 5mg/kg THC	$\Delta^9$ -THC (ng/ml)	9-COOH- $\Delta^9$ - THC (ng/ml)	11-OH- $\Delta^9$ -THC (ng/ml)
1	55.2	6.8	ND
2	48.4	24.6	ND
3	133.5	30.0	ND
4	101.4	41.0	ND
mean	84.6	25.6	

Sample # 75mg/kg THC	$\Delta^9$ -THC (ng/ml)	9-COOH- $\Delta^9$ - THC (ng/ml)	11-OH- $\Delta^9$ -THC (ng/ml)
1	29.9	136.8	2.7
2	64.5	873.3	19.3
3	117.9	317.0	10.1
4	52.4	459.0	9.9
mean	66.2	446.5	10.5

**Table 1. Analysis of  $\Delta^9$ -THC, 9-COOH- $\Delta^9$ -THC, and 11-OH- $\Delta^9$ -THC concentrations in mouse blood serum.** C57BL/6 mice were treated with vehicle (corn oil), 5 mg/kg or 75 mg/kg  $\Delta^9$ -THC for 5 consecutive days. Four hours after the last treatment, mice were anesthetized and whole blood was collected by cardiac puncture.  $\Delta^9$ -THC and its metabolites were chemically extracted from whole blood and analyzed by GC/MS. ND = not detected.

THC. Lastly, the 11-OH- $\Delta^9$ -THC metabolite was modestly elevated with the 75 mg/kg  $\Delta^9$ -THC treatment group with concentrations averaging 10 ng/ml.

## **II. Time-dependent airway epithelial and inflammatory cell responses induced by influenza virus A/PR/8/34 in C57BL/6 mice.**

### **A) PR8 induces time-dependent alterations in epithelial morphology**

No microscopic alterations were present in the examined proximal (at G5 of the main axial airway) and distal (at G11 of the main axial airway) tissue sections from the left lung lobe of mice that were intranasally instilled with vehicle alone (controls) (Figure 5A). The principal pulmonary alteration in mice intranasally instilled with influenza virus and sacrificed 3 dpi (Figure 5 A-D) was an acute necrotizing bronchiolitis characterized by multiple focal areas of necrosis and luminal shedding (exfoliation) of the surface epithelial cells lining the main axial airway (Figure 5C) and smaller diameter pre-terminal and occasional terminal bronchioles. Similar but much less severe lesions were observed in the distal tissue section of some of these exposed mice. Airway epithelial lesions were accompanied by a mild intramural inflammatory cell infiltrate composed principally of mononuclear cells (lymphocytes and monocytes) and lesser numbers of neutrophils. A similar inflammatory cell infiltrate was present in adjacent peribronchiolar and perivascular regions.

Virus instilled mice that were sacrificed 7 dpi had a marked bronchiolitis and alveolitis again restricted mainly to the hilar region of the lung lobe (proximal tissue section). Necrosis and exfoliation of the bronchiolar ciliated epithelium observed at 3 dpi was replaced by a hyperplastic/hypertrophic, nonciliated, cuboidal and basophilic

**Figure 5. Bronchiolar epithelial morphometry following influenza infection.** Light photomicrograph of the respiratory epithelium (e) lining the luminal surface of the main axial airway (generation 5) from mice intranasally instilled with SAL (A, B, E, F, I, J) and PR8 (C, D, G, H, K, L) at 3, 10, and 21 dpi, respectively. A = H&E; SAL instilled mouse 3 dpi with no alterations to the respiratory epithelium lining the airway or to the peribronchiolar tissue (a). B = AB/PAS; SAL instilled mouse 3 dpi with no microscopic evidence of MCM. C = H&E; PR8 instilled mouse 3 dpi with degenerative respiratory epithelium lining the airway and peribronchiolar inflammatory cell infiltrate in the submucosa (sm). D = AB/PAS; PR8 instilled mouse 3 dpi with exfoliation of the epithelium lining the luminal surface of the main axial airway and no microscopic evidence of MCM. E = H&E; SAL instilled mouse 10 dpi with no alterations to the respiratory epithelium lining the airway or to the peribronchiolar tissue. F = AB/PAS; SAL instilled mouse 10 dpi with no microscopic evidence of MCM. G = H&E; PR8 instilled mouse 10 dpi with regenerative epithelium and mucous cell metaplasia (arrows) with marked peribronchiolar inflammatory cell infiltrate (asterisk). H = AB/PAS; PR8 instilled mouse 10 dpi with marked accumulation of mucous-containing epithelial cells. I = H&E; SAL instilled mouse 21 dpi with no alterations to the respiratory epithelium lining the airway or to the peribronchiolar tissue. J = AB/PAS; SAL instilled mouse 21 dpi with no microscopic evidence of MCM. K = H&E; PR8 instilled mouse 21 dpi with cuboidal epithelium and mucous cell metaplasia with decreased peribronchiolar inflammation. L = AB/PAS; PR8 instilled mouse 21 dpi with marked accumulation of mucous-containing epithelial cells lining the airway. Bar = 50 microns. Images in this dissertation are presented in color.

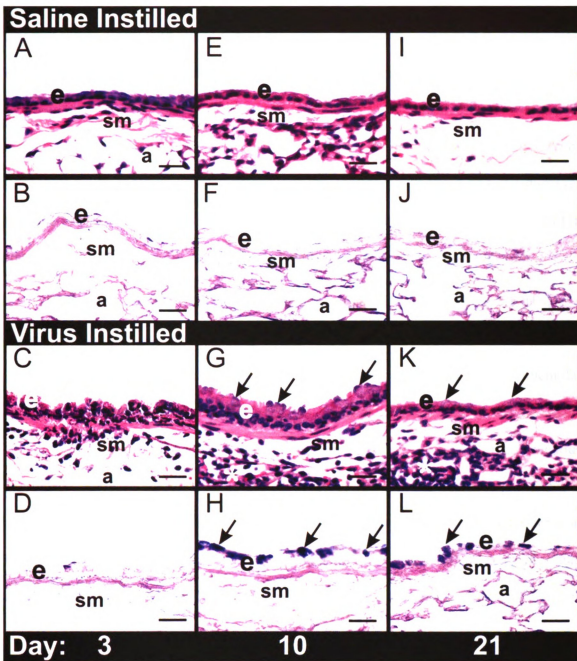


Figure 5. Bronchiolar epithelial morphometry following influenza infection.

epithelium accompanied by a marked lymphocytic inflammatory cell infiltrate in the affected bronchioles and surrounding alveolar parenchyma (interstitial pneumonia). Lesser, but conspicuous, numbers of eosinophils were also intermixed with the mononuclear inflammatory cells. There was also mild to moderate alveolar type II cell hyperplasia and hypertrophy in these affected parenchymal regions along with numerous large highly vacuolated alveolar macrophages, smaller monocytes, and lymphocytes within alveolar air spaces. Various amounts of proteinacious material were also present in some of the alveolar lumens in the affected regions of the pulmonary parenchyma.

Mice that were instilled with virus and sacrificed at 10 dpi (Figure 5 E-H) had a chronic bronchiolitis and alveolitis, again restricted mainly to the proximal tissue section (hilar aspect of the lung lobe). At 10 days post-infection, the affected bronchiolar epithelium was composed of tall cuboidal to columnar ciliated and nonciliated cells (Figure 5G). Many of the nonciliated epithelial cells were mucous cells with conspicuous amounts of AB/PAS stained (Figure 5H), intracytoplasmic mucosubstances (i.e. Mucous cell metaplasia). The associated inflammatory cell infiltrate in and around the bronchiolar walls, adjacent blood vessels and alveolar parenchyma was similar in composition to that observed in mice sacrificed at 7 dpi. However, the most conspicuous change in the affected regions of the alveolar parenchyma at 10 dpi compared to that at 7 dpi was the addition of coalescing regions of alveolar fibrosis accompanying the type II cell hyperplasia and the mainly lymphocytic inflammatory cell infiltrate (chronic alveolitis).

Mice instilled with virus and sacrificed at 15 and 21 dpi (Figure 5 I-L) had similar but less severe airway and parenchymal lesions as compared to those lungs of the mice sacrificed at 10 dpi.

## **B) Temporal analysis of stored intraepithelial mucosubstances following PR8 challenge**

The Vs of intracytoplasmic acidic and neutral mucosubstances (Figure 6) in the airway epithelium was increased by approximately 4-fold in lung lobe sections obtained from PR8 treated mice as compared to respective time-matched SAL controls starting as early as 10 dpi. The marked elevation in mucosubstance Vs was maintained through 21 dpi.

## **C) Expression levels of whole lung MUC5AC mRNA at 7 days post infection**

Recognizing that the time to onset of MCM was established at 10 dpi, RNA from whole lung homogenates at 7 dpi was analyzed for MUC5AC mRNA levels (Figure 7). MUC5AC levels were nearly 3-fold greater in lung homogenates from mice treated with PR8 than those treated with SAL.

## **D) Time-dependent differences in total and PCNA immunopositive epithelial numeric cell densities**

By numeric cell density counts, the total airway epithelial cell counts (Figure 8A) observed at 10 dpi were mildly elevated with respect to counts enumerated in SAL controls. In addition to total cell counts, cells with nuclei staining positive for PCNA (Figure 8B) were also enumerated. PCNA numeric cell density and labeling index (Figure 8C) were significantly elevated as compared to time-matched SAL controls by four to six-fold in the PR8 treated group at 7 and 10 dpi, respectively.

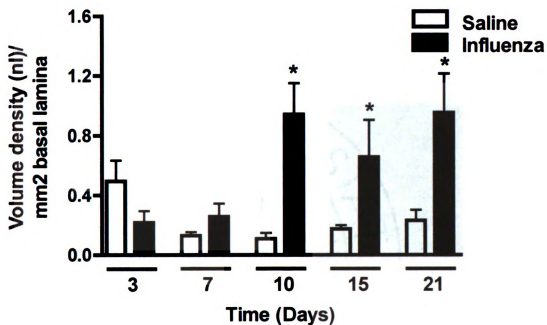


**Figure 6. Time-to-onset of mucous cell metaplasia following influenza infection.** Effects of influenza instillation on the volume density of intraepithelial mucosubstances in the epithelium lining the main axial pulmonary airways at generation 5 of the left lung lobe. Mice were instilled with PR8 or SAL and sacrificed 3, 7, 10, 15, and 21 dpi and tissues collected and processed as described in Materials and Methods. Data is expressed as mean  $\pm$  SEM. \* = significantly different from respective control instilled with SAL.

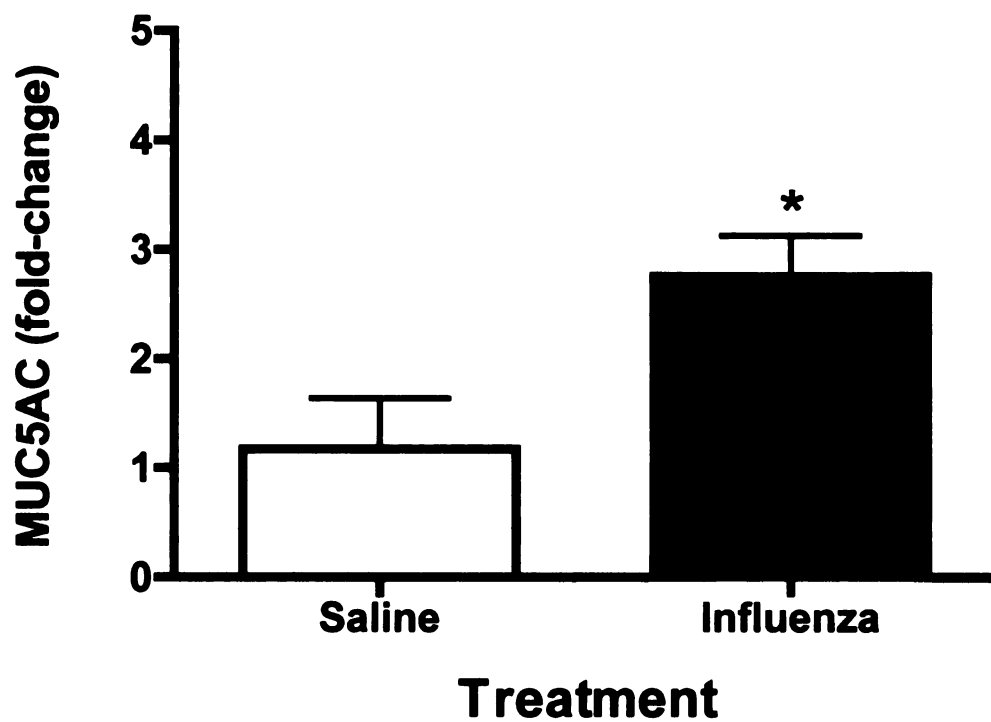


**Figure 7. MUC5AC gene induction by influenza at 7 days post infection.** Effects of influenza instillation on the levels of MUC5AC expression at 7 dpi in the lungs of mice treated with either SAL or PR8. Data is expressed as mean  $\pm$  SEM. \* = significantly different from respective control instilled with SAL.

**Figure 8. Time-dependent proliferation of epithelial cells lining the main axial airway following influenza infection.** Effects of influenza instillation on the numeric cell density of total epithelial cells (A), PCNA positive cells (B), and the labeling index for PCNA (C) in the epithelium lining the main axial pulmonary airways at generation 5 of the left lung lobe. Mice were instilled with PR8 or SAL and sacrificed 3, 7, 10, 15, and 21 dpi and tissues collected and processed as described in Materials and Methods. Data is expressed as mean  $\pm$  SEM. \* = significantly different from respective control instilled with SAL.

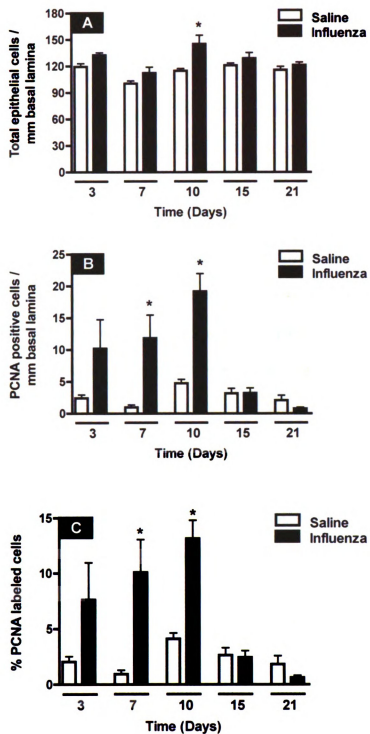


**Figure 8. Time-dependent proliferation of epithelial cells lining the main axial airway following influenza infection.**

## **E) Bronchoalveolar lavage fluid analysis**

### **1. Protein**

BALF-associated protein levels were significantly increased in samples collected from mice infected with PR8 as compared with SAL instilled mice (Figure 9). Increased protein levels were observed between 7 and 21 dpi with an apparent apex at 10 dpi.

### **2. Total and differential inflammatory cell counts**

To further characterize the inflammatory cell milieu that was present in the airways during these epithelial changes, differential cell counts were performed. There was a significant rise in the total BALF-associated leukocytes (Figure 10A) in PR8 infected mice when compared to the respective SAL controls occurring as early as 3 dpi and lasting through 15 dpi with an apparent apex at 10 dpi. The early innate immune response was marked by significant increases in neutrophils (Figure 10B) by 3 dpi that tapered by 10 dpi. Macrophages and other monocytic cells (Figure 10C) were significantly elevated between 7 and 15 dpi. The adaptive immune response was characterized by marked increases in lymphocytes (Figure 10D) between 7 and 21 dpi with peak numbers observed at 10 dpi. Eosinophils (Figure 10E) were also abundant between 7 and 15 dpi.

### **3. Inflammatory chemokines and cytokines**

With ongoing inflammation there are a host of chemokines and cytokines released by activated leukocytes. To characterize the pro-inflammatory chemical mediators retrieved in BALF, a mouse-specific cytometric bead array analysis of the inflammatory

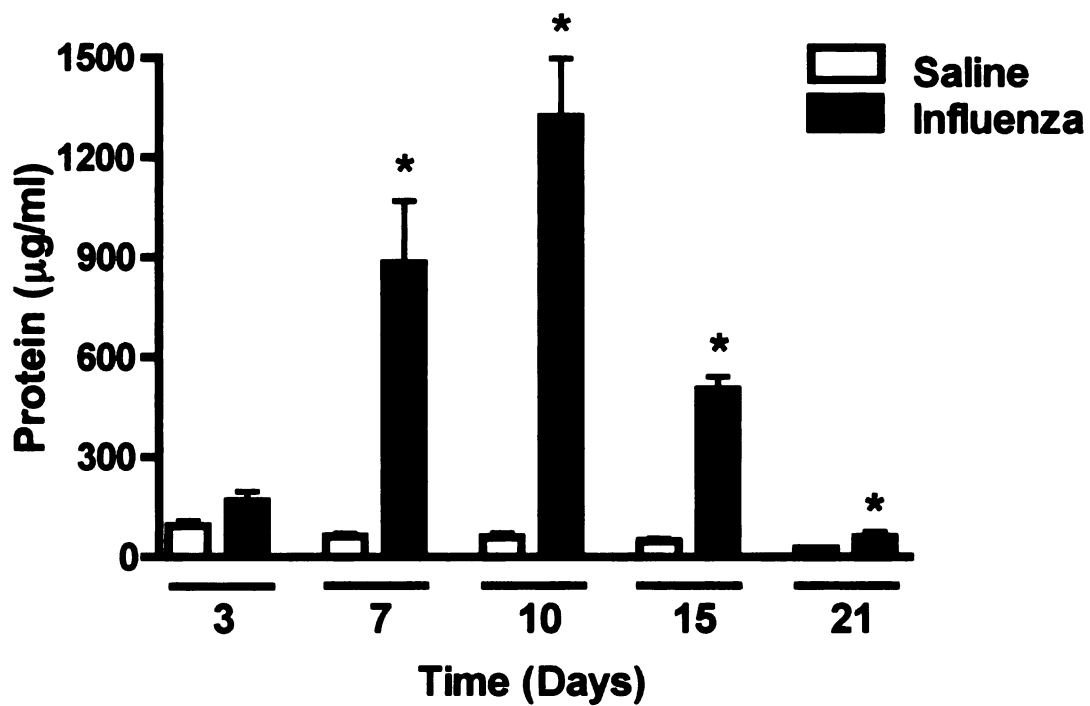


**Figure 9. Time-dependent detection of total protein in bronchoalveolar lavage fluid following influenza infection.** Effects of influenza instillation on total protein detected in BALF supernatants. Mice were instilled with PR8 or SAL and sacrificed 3, 7, 10, 15, and 21 dpi and concentrations of total protein in BALF were determined as described in Materials and Methods. Data is expressed as mean  $\pm$  SEM. \* = significantly different from respective control instilled with SAL.

**Figure 10. Time-dependent recruitment of leukocytes to the pulmonary airways following influenza infection.** Effects of influenza instillation on total cells (A), neutrophil (B), macrophage (C), lymphocyte (D) and eosinophil (E) retrieved in bronchoalveolar lavage fluid (BALF). Mice were instilled with PR8 or SAL and sacrificed 3, 7, 10, 15, and 21 dpi and inflammatory cells were enumerated in BALF as described in Materials and Methods. Data is expressed as mean  $\pm$  SEM. \* = significantly different from respective control instilled with SAL.

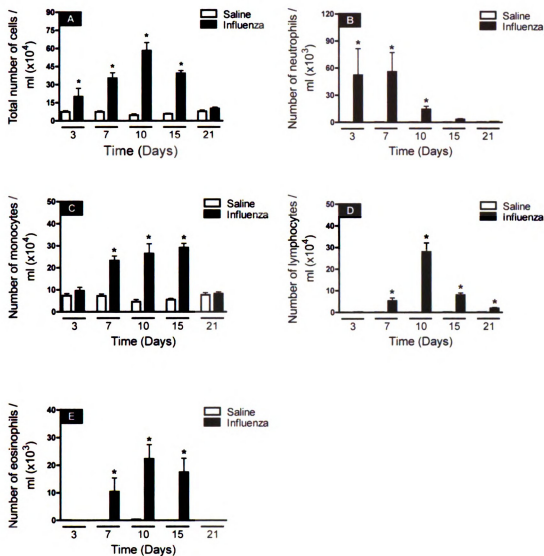


**Figure 10. Time-dependent recruitment of leukocytes to the pulmonary airways following influenza infection.**

cytokines TNF- $\alpha$ , IFN- $\gamma$ , IL-6, MCP-1, IL-10, and IL-12p70 was employed. The BALF-associated concentrations of TNF- $\alpha$  (Figure 11A), IFN- $\gamma$  (Figure 11B), IL-6 (Figure 11C), and MCP-1 (Figure 11D), were significantly elevated in influenza infected mice when compared to SAL controls at 7 dpi. In addition, concentrations of IL-10 (Figure 11E) were significantly decreased in PR8 infected mice as compared to SAL controls at 21 dpi. Levels of TNF- $\alpha$  and IL-6 remained significantly elevated through 10 dpi with similar trends observed with MCP-1. There were no changes in the BALF-associated concentrations reported for IL-12p70 (Figure 11F) with either PR8 or SAL instillation.

#### **4. T<sub>H</sub>2 cytokines IL-4, IL-5, IL-9 and IL-13**

The T<sub>H</sub>2 cytokines IL-4 (Figure 12A), IL-5 (Figure 12B), IL-9 (Figure 12C) and IL-13 (Figure 12D) have been implicated in the development of MCM. By employing cytometric bead array kits and flex sets for these cytokines, we observed marked increases in the levels of IL-5 detected at 7 dpi in the BALF of PR8-infected mice as compared to SAL instilled mice. Furthermore, there were significant, albeit mild increases in the BALF levels of IL-4 and IL-9 detected at 7 dpi in PR8-infected mice as compared to SAL instilled mice. The concentration of IL-13 in BALF was low in all treatment groups with no detectable differences observed between PR8 and SAL instilled mice.

#### **5. Elastase**

In addition to factors derived from lymphocytes, neutrophil-derived elastase has also been implicated as a factor known to induce MCM. In the current study, neutrophil-

**Figure 11. Secretion of chemokines and cytokines into the airways in response to influenza infection.** Effects of influenza instillation on TNF- $\alpha$  (A), IFN- $\gamma$  (B), IL-6 (C), MCP-1 (D), IL-10 (E), and IL-12p70 (F) retrieved in bronchoalveolar lavage fluid (BALF). Mice were instilled with PR8 or SAL and sacrificed 3, 7, 10, 15, and 21 dpi and inflammatory chemokines and cytokines were enumerated in BALF by flow cytometry as described in Materials and Methods. Data is expressed as mean  $\pm$  SEM. \* = significantly different from respective control instilled with SAL.

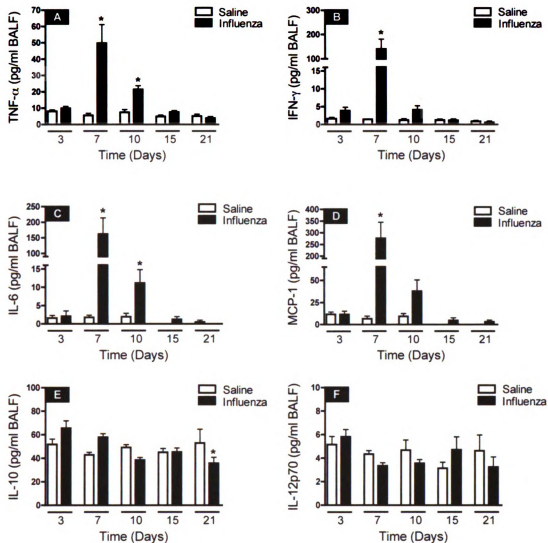


**Figure 11. Secretion of chemokines and cytokines into the airways in response to influenza infection.**

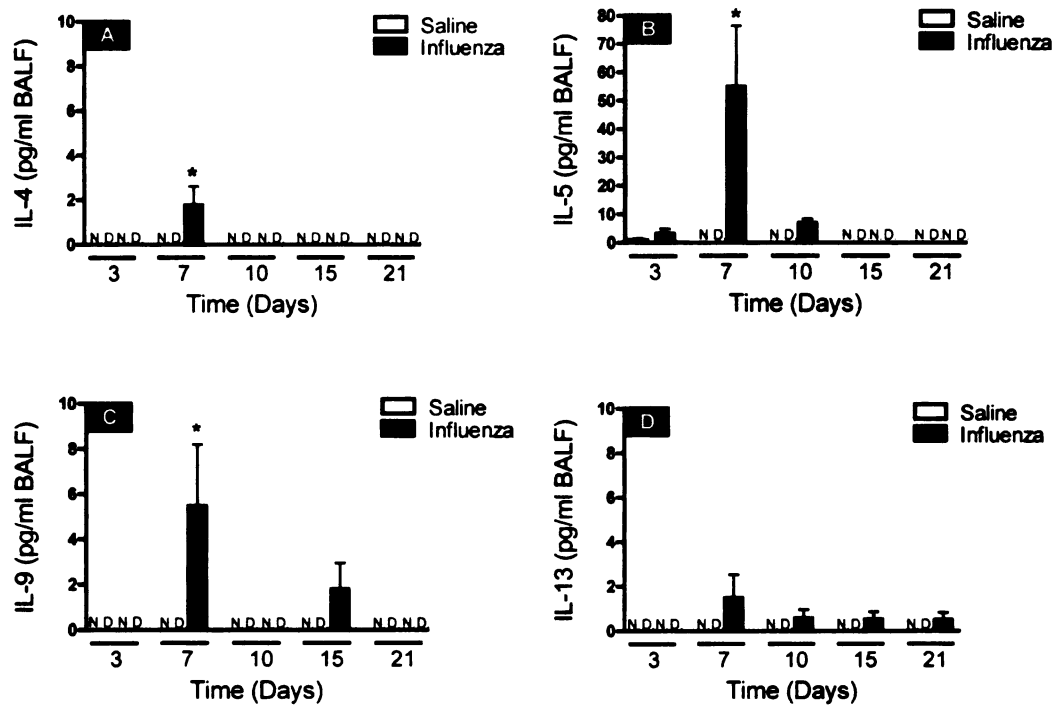


**Figure 12. Detection of  $T_H2$  cytokines secreted into the airways in response to influenza infection.** Effects of influenza instillation on the  $T_H2$  cytokines IL-4 (A), IL-5 (B), IL-9 (C), and IL-13 (D) retrieved in bronchoalveolar lavage fluid (BALF). Mice were instilled with PR8 or SAL and sacrificed 3, 7, 10, 15, and 21 dpi and  $T_H2$  cytokines were enumerated in BALF by flow cytometry as described in Materials and Methods. Data is expressed as mean  $\pm$  SEM. \* = significantly different from respective control instilled with SAL. N.D. = not detected.

derived elastase (Figure 13) was significantly elevated between 7 and 15 dpi in PR8 infected mice as compared to SAL control mice.

### **III. Modulation of airway responses to influenza A/PR/8/34 by delta-9-tetrahydrocannabinol in C57BL/6 mice**

#### **A) $\Delta^9$ -THC increases whole lung H1 mRNA following PR8 challenge**

H1 mRNA levels in the lungs of mice challenged with PR8 in the absence of  $\Delta^9$ -THC treatment were significantly elevated at 7 dpi when compared to SAL control mice (Figure 14). Levels of H1 mRNA detected in the lungs of mice challenged with PR8 and treated with  $\Delta^9$ -THC at a dose of 25 mg/kg were also mildly attenuated when compared to mice challenged with PR8 alone. The levels of H1 mRNA increased with increasing doses of  $\Delta^9$ -THC and were significantly elevated in mice administered 75 mg/kg  $\Delta^9$ -THC when compared to PR8 challenged mice in the absence of  $\Delta^9$ -THC treatment.

#### **B) $\Delta^9$ -THC does not affect total protein levels in BALF**

As a measure of alveolar/capillary membrane integrity, total protein in BALF was assayed. There were marked increases in BALF-associated total protein observed in mice challenged with PR8 at 7 dpi when compared to SAL control mice. However, there were no differences observed in total BALF-associated protein recovered in PR8 challenged mice treated with any dose of  $\Delta^9$ -THC (Figure 15).

#### **C) $\Delta^9$ -THC decreases leukocyte populations retrieved in BALF.**

Consistent with an immune response to viral challenge, the total number of

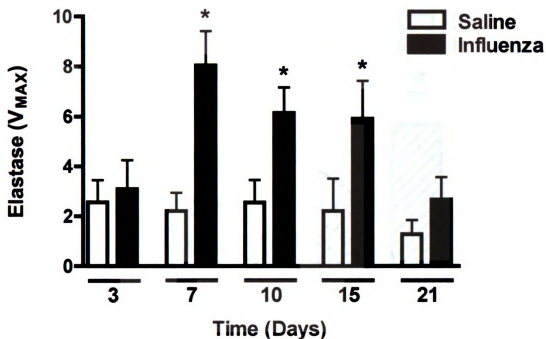


**Figure 13. Secretion of neutrophil-derived elastase into the airways in response to influenza infection.** Effects of influenza instillation on neutrophil elastase detected in BALF supernatants. Mice were instilled with PR8 or SAL and sacrificed 3, 7, 10, 15, and 21 dpi and neutrophil elastase in BALF were determined as described in Materials and Methods. Data is expressed as mean  $\pm$  SEM. \* = significantly different from respective control instilled with SAL.

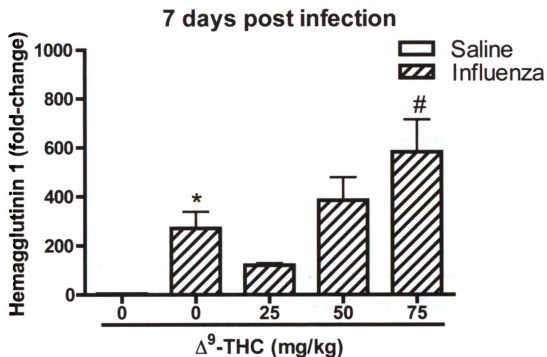


**Figure 14.**  $\Delta^9$ -THC treatment enhances hemagglutinin 1 mRNA levels. Effects of  $\Delta^9$ -THC on Hemagglutinin 1 mRNA levels from influenza challenge in whole lung homogenates at 7 dpi in mice treated with SAL or  $\Delta^9$ -THC (0, 25, 50, or 75 mg/kg) with PR8. Data is expressed as mean  $\pm$  SEM; \* = significantly different from respective control instilled with SAL. # = significantly different from corn oil with PR8 challenge.

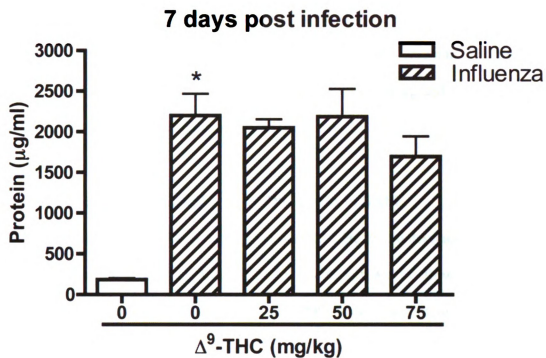


**Figure 15.**  $\Delta^9$ -THC does not alter total protein levels in BALF. Effects of  $\Delta^9$ -THC on total protein detected in BALF supernatants from mice challenged with influenza. Total protein in BALF was determined for mice treated with SAL or  $\Delta^9$ -THC (0, 25, 50, or 75 mg/kg) with PR8 and sacrificed at 7 dpi. Data is expressed as mean  $\pm$  SEM; \* = significantly different from respective control instilled with SAL.

leukocytes retrieved in BALF was significantly elevated in PR8 infected mice at 7 dpi (Table 2). There was a trend toward dose-dependent effects of  $\Delta^9$ -THC treatment on the total number of BALF-associated leukocytes. Treatment of mice with  $\Delta^9$ -THC at all dose levels led to significant reductions in the number of BALF-associated lymphocytes. Additionally, treatment of mice with  $\Delta^9$ -THC at doses of 25 mg/kg and 50 mg/kg led to a reduction in the number of macrophages retrieved in BALF.

**D)  $\Delta^9$ -THC decreases CD4<sup>+</sup> and CD8<sup>+</sup> T cells in BALF.**

Since treatment of PR8 infected mice with  $\Delta^9$ -THC led to decreases in the number of lymphocytes, we evaluated differences in T cell subsets by flow cytometry. The absolute values of BALF-associated CD4<sup>+</sup> and CD8<sup>+</sup> T cells were determined (Table 3). Treatment of PR8 infected mice with  $\Delta^9$ -THC led to significant decreases in the number of CD8<sup>+</sup> T cells at all dose levels with respect to mice challenged with PR8 alone. A similar effect on the number of CD4<sup>+</sup> T cells was observed in PR infected mice administered 50 and 75 mg/kg  $\Delta^9$ -THC as compared to mice challenged with PR8 in the absence of  $\Delta^9$ -THC treatment.

**E)  $\Delta^9$ -THC modestly affects chemokines and cytokines retrieved in BALF.**

Inflammatory chemokines and cytokines secreted into the airways were measured as an indicator of immune cell function in response to PR8 challenge. Mice challenged with PR8 alone exhibited increased BALF concentrations of TNF- $\alpha$ , IFN- $\gamma$ , IL-6, MCP-1, and IL-10 at 7 dpi as compared to the SAL control (Table 4). In PR8 infected mice treated with  $\Delta^9$ -THC, an increase in MCP-1 at a dose of 50 mg/kg  $\Delta^9$ -THC was observed,

Cell type	CO		$\Delta^9$ -THC 25mg/kg	$\Delta^9$ -THC 50mg/kg	$\Delta^9$ -THC 75mg/kg
	SAL	PR8	PR8	PR8	PR8
Total (x10 <sup>4</sup> )	3.1±1.0 (4)	68.2±12.7 * <i>p</i> = 0.020	34.3±9.1 <i>p</i> = 0.170 (4)	31.9±6.7 <i>p</i> = 0.058	59.2±12.5 <i>p</i> = 0.501
Macrophages (x10 <sup>4</sup> )	2.9±0.9 (4)	18.8±3.6 * <i>p</i> = 0.006	6.0±1.3 # <i>p</i> = 0.006 (4)	6.6±1.0 # <i>p</i> = 0.005	13.3±3.4 <i>p</i> = 0.118
Neutrophils (x10 <sup>2</sup> )	2.9±2.0 (4)	1552.5±386.9 * <i>p</i> = 0.010	951.6±324.3 <i>p</i> = 0.391 (4)	1586.3±412.5 <i>p</i> = 0.961	2757.0±829.5 <i>p</i> = 0.210
Lymphocytes (x10 <sup>3</sup> )	1.1±0.2 (4)	334.0±63.4 * <i>p</i> = 0.002	178.8±50.8 # <i>p</i> = 0.019 (4)	90.9±20.7 # <i>p</i> = 0.004	178.2±41.2 # <i>p</i> = 0.047
Eosinophils (x10 <sup>2</sup> )	0 (4)	46.4±16.3 * <i>p</i> = 0.041	43.1±3.0 <i>p</i> = 0.436 (4)	33.9±21.3 <i>p</i> = 0.298	48.6±7.86 <i>p</i> = 0.654

**Table 2. Total and differential cell counts from BALF.** The effects of  $\Delta^9$ -THC on the recruitment of inflammatory cells to the pulmonary airways of mice challenged with influenza. Mice were treated with  $\Delta^9$ -THC (25, 50, or 75 mg/kg) or its corn oil vehicle for 5 consecutive days surrounding the intranasal instillation of influenza virus A/PR/8 or its vehicle SAL. Mice were euthanized on day 7 post infection. BALF was collected by flushing the lungs with 2 ml of sterile SAL. Total leukocyte counts were enumerated by hemacytometer. Differential cell counts were assessed by counting 200 cells from cytopins of the BALF stained with Diff-quick. Data is expressed as mean ± SEM; *n* = 5 except where noted by (*n*); \* = significantly different from respective control instilled with SAL. # = significantly different from corn oil with PR8 challenge.

T-cell type	CO		$\Delta^9$ -THC 25mg/kg	$\Delta^9$ -THC 50mg/kg	$\Delta^9$ -THC 75mg/kg
	SAL	PR8	PR8	PR8	PR8
CD4 <sup>+</sup> (x10 <sup>4</sup> )	154.6±25.4 (4)	883.7±96.8 * <i>p</i> < 0.001	838.2±77.4 <i>p</i> = 0.626	304.4±15.5 # <i>p</i> < 0.001	475.4±64.0 # <i>p</i> < 0.001
CD8 <sup>+</sup> (x10 <sup>4</sup> )	566.7±26.5 (4)	4360.5±133.4 * <i>p</i> < 0.001	3261.9±76.2 # <i>p</i> < 0.001	2483.4±52.1 # <i>p</i> < 0.001	2460.3±74.0 # <i>p</i> < 0.001

**Table 3. CD4<sup>+</sup> and CD8<sup>+</sup> T cell populations observed in BALF by flow cytometry.** The effects of  $\Delta^9$ -THC on lymphocyte populations of CD4<sup>+</sup> and CD8<sup>+</sup> T cells recruited to the airways of mice challenged with PR8. Mice were treated with  $\Delta^9$ -THC (25, 50, or 75 mg/kg) or its corn oil vehicle for 5 consecutive days surrounding the intranasal instillation of influenza virus A/PR/8 or its vehicle SAL. Mice were euthanized on day 7 post infection. BALF was collected by flushing the lungs with 2 ml of sterile SAL. CD4<sup>+</sup> and CD8<sup>+</sup> T cells in BALF were quantified by flow cytometric analysis. Data is expressed as mean ± SEM; *n* = 5 except where noted by (*n*); \* = significantly different from respective control instilled with SAL. # = significantly different from corn oil with PR8 challenge.

Chemokine/ Cytokine	CO		$\Delta^9$ -THC 25mg/kg	$\Delta^9$ -THC 50mg/kg	$\Delta^9$ -THC 75mg/kg
	SAL	PR8	PR8	PR8	PR8
IL-6	0.9±0.5 (4)	497.5±86.2 * <i>p</i> = 0.001 (4)	532.7±120.7 <i>p</i> = 0.830 (4)	954.9±272.4 <i>p</i> = 0.125	1120.0±168.9 <i>p</i> = 0.054
TNF- $\alpha$	6.7±4.7 (4)	145.3±9.9 * <i>p</i> < 0.001 (4)	129.3±2.9 <i>p</i> = 0.663 (4)	145.3±28.0 <i>p</i> = 0.732	155.8±26.2 <i>p</i> = 0.977
MCP-1	7.4±1.1 (4)	1643.0±296.2 * <i>p</i> = 0.013 (4)	2308.0±70.0 <i>p</i> = 0.589 (4)	3301.0±728.4 # <i>p</i> = 0.044 (4)	3239.0±796.0 <i>p</i> = 0.143
IFN- $\gamma$	1.5±0.1 (4)	1411.0±263.2 * <i>p</i> = 0.048	728.1±166.2 <i>p</i> = 0.372 (4)	1475.0±405.0 <i>p</i> = 0.893	1300.0±489.4 <i>p</i> = 0.815
IL-10	46.2±2.9 (4)	151.0±52.0 <i>p</i> = 0.119	120.0±22.4 <i>p</i> = 0.477 (4)	54.2±11.3 <i>p</i> = 0.067	43.8±22.3 <i>p</i> = 0.100
IL-12p70	3.5±0.4 (3)	5.08±0.6 <i>p</i> = 0.051	4.3±0.7 <i>p</i> = 0.884 (4)	5.0±0.4 <i>p</i> = 0.922	4.5±1.2 <i>p</i> = 0.855

**Table 4. Inflammatory cytokines quantified in BALF by cytometric bead array.** The effects of  $\Delta^9$ -THC on soluble mediators released by immune and epithelial cells in the pulmonary airways during an inflammatory response to PR8 challenge. Mice were treated with  $\Delta^9$ -THC (25, 50, or 75 mg/kg) or its corn oil vehicle for 5 consecutive days surrounding the intranasal instillation of influenza virus A/PR/8 or its vehicle SAL. Mice were euthanized on day 7 post infection. BALF was collected by flushing the lungs with 2 ml of sterile SAL. Concentrations of inflammatory cytokines in BALF were enumerated by cytometric bead array analysis on the flow cytometer. Data is expressed as mean  $\pm$  SEM; *n* = 5 except where noted by (*n*); \* = significantly different from respective control instilled with SAL. # = significantly different from corn oil with PR8 challenge.

Treatment of PR8 infected mice with  $\Delta^9$ -THC at any dose, however, did not significantly alter the BALF concentrations of TNF- $\alpha$ , IFN- $\gamma$ , IL-6, IL-10 or IL-12p70 when compared to mice infected with PR8 alone.

**F)  $\Delta^9$ -THC treatment reduces inflammation scores for mouse lung sections.**

The magnitude and severity of inflammation observed in histological sections of lung isolated from the right and left lobes were independently scored (0 to 3, with 0 = no inflammation and 3 = severe inflammation) and compared between treatment groups at 7 dpi (Figure 16A) and 10 dpi (Figure 16B). There was no inflammation observed in the lungs of mice intranasally instilled with SAL. In contrast, there was a marked increase in the inflammation score noted for lung sections obtained from mice challenged with PR8 alone at both 7 and 10 dpi, representing a moderate to severe inflammatory response. There was a trend toward decreased inflammation scores for sections obtained from  $\Delta^9$ -THC treated mice challenged with PR8 at 7 dpi. The inflammation scores for sections obtained from  $\Delta^9$ -THC treated mice challenged with PR8 were, however, significantly attenuated at 10 dpi, representing mild to moderate levels of inflammation.

**G) Effect of  $\Delta^9$ -THC on the observed pulmonary histopathology to PR8.**

Exposure of mice to the corn oil vehicle or  $\Delta^9$ -THC alone did not result in significant histologic changes within the control mice (Figure 17A). Infection of mice with influenza induced a significant cellular and inflammatory reaction 7 dpi in all lung regions examined. The inflammatory infiltrate was centered upon the bronchiolo-alveolar duct junction, and extended out into the surrounding alveolar parenchyma. The

**Figure 16.  $\Delta^9$ -THC decreases inflammation scores in a time-dependent manner.** Effects of  $\Delta^9$ -THC on the inflammatory response gathered within the subepithelial interstitium and alveolar parenchyma following influenza challenge. Inflammation scores were recorded from lung sections taken at 7 dpi (A) and 10 dpi (B). Scores were tabulated as discussed in Materials and Methods. Data is expressed as mean  $\pm$  SEM; N.D. = not detectable. \* = significantly different from respective control instilled with SAL. # = significantly different from corn oil with PR8 challenge.

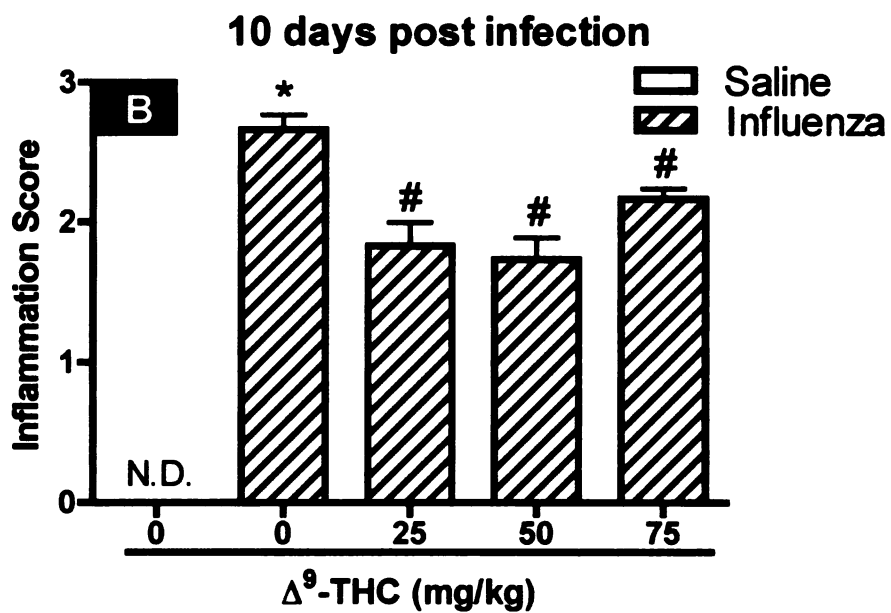
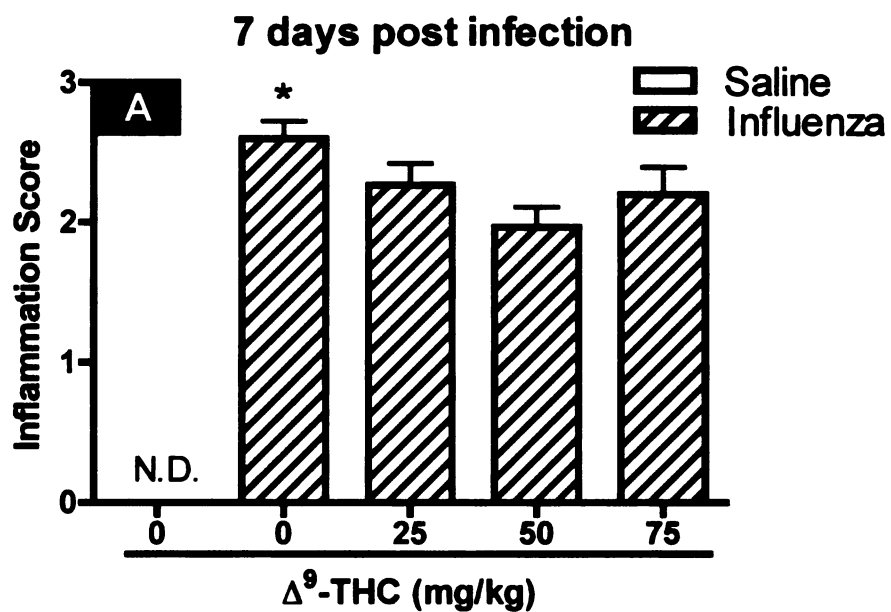


**Figure 16.  $\Delta^9$ -THC decreases inflammation scores in a time-dependent manner.**

**Figure 17. Examination of the effects of  $\Delta^9$ -THC on the inflammatory response to influenza challenge by histopathology.** Effects of  $\Delta^9$ -THC on the inflammatory response observed at generation 5 of the main axial airway on day 10 post infection. Mice were treated with  $\Delta^9$ -THC (25, 50, or 75 mg/kg) or its corn oil vehicle for 5 consecutive days surrounding the intranasal instillation of influenza virus A/PR/8 or its vehicle SAL. Mice were euthanized on day 10 post infection. Lungs were fixed with 10% neutral-buffered formalin for 24 hours, then sectioned and stained with hematoxylin and eosin (H&E). Light photomicrographs were taken for lung sections at generation 5 of the main axial airway (MAA) to include the bronchiolar artery (a) and alveolar parenchyma (p). A = lung section from a mouse receiving corn oil gavage surrounding a SAL instillation. There was no evidence of inflammation in the perivascular/peribronchiolar submucosal compartment (sm) or alveolar parenchyma. B = lung section from a mouse receiving corn oil gavage surrounding an influenza instillation. There was severe inflammation of the perivascular/peribronchiolar submucosal compartment with marked extension into the alveolar parenchyma. C = lung section from a mouse receiving THC (75 mg/kg) gavage surrounding an influenza instillation. There was severe inflammation of the perivascular/peribronchiolar submucosal compartment with modest extension into the alveolar parenchyma. Bar = 100 microns. Images in this dissertation are presented in color.

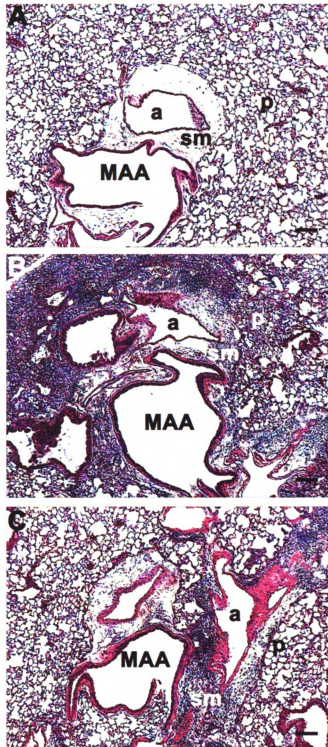


Figure 17. Examination of the effects of  $\Delta^9$ -THC on the inflammatory response to influenza challenge by histopathology.

inflammatory cells were a mix of primarily lymphocytes and neutrophils, with fewer macrophages and plasma cells. The lymphocytic and neutrophilic population often filled the alveoli, and there was moderate alveolar interstitial infiltration with similar inflammatory cells. The lymphocytes often formed well-organized perivascular and peribronchiolar aggregates. Acute epithelial necrosis was present in small numbers of bronchioles, and the remaining epithelial cells were moderately attenuated. At 10 dpi with influenza the inflammation was more severe, and often obscured the alveolar parenchyma (Figure 17B). The inflammatory cells 10 dpi were primarily lymphocytes, with smaller numbers of neutrophils. The bronchiolar epithelium 10 dpi was moderately hyperplastic and hypertrophied, and there were scattered foci of alveolar bronchiolarization (extension of bronchiolar epithelium into the adjacent alveolar spaces). PR8-infected mice treated with  $\Delta^9$ -THC resulted in no observed decreases in inflammation 7 dpi at each  $\Delta^9$ -THC dose. At 10 dpi, exposure of PR8-infected mice with all dose levels of  $\Delta^9$ -THC resulted in a mild to moderate decrease in histologically apparent inflammation within the lungs (Figure 17C). The inflammation within the mice was not uniformly distributed throughout all lung regions, as found in the control PR8-infected mice. The decreases in inflammation included both decreases in inflammatory cell numbers, as well as extent of distribution within the tissue. The bronchiolar epithelial changes noted above were still present 10 dpi in the  $\Delta^9$ -THC co-exposed mice.

#### **H) Caspase-3 mRNA expression levels and G5 numeric cell densities**

CAS-3 is a cellular biochemical marker of committed activation of signaling pathways that lead to cell death by apoptosis. In the current study, there were markedly

higher CAS-3 mRNA levels observed at 7 dpi in total lung homogenates from mice challenged with PR8 alone as compared to mice instilled with SAL alone. The increase in CAS-3 mRNA suggests an increased commitment to apoptotic cell death by cells present in the lung in response to PR8 infection (Figure 18A).  $\Delta^9$ -THC treated mice infected with PR8 exhibited a trend toward increasing levels of CAS-3 mRNA with increasing doses of  $\Delta^9$ -THC when compared to mice infected with PR8 alone. In addition, immunohistochemical staining for CAS-3 revealed marked increases in the number of CAS-3 positive cells in lung sections obtained from mice infected with PR8 alone at 7 dpi (Figure 18B). There was a marked decrease ( $p = 0.056$ ) in CAS-3 immunoreactive epithelial cells at 7 dpi in PR8 infected mice treated with 25 mg/kg  $\Delta^9$ -THC when compared to mice challenged with PR8 alone (Figure 18B). At 10 dpi, there were no significant differences observed in the numeric cell densities for CAS-3 with any of the treatments.

#### **I) MUC5AC mRNA expression levels and G5 numeric cell densities**

Increases in *MUC5AC* gene transcription might be an early indicator of increased mucin production and possibly MCM in the bronchiolar epithelium. In the current study, the levels of *MUC5AC* mRNA were increased in mice challenged with PR8 alone when compared to mice instilled with SAL alone (Figure 19A). In  $\Delta^9$ -THC treated mice challenged with PR8, a dose of 25 mg/kg  $\Delta^9$ -THC led to a four-fold increase in *MUC5AC* mRNA levels as compared to mice infected with PR8 alone. In addition to changes in *MUC5AC* gene expression, there were marked increases in the number of epithelial cells staining for alcian blue (acidic mucosubstances) in lung sections obtained from mice

**Figure 18.  $\Delta^9$ -THC has no effect on Caspase-3 mRNA levels and epithelial numeric cell densities.** The effects of  $\Delta^9$ -THC on apoptotic cell death in response to influenza challenge were measured by the expression of CAS-3 mRNA (A) and immunohistochemical staining of CAS-3 in the epithelium lining the main axial airway at generation 5 of the left lung lobe at 7 dpi (B) and 10 dpi (C). Mice were treated with SAL or  $\Delta^9$ -THC (0, 25, 50, or 75 mg/kg) with PR8. Data is expressed as mean  $\pm$  SEM; N.D. = not detectable. \* = significantly different from respective control instilled with SAL.

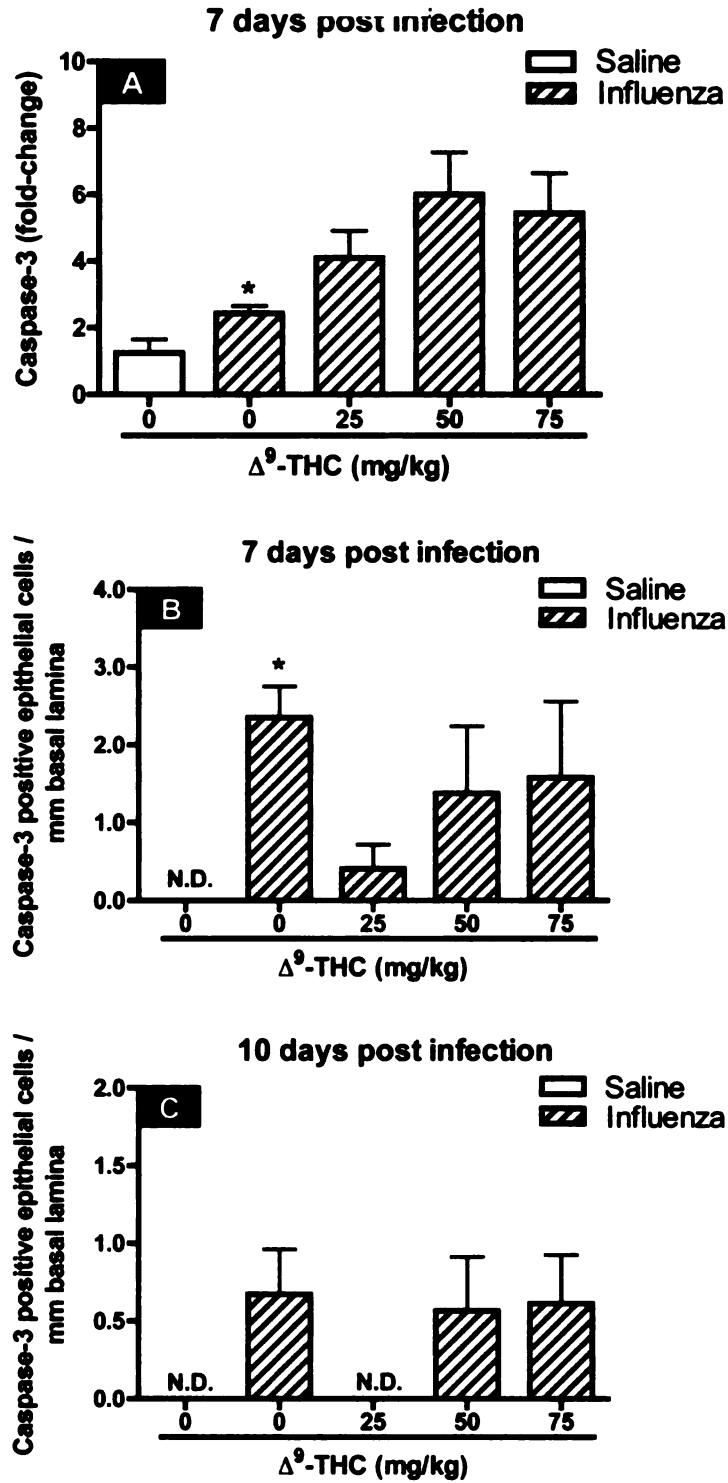


Figure 18.  $\Delta^9$ -THC has no effect on Caspase-3 mRNA levels and epithelial numeric cell densities.

**Figure 19.  $\Delta^9$ -THC increases MUC5AC mRNA levels and decreases epithelial numeric cell densities for acidic mucosubstances.** The effects of  $\Delta^9$ -THC on the development of mucous cell metaplasia in the epithelium lining the main axial airway following influenza challenge and subsequent inflammatory cell responses. Expression levels of MUC5AC mRNA (A) and G5 main axial airway labeling indexes of alcian blue were determined at 7 dpi (B) and 10 dpi for mice treated with SAL or  $\Delta^9$ -THC (0, 25, 50, or 75 mg/kg) with PR8. Data is expressed as mean  $\pm$  SEM; \* = significantly different from respective control instilled with SAL. # = significantly different from corn oil with PR8 challenge.

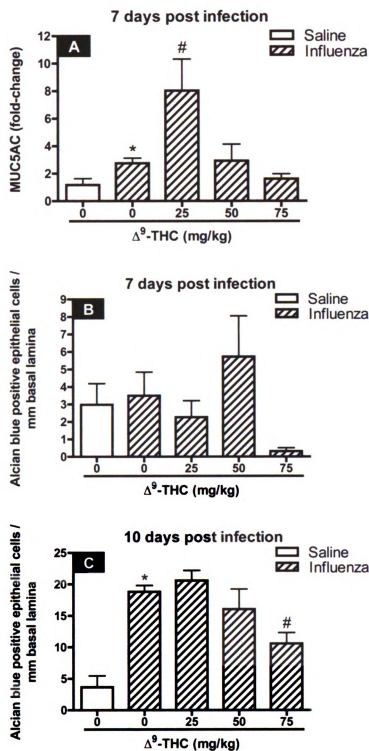


Figure 19.  $\Delta^9$ -THC increases MUC5AC mRNA levels and decreases epithelial numeric cell densities for acidic mucosubstances.

infected with PR8 alone at 10 dpi but not at 7 dpi (Figures 19B and C).  $\Delta^9$ -THC treatment of PR8 infected mice did not affect the number of alcian blue stained epithelial cells observed along the main axial airway at 7 dpi (Figure 19B), but did attenuate the number of alcian blue-positive cells observed at 10 dpi in mice receiving 75 mg/kg  $\Delta^9$ -THC (Figure 19C) when compared to mice challenged with PR8 alone.

#### **J) $\Delta^9$ -THC modestly enhances neutrophil-derived elastase levels in BALF**

Neutrophil-derived elastase is another soluble mediator secreted into the airways during ongoing inflammation that has been shown to have an influence on the development of MCM. Neutrophil-derived elastase was not detectable in BALF from SAL instilled mice (Figure 20). However, BALF-associated elastase was markedly increased in mice infected with PR8 alone.  $\Delta^9$ -THC treated mice infected with PR8 exhibited a modest increase in elastase levels at a dose of 75 mg/kg  $\Delta^9$ -THC when compared to mice challenged with PR8 alone.

### **IV. Pulmonary airway responses to influenza A/PR/8/34 in $CB_1^{-/-}/CB_2^{-/-}$ mice exposed to $\Delta^9$ -tetrahydrocannabinol: An examination for the role of cannabinoid receptors**

#### **A) Qualitative health assessment of $CB_1^{-/-}/CB_2^{-/-}$ and wild type mice challenged with PR**

$CB_1^{-/-}/CB_2^{-/-}$  and wild type mice treated with corn oil or  $\Delta^9$ -THC and intranasally instilled with SAL were normal in appearance and activity level. Infection with PR8 in the presence or absence of  $\Delta^9$ -THC treatment, however, led to marked differences in the

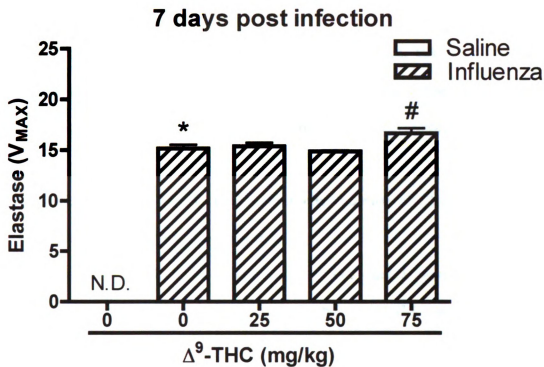


**Figure 20.  $\Delta^9$ -THC modestly increases neutrophil-derived elastase levels secreted in the pulmonary airways.** Effects of  $\Delta^9$ -THC on the secretion of elastase by neutrophils in response to influenza infection within the pulmonary airways at 7 dpi. Neutrophil-derived elastase in BALF was determined for mice treated with SAL or  $\Delta^9$ -THC (0, 25, 50, or 75 mg/kg) with PR8. Data is expressed as mean  $\pm$  SEM; \* = significantly different from respective control instilled with SAL. N.D. = not detectable. # = significantly different from corn oil with PR8 challenge.

gross appearance of  $CB_1^{-/-}/CB_2^{-/-}$  and wild type mice. Specifically,  $CB_1^{-/-}/CB_2^{-/-}$  mice were notably more gaunt in comparison to wild type mice, suggesting that the mice were dehydrated. In addition, the  $CB_1^{-/-}/CB_2^{-/-}$  mice were lethargic and displayed unkempt fur. In contrast, wild type mice infected with PR8 in the presence or absence of  $\Delta^9$ -THC treatment maintained normal grooming habits and exhibited similar activity levels as the SAL instilled controls. Upon gross examination of the lungs,  $CB_1^{-/-}/CB_2^{-/-}$  mice had extensive hemorrhaging across all lung lobes. Wild type mice also displayed evidence of hemorrhaging, however, to a much lesser extent than  $CB_1^{-/-}/CB_2^{-/-}$  mice.

**B) The viral load of PR8 in the pulmonary airways of  $CB_1^{-/-}/CB_2^{-/-}$  and wild type mice measured 7 days after challenge.**

The levels of mRNA for the highly antigenic viral surface protein, hemagglutinin 1, were assessed by quantitative real time PCR. For both  $CB_1^{-/-}/CB_2^{-/-}$  and wild type mice, viral H1 expression was markedly elevated above SAL controls at 7 dpi in the lungs of all mice challenged with PR8 (Figure 21). Infection of  $\Delta^9$ -THC treated  $CB_1^{-/-}/CB_2^{-/-}$  mice with PR8 resulted in an increase ( $p = 0.056$ ) in H1 mRNA levels when compared to mice instilled with PR8 alone. In  $\Delta^9$ -THC treated wild type mice infected with PR8, there was a significant increase in viral H1 mRNA levels when compared to wild type mice instilled with PR8 alone. The overall level of expression of H1 mRNA, though, was greatly reduced in  $CB_1^{-/-}/CB_2^{-/-}$  mice when compared to wild type mice.

**C)  $\Delta^9$ -THC affects vascular permeability induced by PR8 infection of the airways in  $CB_1^{-/-}/CB_2^{-/-}$  and wild type mice.**

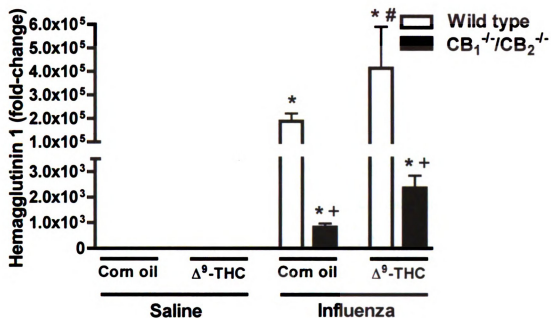


**Figure 21. Effects of  $\Delta^9$ -THC treatment on the expression levels of H1 mRNA in  $CB_1^{-/-}/CB_2^{-/-}$  and wild type mice.** The effects of  $\Delta^9$ -THC on Hemagglutinin 1 mRNA levels in lungs from  $CB_1^{-/-}/CB_2^{-/-}$  and wild type mice challenged with PR8. Mice were treated with  $\Delta^9$ -THC (75 mg/kg) or its corn oil vehicle for 5 consecutive days surrounding the intranasal instillation of influenza virus A/PR/8 or its vehicle SAL. Mice were euthanized on day 7 post infection. Whole lungs were immersed in TRI reagent and homogenized prior to the isolation of total RNA. The mRNA levels for Hemagglutinin 1 were determined by real-time PCR with 18S utilized as an internal loading control. The fold-change in gene expression is normalized to mice instilled with SAL. Data is expressed as mean  $\pm$  SEM; \* = significantly different from respective control instilled with SAL. # = significantly different from respective control gavaged with corn oil. + = significantly different from respective group in wild type mice.

The detection of increased levels of total BALF-associated protein is indicative of increased vascular permeability at the alveolar/capillary interface during the inflammatory response to PR8. The total BALF-associated protein levels in PR8 infected  $CB_1^{-}/CB_2^{-}$  and wild type mice, in the absence of  $\Delta^9$ -THC treatment, were 2-fold greater than SAL controls (Figure 22).  $\Delta^9$ -THC treated  $CB_1^{-}/CB_2^{-}$  mice infected with PR8 exhibited a 33% increase in total protein when compared to  $CB_1^{-}/CB_2^{-}$  mice challenged with PR8 alone. Conversely,  $\Delta^9$ -THC treated wild type mice infected with PR8 had a 50% decrease in total protein when compared to wild type mice challenged with PR8 alone. When comparing  $CB_1^{-}/CB_2^{-}$  and wild type mice, the amount of total protein detected in mice treated with  $\Delta^9$ -THC and infected with PR8 was 2-fold greater in  $CB_1^{-}/CB_2^{-}$  mice than amounts of total protein observed in wild type mice receiving the same treatment.

**D)  $CB_1^{-}/CB_2^{-}$  mice treated with  $\Delta^9$ -THC exhibit a distinctly different composition of leukocytes recruited to the airways in response to PR8 infection when compared to wild type.**

Primary influenza infection elicits an inflammatory response consisting of a mixed population of leukocytes that infiltrate the pulmonary airways. In particular, there is a marked influx of neutrophils and lymphocytes into the airways with monocytes and eosinophils representing a smaller portion of the total population of BALF-associated leukocytes. In the current study, the total number of BALF-associated leukocytes was 3-fold greater in PR8-infected wild type mice and 4-fold greater in  $CB_1^{-}/CB_2^{-}$  mice when compared to their respective non-infected controls (Figure 23A).  $\Delta^9$ -THC treated mice infected with PR8 exhibited a 2-fold increase above SAL instilled controls in both

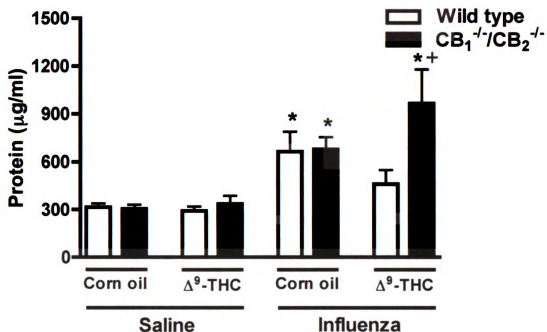


**Figure 22. Effects of  $\Delta^9$ -THC treatment on total protein in BALF in  $CB_1^{-/-}/CB_2^{-/-}$  and wild type mice.** The effects of  $\Delta^9$ -THC on total protein detected in BALF supernatants from  $CB_1^{-/-}/CB_2^{-/-}$  and wild type mice challenged with PR8. Mice were treated with  $\Delta^9$ -THC (75 mg/kg) or its corn oil vehicle for 5 consecutive days surrounding the intranasal instillation of influenza virus A/PR/8 or its vehicle SAL. Mice were euthanized on day 7 post infection. BALF was collected by flushing the lungs with 2 ml of sterile SAL. Total protein was assessed for supernatants from BALF that had been centrifuged to remove cellular debris. Data is expressed as mean  $\pm$  SEM; \* = significantly different from respective control instilled with SAL. + = significantly different from respective group in wild type mice.

CB<sub>1</sub><sup>-/-</sup>/CB<sub>2</sub><sup>-/-</sup> and wild type mice. However, the difference in total leukocytes retrieved in the Δ<sup>9</sup>-THC treated CB<sub>1</sub><sup>-/-</sup>/CB<sub>2</sub><sup>-/-</sup> mice infected with PR8 was significantly less than CB<sub>1</sub><sup>-/-</sup>/CB<sub>2</sub><sup>-/-</sup> mice challenged with PR8 alone. To further assess differences in individual leukocyte populations retrieved by lavage, differential cell counts were performed. Neutrophils (Figure 23B) were markedly increased in PR8-infected CB<sub>1</sub><sup>-/-</sup>/CB<sub>2</sub><sup>-/-</sup> and wild type mice. Specifically, Δ<sup>9</sup>-THC treated wild type mice infected with PR8 exhibited 2-fold increases in neutrophils when compared to wild type mice challenged with PR8 alone. Conversely, there were marked decreases in the number of BALF-associated neutrophils for PR8-infected CB<sub>1</sub><sup>-/-</sup>/CB<sub>2</sub><sup>-/-</sup> mice treated with Δ<sup>9</sup>-THC when compared to CB<sub>1</sub><sup>-/-</sup>/CB<sub>2</sub><sup>-/-</sup> mice challenged with PR8 alone. BALF-associated lymphocytes were markedly increased (Figure 23C) with PR8 infection in both CB<sub>1</sub><sup>-/-</sup>/CB<sub>2</sub><sup>-/-</sup> and wild type mice. Δ<sup>9</sup>-THC treated CB<sub>1</sub><sup>-/-</sup>/CB<sub>2</sub><sup>-/-</sup> and wild type mice infected with PR8 exhibited attenuation in the number of lymphocyte retrieved. There were no apparent changes in the number of macrophages retrieved in BALF from PR8 challenged wild type mice. A 2-fold increase was observed, however, in the number of BALF-associated macrophages from PR8-infected CB<sub>1</sub><sup>-/-</sup>/CB<sub>2</sub><sup>-/-</sup> mice that was attenuated in Δ<sup>9</sup>-THC treated CB<sub>1</sub><sup>-/-</sup>/CB<sub>2</sub><sup>-/-</sup> mice infected with PR8 (Figure 23D). Lastly, PR8-infection of CB<sub>1</sub><sup>-/-</sup>/CB<sub>2</sub><sup>-/-</sup> and wild type mice resulted in an increase in the number of eosinophils retrieved in BALF (Figure 23E). Δ<sup>9</sup>-THC treated CB<sub>1</sub><sup>-/-</sup>/CB<sub>2</sub><sup>-/-</sup> and wild type mice infected with PR8 exhibited no effect in the number of BALF-associated eosinophils counted.

**Figure 23. Effects of  $\Delta^9$ -THC treatment on total and differential leukocyte counts in BALF in  $CB_1^{-}/CB_2^{-}$  and wild type mice.** The effects of  $\Delta^9$ -THC on leukocyte recruitment to the pulmonary airways of  $CB_1^{-}/CB_2^{-}$  and wild type mice challenged with PR8 were enumerated. Mice were treated with  $\Delta^9$ -THC (75 mg/kg) or its corn oil vehicle for 5 consecutive days surrounding the intranasal instillation of influenza virus A/PR/8 or its vehicle SAL. Mice were euthanized on day 7 post infection. BALF was collected by flushing the lungs with 2 ml of sterile SAL. Total leukocyte (A) counts were enumerated by hemacytometer. Differential cell counts of neutrophils (B), lymphocytes (C), macrophages (D), and eosinophils (E) were assessed by counting 200 cells from cytopins of the BALF stained with Diff-quick. Data is expressed as mean  $\pm$  SEM; \* = significantly different from respective control instilled with SAL. # = significantly different from respective control gavaged with corn oil. + = significantly different from respective group in wild type mice.

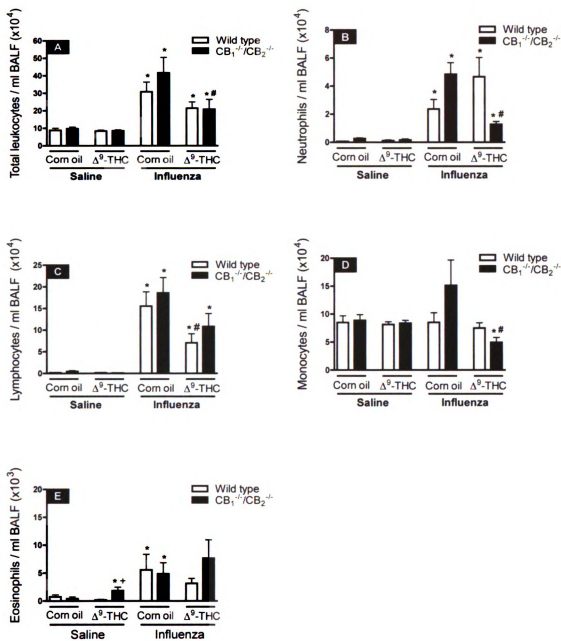


**Figure 23. Effects of  $\Delta^9$ -THC treatment on total and differential leukocyte counts in BALF in  $CB_1^{-/-}/CB_2^{-/-}$  and wild type mice.**

**E) BALF-associated CD4<sup>+</sup> and CD8<sup>+</sup> T cell levels following PR8 challenge in CB<sub>1</sub><sup>-/-</sup>/CB<sub>2</sub><sup>-/-</sup> and wild type mice.**

To evaluate the contribution of CD4<sup>+</sup> and CD8<sup>+</sup> T cells within the pool of BALF-associated lymphocytes responding to PR8 challenge, the number of CD4<sup>+</sup> T cells (Figure 24A) and CD8<sup>+</sup> T-cells (Figure 24B) were enumerated by flow cytometric analysis. Wild type mice treated with either corn oil or  $\Delta^9$ -THC exhibited modest levels of BALF-associated CD4<sup>+</sup> T cells. Interestingly, background levels of CD4<sup>+</sup> T cells were greater in corn oil and  $\Delta^9$ -THC treated CB<sub>1</sub><sup>-/-</sup>/CB<sub>2</sub><sup>-/-</sup> mice than in wild type mice with the same treatments. As a result, there was no observed difference in the number of CD4<sup>+</sup> T cells retrieved in BALF between SAL instilled controls and CB<sub>1</sub><sup>-/-</sup>/CB<sub>2</sub><sup>-/-</sup> mice infected with PR8 alone. Alternatively,  $\Delta^9$ -THC treated CB<sub>1</sub><sup>-/-</sup>/CB<sub>2</sub><sup>-/-</sup> mice infected with PR8 exhibited a significant increase in CD4<sup>+</sup> T cells above background. The increase in BALF-associated CD4<sup>+</sup> T cells in CB<sub>1</sub><sup>-/-</sup>/CB<sub>2</sub><sup>-/-</sup> mice treated with  $\Delta^9$ -THC and infected with PR8 was comparatively greater than the respective treatment group in wild type mice. CD8<sup>+</sup> T cells were not detected in BALF from SAL instilled controls in both CB<sub>1</sub><sup>-/-</sup>/CB<sub>2</sub><sup>-/-</sup> and wild type mice. However, there were marked increases in the number of BALF-associated CD8<sup>+</sup> T cells for both CB<sub>1</sub><sup>-/-</sup>/CB<sub>2</sub><sup>-/-</sup> and wild type mice challenged with PR8. In addition, there was a trend toward decreased numbers of BALF-associated CD8<sup>+</sup> T cells in  $\Delta^9$ -THC treated wild type mice infected with PR8.

**Figure 24. Effects of  $\Delta^9$ -THC treatment on CD4<sup>+</sup> and CD8<sup>+</sup> T cells retrieved in BALF in CB<sub>1</sub><sup>-/-</sup>/CB<sub>2</sub><sup>-/-</sup> and wild type mice.** The effects of  $\Delta^9$ -THC on CD4<sup>+</sup> T cell (A) and CD8<sup>+</sup> T cell counts (B) recruited to the airways of CB<sub>1</sub><sup>-/-</sup>/CB<sub>2</sub><sup>-/-</sup> and wild type mice challenged with influenza. Mice were treated with  $\Delta^9$ -THC (75 mg/kg) or its corn oil vehicle for 5 consecutive days surrounding the intranasal instillation of influenza virus A/PR/8 or its vehicle SAL. Mice were euthanized on day 7 post infection. BALF was collected by flushing the lungs with 2 ml of sterile SAL. CD4<sup>+</sup> and CD8<sup>+</sup> T cells in BALF were quantified by flow cytometric analysis. Data is expressed as mean  $\pm$  SEM; \* = significantly different from respective control instilled with SAL. # = significantly different from respective control gavaged with corn oil. + = significantly different from respective group in wild type mice. N.D.= not detected.

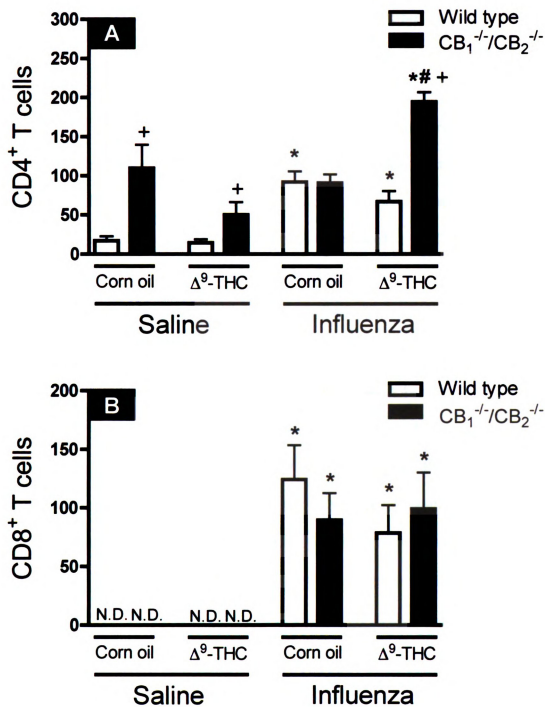


Figure 24. Effects of  $\Delta^9$ -THC treatment on CD4<sup>+</sup> and CD8<sup>+</sup> T cells retrieved in BALF in CB<sub>1</sub><sup>-/-</sup>/CB<sub>2</sub><sup>-/-</sup> and wild type mice.

**F) Cannabinoid receptor deficient mice exhibit unique differences in epithelial and leukocytic chemokine and cytokine secretion in the pulmonary airways.**

One mechanism of cellular communication within a mixed population of leukocytes and between infected epithelium and leukocytes is through secretion of cytokines and chemokines. PR8-infected  $CB_1^{-/-}/CB_2^{-/-}$  mice exhibited marked increases in the chemokine MCP-1 (Figure 25A), and pro-inflammatory cytokines TNF- $\alpha$  (Figure 25B), IL-6 (Figure 25C), and IFN- $\gamma$  (Figure 25D) measured in BALF. Likewise, wild type mice challenged with PR8 exhibited increased levels of BALF-associated MCP-1, TNF- $\alpha$ , IL-6, and IFN- $\gamma$ . In addition, there was a modest enhancement of IL-10 concentrations (Figure 25E) following PR8 challenge in  $CB_1^{-/-}/CB_2^{-/-}$  and wild type mice. There were no changes in BALF-associated IL-12p70 in the presence or absence of  $\Delta^9$ -THC treatment or PR8 challenge (Figure 25F) in either  $CB_1^{-/-}/CB_2^{-/-}$  or wild type mice.  $\Delta^9$ -THC treated  $CB_1^{-/-}/CB_2^{-/-}$  mice infected with PR8 exhibited an attenuation of BALF-associated IFN- $\gamma$  and IL-10 concentrations. Conversely, the concentrations of chemokines and cytokines detected in BALF in PR8-infected wild type mice were unaffected by  $\Delta^9$ -THC treatment. There were, however, comparative differences between detectable levels of BALF-associated TNF- $\alpha$ , and IFN- $\gamma$  ( $p = 0.061$ ) in PR8-infected wild type and  $CB_1^{-/-}/CB_2^{-/-}$  mice.

The BALF-associated  $T_H2$  cytokines IL-2 (Figure 26A), IL-4 (Figure 26B), and IL-5 (Figure 26C) were also quantified by cytometric bead array. Of particular interest, PR-8 infected  $CB_1^{-/-}/CB_2^{-/-}$  mice exhibited marked increases in concentrations of IL-5 that were comparatively 2-fold less than concentrations observed in the cognate PR8-infected

**Figure 25. Effects of  $\Delta^9$ -THC treatment on inflammatory chemokines and cytokines in secreted into the pulmonary airways in  $CB_1^{-/-}/CB_2^{-/-}$  and wild type mice.** The effects of  $\Delta^9$ -THC on the release of soluble chemical mediators from leukocytes and epithelium in response to PR8 challenge of the pulmonary airways of  $CB_1^{-/-}/CB_2^{-/-}$  and wild type mice. Mice were treated with  $\Delta^9$ -THC (75 mg/kg) or its corn oil vehicle for 5 consecutive days surrounding the intranasal instillation of influenza virus A/PR/8 or its vehicle SAL. Mice were euthanized on day 7 post infection. BALF was collected by flushing the lungs with 2 ml of sterile SAL. Concentrations of the inflammatory chemokine MCP-1 (A) and cytokines TNF-a (B), IL-6 (C), IFN-g (D), IL-10 (E) and IL-12p70 (F) were determined by cytometric bead array analysis. Data is expressed as mean  $\pm$  SEM; \* = significantly different from respective control instilled with SAL. # = significantly different from respective control gavaged with corn oil. + = significantly different from respective group in wild type mice.

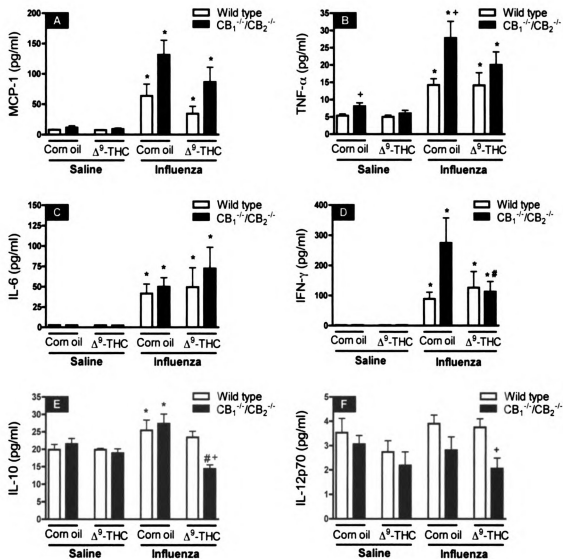


**Figure 25.** Effects of  $\Delta^9$ -THC treatment on inflammatory chemokines and cytokines released into the pulmonary airways in  $CB_1^{-/-}/CB_2^{-/-}$  and wild type mice.

**Figure 26. Effects of  $\Delta^9$ -THC treatment on  $T_H2$  cytokines secreted into the pulmonary airways in  $CB_1^{-}/CB_2^{-}$  and wild type mice.** The effects of  $\Delta^9$ -THC on the concentrations of the  $T_H2$  cytokines IL-2 (A), IL-4 (B), and IL-5 (C) in BALF from  $CB_1^{-}/CB_2^{-}$  and wild type mice challenged with PR8. Mice were treated with  $\Delta^9$ -THC (75 mg/kg) or its corn oil vehicle for 5 consecutive days surrounding the intranasal instillation of influenza virus A/PR/8 or its vehicle SAL. Mice were euthanized on day 7 post infection. BALF was collected by flushing the lungs with 2 ml of sterile SAL. Cytometric bead array was performed on BALF to enumerate the  $T_H2$  cytokines. Data is expressed as mean  $\pm$  SEM; \* = significantly different from respective control instilled with SAL. # = significantly different from respective control gavaged with corn oil. + = significantly different from respective group in wild type mice.

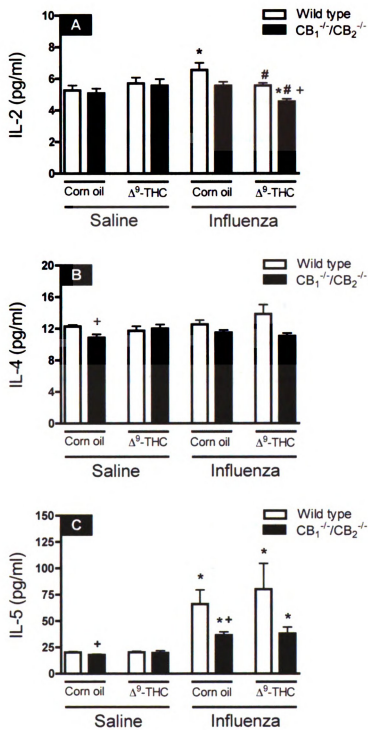


**Figure 26.** Effects of  $\Delta^9$ -THC treatment on T<sub>H</sub>2 cytokines secreted into the pulmonary airways in CB<sub>1</sub><sup>-/-</sup>/CB<sub>2</sub><sup>-/-</sup> and wild type mice.

wild type mice. The concentrations of IL-2 and IL-4 in BALF were unaffected by PR8 challenge in  $CB_1^{-}/CB_2^{-}$  mice.  $\Delta^9$ -THC treated  $CB_1^{-}/CB_2^{-}$  mice infected with PR8 had modestly attenuated concentrations of BALF-associated IL-2, but exhibited no effect on the concentrations of IL-4 or IL-5. PR8-infected wild type mice exhibited marked increases in BALF IL-5 concentrations, subtle increases in the concentrations of IL-2, and no detectable differences for IL-4 when compared to SAL instilled mice.  $\Delta^9$ -THC treated wild type mice infected with PR8 had a modest attenuation of BALF IL-2 concentrations with no observed effect on either IL-4 or IL-5 concentrations.

### **G) Cytokines and chemokines detected in blood serum.**

In  $CB_1^{-}/CB_2^{-}$  mice, PR8 challenge alone resulted in marked increases in serum associated MCP-1 (Figure 27A), TNF- $\alpha$  (Figure 27B), IL-6 (Figure 27C), and IFN- $\gamma$  (Figure 27D) with respect to SAL control. In wild type mice, PR8 challenge increased circulating levels of the chemokine, MCP-1 and the cytokine IFN- $\gamma$  with respect to SAL instilled mice. In  $CB_1^{-}/CB_2^{-}$  there was no difference observed between SAL controls and PR8 challenge for serum concentrations of IL-12p70 (Figure 27E). In wild type mice there were modest, yet significant, increases observed in the concentrations of IL-12p70 with PR8 instillation as compared to SAL instillation alone in the presence or absence of  $\Delta^9$ -THC.  $CB_1^{-}/CB_2^{-}$  mice treated with  $\Delta^9$ -THC had attenuated concentrations of MCP-1 and IFN- $\gamma$  with respect to PR8 challenge alone, whereas wild type mice treated with  $\Delta^9$ -THC exhibited markedly enhanced circulating levels of IL-6 with respect to mice challenged with PR8 alone. In addition, there were comparative differences observed between  $CB_1^{-}/CB_2^{-}$  and wild type mice with PR8 challenge for the concentrations of

**Figure 27. Effects of  $\Delta^9$ -THC treatment on inflammatory chemokines and cytokines released into blood serum in  $CB_1^{-/-}/CB_2^{-/-}$  and wild type mice.** The effects of  $\Delta^9$ -THC on the dispersion of soluble chemical mediators from leukocytes and epithelium into the circulation in response to PR8 challenge of the pulmonary airways of  $CB_1^{-/-}/CB_2^{-/-}$  and wild type mice. Mice were treated with  $\Delta^9$ -THC (75 mg/kg) or its corn oil vehicle for 5 consecutive days surrounding the intranasal instillation of influenza virus A/PR/8 or its vehicle SAL. Mice were euthanized on day 7 post infection. Serum was collected from the abdominal aorta. Concentrations of the inflammatory chemokine MCP-1 (A) and cytokines TNF-a (B), IL-6 (C), IFN-g (D), and IL-12p70 (E) were determined by cytometric bead array analysis. Data is expressed as mean  $\pm$  SEM; \* = significantly different from respective control instilled with SAL. # = significantly different from respective control gavaged with corn oil. N.D.= not detected.

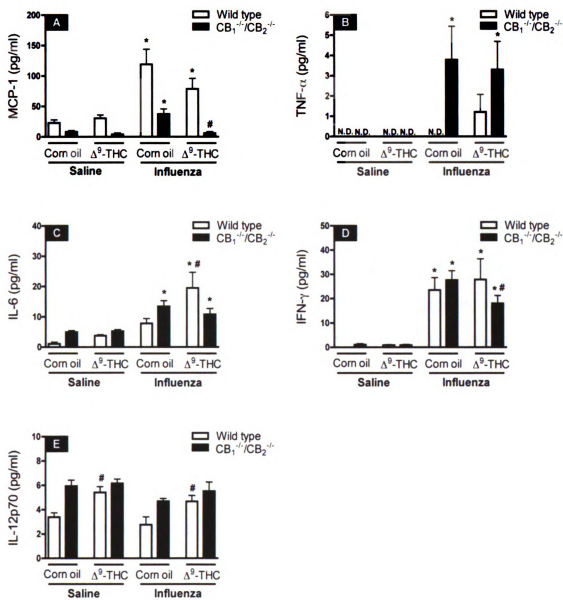


**Figure 27. Effects of  $\Delta^9$ -THC treatment on inflammatory chemokines and cytokines released into blood serum in  $CB_1^{-}/CB_2^{-}$  and wild type mice.**

MCP-1 detected.

**H) The absence of cannabinoid receptors CB<sub>1</sub> and CB<sub>2</sub> enhances the observed pulmonary histopathology.**

As previously reported by our laboratory, infection of mice with PR8 induces significant pulmonary inflammation 7 dpi in wild-type mice (Figure 28A-D) (113). Infection of the CB<sub>1</sub><sup>-/-</sup>/CB<sub>2</sub><sup>-/-</sup> mice with PR8 resulted in a similar inflammatory reaction (Figure 28E). As we have reported, the inflammation consists of primarily lymphocytes and neutrophils, with fewer macrophages and plasma cells centered upon the bronchiole-alveolar junction, and extending out into the surrounding parenchyma. Treatment of PR8 infected wild-type mice with Δ<sup>9</sup>-THC resulted in a significant decrease in inflammation 7 dpi compared to corn oil treated mice infected with PR8 (Figure 28D). These mice often had no to few inflammatory cells present; the remaining inflammation, was comprised of primarily lymphocytes and alveolar macrophages. In contrast, treatment of PR8 infected CB<sub>1</sub><sup>-/-</sup>/CB<sub>2</sub><sup>-/-</sup> mice with Δ<sup>9</sup>-THC resulted in a vigorous inflammatory and cellular reaction in the mice (Figure 28F). In these mice there were large numbers of mature lymphocytes around the conducting airways and extending into the surrounding alveolar parenchyma where they were admixed with fewer macrophages and neutrophils. The bronchiolar epithelium was moderately hypertrophied. Treatment of wild type and CB<sub>1</sub><sup>-/-</sup>/CB<sub>2</sub><sup>-/-</sup> mice with corn oil vehicle or Δ<sup>9</sup>-THC alone did not result in significant histologic changes in any of the lung sections examined.

**Figure 28. Inflammatory response to PR8 in the proximal section of the left lung lobe in  $CB_1^{-/-}/CB_2^{-/-}$  and wild type mice.** Light photomicrographs of the hilar region of the left lung lobe of wild type (WT) and  $CB_1^{-/-}/CB_2^{-/-}$  (KO) mice sectioned at generation 5 along the main axial airway (maa). Panel (A): corn oil treated wild type mouse instilled with saline (SAL) with no evidence of an inflammatory cell infiltrate (arrow) in the peribronchiolar (maa)/perivascular (a) submucosa (sm) and no evidence of inflammation in the alveolar parenchyma (p). Panel (B):  $\Delta^9$ -THC-treated wild type mouse instilled with saline with marked inflammatory cell infiltrate of the submucosa and diffuse inflammation within the alveolar airspace. Panel (C): corn oil treated wild type mouse instilled with PR8 with marked inflammatory cell infiltrate in the peribronchiolar /perivascular submucosa and alveolar airspace. Panel (D):  $\Delta^9$ -THC-treated wild type mouse instilled with PR8 with modest to no inflammatory cell infiltrate of the submucosa and alveolar airspace. Panel (E): corn oil treated  $CB_1^{-/-}/CB_2^{-/-}$  mouse instilled with PR8 with marked inflammatory cell infiltrate in the peribronchiolar /perivascular submucosa and alveolar airspace. Panel (F):  $\Delta^9$ -THC-treated  $CB_1^{-/-}/CB_2^{-/-}$  mouse instilled with PR8 with severe inflammation within the submucosa and alveolar airspace. Bar = 50 microns. Images provided in this dissertation are in color.

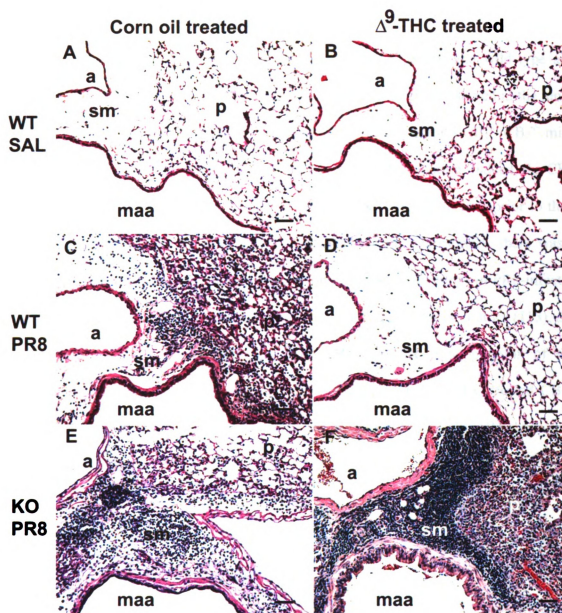


**Figure 28. Inflammatory response to PR8 in the proximal section of the left lung lobe from wild type mice.**

**I)  $\Delta^9$ -THC affects the magnitude of the inflammatory response to PR8 in wild type and CB<sub>1</sub> and CB<sub>2</sub> deficient mice.**

The magnitude and severity of inflammation observed in tissue sections isolated from the left lung lobe were independently scored (0 to 3, with 0 = no inflammation and 3 = severe inflammation) and compared between treatment groups and wild type and CB<sub>1</sub><sup>-/-</sup>/CB<sub>2</sub><sup>-/-</sup> mice at 7 dpi (Figures 29). There was no inflammation observed in the lungs of wild type mice intranasally instilled with SAL. However, 2 out of 8 CB<sub>1</sub><sup>-/-</sup>/CB<sub>2</sub><sup>-/-</sup> mice instilled with SAL exhibited modest evidence of ongoing inflammation. Indeed, the CB<sub>1</sub><sup>-/-</sup>/CB<sub>2</sub><sup>-/-</sup> mice were subjected to an extensive battery of serological screens prior to their use and were found to be negative for all pathogens tested. Interestingly, there was a marked and identical increase in the inflammation score noted for lungs in PR8-infected wild type and CB<sub>1</sub><sup>-/-</sup>/CB<sub>2</sub><sup>-/-</sup> mice. Similar to previous findings by our laboratory (113),  $\Delta^9$ -THC treated wild type mice challenged with PR8 exhibited a suppression of the inflammatory response in the lung airways. In marked contrast,  $\Delta^9$ -THC treated CB<sub>1</sub><sup>-/-</sup>/CB<sub>2</sub><sup>-/-</sup> mice infected with PR8 had a trend toward increased ( $p = 0.079$ ) inflammation of the pulmonary airways.

**J) Effects of CB<sub>1</sub> and CB<sub>2</sub> deficiency on the numeric cell densities of apoptotic cells and metaplastic goblet cells.**

Bronchiolar epithelial cell apoptosis in influenza-infected mice is directed by cell-mediated immune responses to virally infected cells (114). The numeric cell density for the apoptotic cell marker, CAS-3 (Figure 30) was quantified at 7 dpi in the epithelium lining generation 5 of the main axial airway. CAS-3 numeric cell densities were not

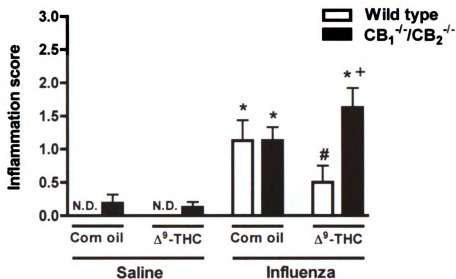


**Figure 29.** Effects of  $\Delta^9$ -THC treatment on histopathology-based inflammation scores in  $CB_1^{-/-}/CB_2^{-/-}$  and wild type mice. Effects of  $\Delta^9$ -THC on the inflammatory response gathered within the subepithelial interstitium and alveolar parenchyma following influenza challenge of the pulmonary airways in  $CB_1^{-/-}/CB_2^{-/-}$  and wild type mice. Mice were treated with  $\Delta^9$ -THC (75 mg/kg) or its corn oil vehicle for 5 consecutive days surrounding the intranasal instillation of influenza virus A/PR/8 or its vehicle SAL. Mice were euthanized on day 7 post infection. Lungs were fixed with 10% neutral-buffered formalin for 24 hours, then sectioned and stained with hematoxylin and eosin (H&E). Inflammation scores were recorded from lung sections taken on 7 dpi. Scores were tabulated and averaged for the two sections taken from generations 5 and 11 of the left lung lobe. Scores: 0 = no inflammation, 1 = mild, inflammatory cell infiltrate of the perivascular/peribronchiolar compartment, 2 = moderate, inflammatory cell infiltrate of the perivascular/peribronchiolar space with modest extension into the alveolar parenchyma, and 3 = severe, inflammatory cell infiltrate of the perivascular/peribronchiolar space with a greater magnitude of inflammatory foci found in the alveolar parenchyma. Data is expressed as mean  $\pm$  SEM; N.D. = not detectable. \* = significantly different from respective control instilled with SAL. + = significantly different from respective group in wild type mice.

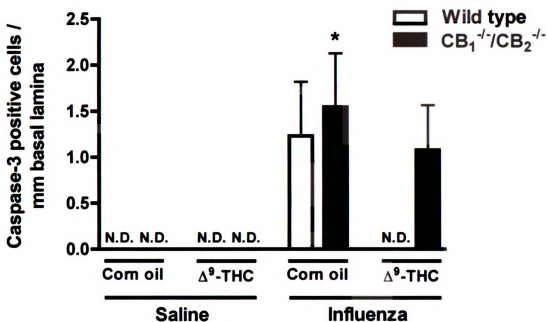


**Figure 30. Effects of  $\Delta^9$ -THC treatment on the numeric cell density of caspase-3 positive epithelial cells in  $CB_1^{-/-}/CB_2^{-/-}$  and wild type mice.** The effects of  $\Delta^9$ -THC on apoptotic cell death in response to influenza challenge.  $CB_1^{-/-}/CB_2^{-/-}$  and wild type mice were treated with  $\Delta^9$ -THC (75 mg/kg) or its corn oil vehicle for 5 consecutive days surrounding the intranasal instillation of influenza virus A/PR/8 or its vehicle SAL. Mice were euthanized on day 7 and 10 post infection. Lungs were immersed in TRI reagent for the isolation of total RNA or fixed with 10% neutral-buffered formalin for 24 hours, then sectioned and stained by immunohistochemistry for Caspase-3. Numeric cell densities were determined by enumerating caspase-3 positive nuclei per length of basal lamina. Data is expressed as mean  $\pm$  SEM; \* = significantly different from respective control instilled with SAL. # = significantly different from respective control gavaged with corn oil. + = significantly different from respective group in wild type mice.

distinguishably different between treatment groups in wild type mice. In PR8-infected  $CB_1^{-}/CB_2^{-}$  mice, CAS-3 levels were modestly increased above SAL instilled controls, but were no different than cell densities enumerated for  $CB_1^{-}/CB_2^{-}$  mice infected with PR8 and treated with  $\Delta^9$ -THC. During the recovery from viral infection a metaplastic change occurs in the epithelium lining the bronchi that includes increased numbers of mucus producing goblet cells (115). Consistent with our previous finding (113), there was no difference in the numeric cell density of mucus production (Figure 31) quantified at 7 dpi in wild type mice with any treatment. Rather interestingly,  $\Delta^9$ -THC treated  $CB_1^{-}/CB_2^{-}$  mice in the presence or absence of PR8 infection, exhibited significant increases in the numeric cell density for mucin-positive epithelial cells as compared to wild type mice.

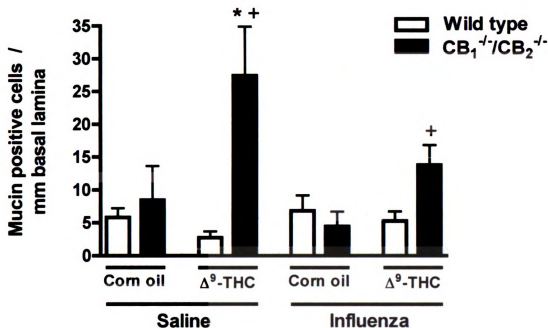


**Figure 31. Effects of  $\Delta^9$ -THC treatment on the numeric cell density of mucosubstances in airway epithelial cells in  $CB_1^{-}/CB_2^{-}$  and wild type mice.** The effects of  $\Delta^9$ -THC on the development of mucous cell metaplasia in the epithelium lining the main axial airway following influenza challenge and subsequent inflammatory cell responses.  $CB_1^{-}/CB_2^{-}$  and wild type mice were treated with  $\Delta^9$ -THC (75 mg/kg) or its corn oil vehicle for 5 consecutive days surrounding the intranasal instillation of influenza virus A/PR/8 or its vehicle SAL. Mice were euthanized on days 7 and 10 post infection. Lungs were fixed with 10% neutral-buffered formalin for 24 hours, then sectioned and stained with alcian blue/periodic acid Schiff (neutral and acidic mucosubstances). Numeric cell densities were determined by enumerating alcian blue positive secretory vesicles in epithelial cells per length of basal lamina from stained sections. Data is expressed as mean  $\pm$  SEM; \* = significantly different from respective control instilled with SAL. # = significantly different from respective control gavaged with corn oil. + = significantly different from respective group in wild type mice.

## **DISCUSSION**

The studies outlined in this dissertation were a part of an effort to evaluate the effects of  $\Delta^9$ -THC and the role of the cannabinoid receptors CB<sub>1</sub> and CB<sub>2</sub> on immune and pulmonary epithelial cell responses in a murine model of host-resistance to influenza virus A/PR/8/34 (Table 5).

### **I. Animals utilized in these studies**

In the studies outlined in this dissertation, C57BL/6 mice were utilized. C57BL/6 mice do not exhibit a genetically determined preference to either a T<sub>H</sub>1 or T<sub>H</sub>2 predominant immune response to pathogens like other mouse strains (e.g. AJ or BALB-C mice). In addition, CB<sub>1</sub>/CB<sub>2</sub> receptor knockout mice were developed on a C57BL/6 background.

### **II. The method of delivery and the dose of PR utilized**

In the studies outlined in this dissertation, a PR8 exposure paradigm was chosen such that the mice were instilled with a low concentration (50 pfu) of PR8 to ensure the survival of the mice for the duration of the kinetic study (21 days). In addition, PR8 was intranasally instilled in a large volume of SAL (50  $\mu$ l) to facilitate the delivery of PR8 to the lower airways. This paradigm is unlike most studies, wherein immune responses to influenza are examined within the first 6 – 10 days following a high concentration virus exposure.

### **III. The method of delivery and dose of $\Delta^9$ -THC utilized in these studies**

There are two major routes of exposure to  $\Delta^9$ -THC in humans, inhalation and oral

Effect of corn oil on:	Wild Type		CB <sub>1</sub> <sup>-/-</sup> /CB <sub>2</sub> <sup>-/-</sup>	
	Saline	PR8	Saline	PR8
<b>Epithelium</b>				
MCM	---	---	---	---
H&E	---	+	---	+
<b>Inflammatory cells</b>				
BALF Leukocytes	---	++	---	+++
BALF Cytokines	---	++	---	++
Histochemistry	---	++	---	++
<b>Effect of Δ<sup>9</sup>-THC on:</b>				
	Wild Type		CB <sub>1</sub> <sup>-/-</sup> /CB <sub>2</sub> <sup>-/-</sup>	
	Saline	PR8	Saline	PR8
<b>Epithelium</b>				
MCM	---	---	+++	+
H&E	---	+	---	++
<b>Inflammatory cells</b>				
BALF Leukocytes	---	+	---	+
BALF Cytokines	---	+	---	+
Histochemistry	---	+	---	+++

**Table 5. Summary of the effects of corn oil and Δ<sup>9</sup>-THC on BALF and histochemistry measurements taken for epithelial and inflammatory cells in wild type and CB<sub>1</sub><sup>-/-</sup>/CB<sub>2</sub><sup>-/-</sup> mice. Dashed line denotes no effect. A single plus denotes a mild effect, a double plus indicates a modest effect, and a triple plus signifies a marked response.**

consumption. In the studies outlined in this dissertation,  $\Delta^9$ -THC was administered orally in corn oil for five consecutive days. The oral route of administration was selected due to the fact that  $\Delta^9$ -THC is a highly lipophilic molecule requiring a nonaqueous diluent for drug delivery, which in itself has the likely potential for inducing irritation and damage to the airways. In contrast, oral administration of  $\Delta^9$ -THC in corn oil is well tolerated but poorly absorbed from the gastrointestinal tract resulting in modest blood concentrations of  $\Delta^9$ -THC and its metabolites. Oral administration of 75 mg/kg  $\Delta^9$ -THC for 5 consecutive days resulted in a serum concentration of 66.2 ng/ml of the parent compounds, 446.5 ng/ml of the 9-COOH metabolite and 10.5 ng/ml of the 11-OH metabolite, four hours after the last  $\Delta^9$ -THC dose. The levels of  $\Delta^9$ -THC observed systemically correlate well with a previous report by Azorlosa and coworkers (1992) (116) in which peak human plasma levels ranged from 57 to 268 ng/ml. PR8 was administered by intranasal instillation in SAL on Day 3, with  $\Delta^9$ -THC co-administration surrounding the day of infection. The rationale for this dosing paradigm was to investigate the putative effects of  $\Delta^9$ -THC treatment on the immune response to PR8 during the early stages of the primary infection.

#### **IV. Effect of $\Delta^9$ -THC on viral H1 mRNA levels in wild type and $CB_1^{-/-}/CB_2^{-/-}$ mice.**

Viral H1 mRNA levels were quantified by real-time PCR, which allows for the analysis of large numbers of samples in a rapid manner while retaining the specificity and sensitivity of conventional methods such as the hemagglutination assays (56, 117).  $\Delta^9$ -THC treated mice exhibited a higher pulmonary viral H1 mRNA content, that was dose-dependent and without an effect on mortality, when compared to PR8 infected mice

treated with corn oil. These results suggest that  $\Delta^9$ -THC administration impairs immune effectors involved in the clearance of PR8. By 10 dpi H1 mRNA levels approached the level of detection in all groups, hence suggesting that the clearance of the virus had occurred in all PR8 treatment groups. In comparison, influenza viral titres have been shown to return to baseline within 8 days of an uncomplicated influenza infection in humans (118).

In the comparison of wild type and  $CB_1^{-/-}/CB_2^{-/-}$  mice, we observed greater H1 mRNA levels in the lungs of  $\Delta^9$ -THC treated mice challenged with PR8 when compared to mice challenged with PR8 alone in both wild type and  $CB_1^{-/-}/CB_2^{-/-}$  mice (113). Similar to our previous observation, we observed H1 mRNA levels in the lungs of  $\Delta^9$ -THC treated  $CB_1^{-/-}/CB_2^{-/-}$  and wild type mice challenged with PR8 that were greater than H1 mRNA levels in  $CB_1^{-/-}/CB_2^{-/-}$  and wild type mice challenged with PR8 alone. Interestingly, H1 mRNA levels were reduced in the lungs of  $CB_1^{-/-}/CB_2^{-/-}$  mice by two orders of magnitude when compared to H1 mRNA levels observed for wild type mice. The profound reduction in H1 mRNA levels suggests that the cellular environment that supports viral entry or growth in the airway epithelium has been impaired in  $CB_1^{-/-}/CB_2^{-/-}$  mice when compared to wild type mice, or that the kinetics of the cell-mediated immune response are markedly enhanced in  $CB_1^{-/-}/CB_2^{-/-}$  mice. Our findings of increased background levels of  $CD4^+$  T cells in  $CB_1^{-/-}/CB_2^{-/-}$  mice, in the current study, support the latter explanation by suggesting that a hyper-responsive immunity toward PR8 infection brought about by the absence of functional cannabinoid receptors  $CB_1$  and  $CB_2$  exists. Moreover, since cannabinoid-mediated effects occurring through  $CB_1$  and  $CB_2$  receptors on the immune system are most often associated with the suppression of immune

responses, the results presented herein would be consistent with the idea that CB<sub>1</sub> and CB<sub>2</sub> receptors play a role in dampening immune responses to maintain immune homeostasis.

**V. Effect of PR8 on inflammatory cell recruitment to the pulmonary airways in the presence or absence of  $\Delta^9$ -THC in wild type and CB<sub>1</sub><sup>-/-</sup>/CB<sub>2</sub><sup>-/-</sup> mice.**

Inflammatory cells entering the airways of PR8 infected mice followed a classic pattern of inflammation, in which an early pro-inflammatory response, represented by neutrophilic influx followed by monocytes and macrophages, was observed early at 3 and 7 dpi, respectively, and a delayed host-immune response, characterized predominantly by an influx of lymphocytes and to a lesser extent eosinophils peaked by 10 dpi.

$\Delta^9$ -THC treatment did not influence the total number of leukocytes retrieved in BALF between mice challenged with PR8 in the absence and presence of  $\Delta^9$ -THC treatment. In spite of trends toward decreased total leukocytes in BALF with  $\Delta^9$ -THC treatment, further analysis of differential cell counts indicated that  $\Delta^9$ -THC treatment decreased, in a dose-related manner, the number of macrophages and lymphocytes in the airways. Berdyshev and coworkers (119) have previously reported similar findings with the dose-dependent modulation of immune cell recruitment to the lungs by  $\Delta^9$ -THC following endotoxin exposure.

In light of the observation that  $\Delta^9$ -THC modulated the differential leukocyte counts present in BALF, we further quantified the absolute number of CD4<sup>+</sup> and CD8<sup>+</sup> lymphocytes. Interestingly,  $\Delta^9$ -THC administration attenuated both CD4<sup>+</sup> and CD8<sup>+</sup> cell counts by 2-fold. It is noteworthy that measurements of BALF primarily provided

information on the cellular and soluble mediators present in the alveolar air space and not from cells within the alveolar tissue. Given the marked lymphocytic and monocytic infiltration of the airway submucosa, it was important to consider these data in conjunction with histopathology, which suggest that  $\Delta^9$ -THC modulated the immune response to PR8 through an influence on leukocyte migration. These findings are consistent with the effects of cannabinoids on lymphocyte and macrophage chemotaxis reported by others (120-123).

In the comparison between wild type and  $CB_1^{-}/CB_2^{-}$  mice, the magnitude of total leukocyte recruitment to the pulmonary airways and the cellular subsets present were similar between  $CB_1^{-}/CB_2^{-}$  and wild type mice challenged with PR8, in the absence of  $\Delta^9$ -THC treatment, suggesting that mice lacking functional  $CB_1/CB_2$  receptors were capable of mounting an aggressive immune response to PR8 infection. Differential cell counts provided evidence that the immune response to PR8 by  $CB_1^{-}/CB_2^{-}$  mice was more robust or efficient than the immune response mounted against PR8 in wild type mice. More specifically, the BALF-associated leukocytic subsets of macrophages and neutrophils were notably decreased in  $\Delta^9$ -THC treated  $CB_1^{-}/CB_2^{-}$  mice infected with PR8. The decreased recruitment of macrophages and neutrophils to the airways might point to a cannabinoid receptor dependent effect on the chemotaxis of these leukocytes. Contrary to findings with macrophages and neutrophils, there were remarkable similarities in the total number of BALF-associated lymphocytes among all treatment groups for  $CB_1^{-}/CB_2^{-}$  and wild type mice. Upon further examination of the T cell subsets retrieved in BALF, there was evidence that the T cell response to PR8 challenge with  $\Delta^9$ -THC treatment was predominantly  $CD4^+$  T cells in  $CB_1^{-}/CB_2^{-}$  mice. As

mentioned previously, increased numbers of CD4<sup>+</sup> T cells might suggest hyperresponsive immunity in CB<sub>1</sub><sup>-/-</sup>/CB<sub>2</sub><sup>-/-</sup> mice. However, the balance of the T-helper subset population, and the level of activity of these cells in the pulmonary airways remain unresolved.

**VI. Effect of PR8 on the release of soluble mediators into the pulmonary airways in the presence or absence of Δ<sup>9</sup>-THC in wild type and CB<sub>1</sub><sup>-/-</sup>/CB<sub>2</sub><sup>-/-</sup> mice.**

In addition to replicating in the epithelial cells of the respiratory tract, influenza also infects monocytes/macrophages and other leukocytes by binding to sialic acid receptor moieties on these cell types (28). Virus infection activates several transcription factors within these cells that are involved in the induction of chemokine and cytokine gene expression. These include nuclear factor kappa B (NF-κB), interferon regulatory factors (IRFs), activating protein (AP)-1, signal transducers and activators of transcription (STATs) and nuclear factor-interleukin 6 (NF-IL-6 or C/EBPβ) (36). Therefore, influenza plays a direct role in influencing the chemokine and cytokine makeup of the inflammatory response (reviewed by Julkunen (2001) (36) and Julkunen (2000) (29)). In these studies, the BALF-associated concentrations of MCP-1, TNF-α, IL-6, and IFN-γ were primarily affected by PR8 infection of mice as compared to mice instilled with SAL. MCP-1 is a chemokine that can be derived from either influenza-infected epithelia or infected monocytes/macrophages. IL-6 and TNF-α are pro-inflammatory cytokines produced predominantly by monocytes/macrophages. Instead of participating in an anti-viral capacity, TNF-α has been suggested to be a driving force for MCP-1 expression. IL-6 serves as a differentiation factor for lymphocytes and stimulates immunoglobulin production by B cells. Interferon-γ, produced by NK cells and/or T<sub>H</sub>1

cells, enhances the overall development of cell-mediated immunity, macrophage activation, antigen presentation, and chemokine gene expression. In these studies, each of these cytokines was significantly elevated at 7 dpi.

As shown in the kinetic study (115), the immune response to PR8 treatment resulted in increased levels of IL-6, TNF- $\alpha$ , IFN- $\gamma$ , MCP-1 and IL-10 by 7 dpi in BALF in the study that examined the dose-related effects of  $\Delta^9$ -THC. Collectively, no clear or obvious profile of activity emerged concerning the effects of  $\Delta^9$ -THC on PR8 cytokine or chemokine induction. This should not be altogether surprising as each cytokine and chemokine is regulated in its own unique manner with its own distinct kinetics. In addition, the molecular mechanism by which certain cytokines and chemokines are modulated by cannabinoids is only partially understood. In spite of this, several of the soluble inflammatory mediators evaluated in this study did exhibit dose-dependent modulation in response to  $\Delta^9$ -THC treatment. Specifically, treatment of PR8 infected mice with  $\Delta^9$ -THC at 50 mg/kg and 75 mg/kg led to increased levels of MCP-1 and IL-6 in the BALF, whereas IL-10 concentrations were decreased at these dosage levels of  $\Delta^9$ -THC. The modulation of these cytokines in response to cannabinoids is supported by previous findings in other experimental models (121, 124).

In the comparison of wild type and  $CB_1^{-/-}/CB_2^{-/-}$  mice, we observed increased total BALF associated protein in wild type mice challenged with PR8 that was mildly attenuated in  $\Delta^9$ -THC treated wild type mice infected with PR8. Interestingly, total protein levels in BALF from  $CB_1^{-/-}/CB_2^{-/-}$  mice challenged with PR8 alone were similar to wild type mice challenged with PR8 alone, yet were enhanced in  $\Delta^9$ -THC treated  $CB_1^{-/-}/CB_2^{-/-}$  mice challenged with PR8. Comparatively, a marked difference existed between

$\Delta^9$ -THC treated  $CB_1^{-/-}/CB_2^{-/-}$  and wild type mice infected with PR8, suggesting an increased severity in either vascular leakiness or inflammatory cell secretions in  $CB_1^{-/-}/CB_2^{-/-}$  mice. Consistent with increased amounts of total protein in BALF, inflammation scores accurately reflected changes observed in vascular leakiness. In addition to total protein, we also measure the BALF-associated chemokine/cytokine levels to provide information regarding the activity of leukocytes transient to the pulmonary airways. BALF-associated concentrations of MCP-1, TNF- $\alpha$ , and IFN- $\gamma$  in  $CB_1^{-/-}/CB_2^{-/-}$  mice infected with PR8, in the absence of  $\Delta^9$ -THC treatment were modestly elevated with respect to PR8 infected wild type mice. There was a trend toward decreased concentrations of these same cytokines in  $\Delta^9$ -THC-treated  $CB_1^{-/-}/CB_2^{-/-}$  mice infected with PR8; however, the collective findings did not provide evidence for  $CB_1$  and/or  $CB_2$  receptor-dependent or -independent regulation of the secretion of these cytokines. Since  $CB_1^{-/-}/CB_2^{-/-}$  mice had a lymphocytic response consisting of greater numbers of  $CD4^+$  T cells, and  $\Delta^9$ -THC treatment of  $CB_1^{-/-}/CB_2^{-/-}$  mice challenged with PR8 resulted in decreased concentrations of IFN- $\gamma$ , we also measured the BALF-associated concentrations of the  $T_H2$  cytokines IL-2, IL-4, and IL-5. It has been suggested that  $\Delta^9$ -THC treatment modulates cytokine production in a way that results in decreased  $T_H1$  cell-mediated immunity and increased  $T_H2$  humoral immunity (125, 126). Hence, we explored the potential for decreased  $T_H1$ -type with concomitantly increased  $T_H2$ -type cytokines in BALF. Only the cytokine IL-5 was markedly influenced by PR8 infection in wild type mice in the presence or absence of  $\Delta^9$ -THC. IL-5 concentrations were reduced in PR8-infected  $CB_1^{-/-}/CB_2^{-/-}$  mice in the presence or absence of  $\Delta^9$ -THC.  $\Delta^9$ -THC treatment of  $CB_1^{-/-}/CB_2^{-/-}$  or wild type mice infected with PR8 exhibited no effect on the levels of IL5

when compared to  $CB_1^{-}/CB_2^{-}$  or wild type mice infected with PR8 alone. The data suggest that the increased numbers of  $CD4^+$  T cells observed in  $CB_1^{-}/CB_2^{-}$  mice were not actively secreting more  $T_H2$ -type cytokines than wild type mice and that there was not an imbalance between  $T_H1$ - type and  $T_H2$ -type cytokines secreted due to  $\Delta^9$ -THC treatment in response to PR8.

We further evaluated the magnitude of the inflammatory response to PR8 by measuring serum chemokine/cytokine levels. The serum profile of the pro-inflammatory chemokine MCP-1 is markedly reduced for  $CB_1^{-}/CB_2^{-}$  mice challenged with PR8 in the presence or absence of  $\Delta^9$ -THC as compared to wild type mice. The reduction in serum MCP-1 is in stark contrast to elevated MCP-1 concentrations for the same treatment groups observed locally in BALF in  $CB_1^{-}/CB_2^{-}$  mice. The cytokines TNF- $\alpha$ , IL-6 and IFN- $\gamma$  were elevated with PR8 challenge in the presence or absence of  $\Delta^9$ -THC. However, these cytokines were elevated modestly with respect to the detection limits of the assay. To glean a better understanding of the possible kinetic contribution of these chemokines/cytokines to the status of immune effectors responding to PR8, their combined serum and BALF concentrations were considered. The combined local and serum concentrations for MCP-1 following PR8 challenge in the presence or absence of  $\Delta^9$ -THC suggest that macrophage recruitment signals are localized to the pulmonary airways in  $CB_1^{-}/CB_2^{-}$  mice and are more peripherally abundant in wild type mice. Furthermore, macrophage activity, as measured by TNF- $\alpha$  secretion, is enhanced both locally and peripherally with PR8 challenge in the presence and absence of  $\Delta^9$ -THC in  $CB_1^{-}/CB_2^{-}$  mice. More importantly, IFN- $\gamma$ , a cytokine derived from  $T_H1$  cells, is markedly elevated in  $CB_1^{-}/CB_2^{-}$  mice challenged with PR8 alone and suppressed by  $\Delta^9$ -

THC co-treatment. The combined peripheral and local chemokine/cytokine profiles in  $CB_1^{-}/CB_2^{-}$  mice suggest a more vigorous recruitment of leukocytes to the pulmonary airways following PR8 challenge.

## **VII. Effect of a single PR8 instillation on pulmonary histopathology in the presence or absence of $\Delta^9$ -THC in wild type and $CB_1^{-}/CB_2^{-}$ mice.**

To clarify the relationship between cellular and biochemical findings in BALF with the dynamic process of airway inflammation, we examined differences in immune cell recruitment and associated epithelial cell morphology by histopathology. Challenging mice with PR8 yielded an observed airway epithelial degeneration and necrosis by 3 dpi with more extensive epithelial regeneration by 7 and 10 dpi, evidenced by the basophilic nature of the epithelium observed with H&E staining and the positive staining of cellular nuclei with antibodies directed against PCNA. Epithelial regeneration peaked at 10 dpi, and resolved by 15 dpi. Coincident with the regenerative process, was an increase in the total number of epithelial cells enumerated in the PR8 infected group. While epithelial regeneration was still active at 10 dpi, we observed a metaplastic change of the epithelium to include more mucus-producing goblet cells that did not resolve by 21 dpi.

Given the marked inflammatory response evident at 7 dpi and the unique finding of MCM at 10 dpi, we examined the effects of  $\Delta^9$ -THC on leukocyte infiltration and morphologic changes of the airway epithelium associated with influenza infection. Inflammation scores for histopathology were assigned to assess the influence of  $\Delta^9$ -THC on the host immune cell responses to influenza infection.  $\Delta^9$ -THC, at all dose levels, attenuated the magnitude of inflammation at 10 dpi. Most impressively, the

histopathology clearly demonstrates that the inflammatory response in the lungs of mice challenged with influenza alone extends well beyond the perivascular/peribronchiolar submucosal compartment and into the alveolar parenchyma. With  $\Delta^9$ -THC treatment, the inflammatory response was still centered around the perivascular/peribronchiolar submucosal compartment; however, the magnitude and severity of inflammation extending into the alveolar parenchyma was greatly reduced. Therefore, there was less tissue injury observed with  $\Delta^9$ -THC treatment.

In the comparison of wild type and  $CB_1^{-/-}/CB_2^{-/-}$  mice, lung sections taken from the levels of the fifth (proximal) and eleventh (distal) airway generations to the main axial airway of the left lung lobe were scored for the magnitude and severity of inflammation present. Within saline instilled wild type mice there was no inflammation observed. On the other hand, in  $CB_1^{-/-}/CB_2^{-/-}$  mice there were 2 out of 8 mice instilled with saline, in the presence or absence of  $\Delta^9$ -THC treatment, which had modest evidence of inflammatory foci (Figures 8A and 8C). It remains unclear whether the isolated incidence of inflammation was the result of a subclinical infection in  $CB_1^{-/-}/CB_2^{-/-}$  mice that went undetected by serological screens or was a spontaneous occurrence of an underlying pathology in a mouse for which the absence of the cannabinoid receptors  $CB_1$  and  $CB_2$  might have rendered them immunologically hyper-responsive. Indeed, the  $CB_1^{-/-}/CB_2^{-/-}$  mice were subjected to an extensive battery of serological screens prior to their use and were found to be negative for all pathogens tested. Regardless, inflammation scores were similar for lung sections from  $CB_1^{-/-}/CB_2^{-/-}$  and wild type mice challenged with PR8, in the absence of  $\Delta^9$ -THC treatment. In fact, the histopathology for both PR8-infected  $CB_1^{-/-}/CB_2^{-/-}$  and wild type mice demonstrated a similar pattern of inflammatory

cells infiltrating the perivascular/peribronchiolar submucosa and exhibiting a diffuse infiltration of the alveolar airspace (Figures 7B and 8B). In  $\Delta^9$ -THC treated wild type mice challenged with PR8 there was a marked reduction in the inflammation score that was consistent with our previous finding (113). Also similar to our previous finding was the localization of inflammation to the submucosa with occasional inflammatory foci appearing in the alveolar parenchyma (Figure 8D). In contrast, inflammation scores for lung sections from  $\Delta^9$ -THC-treated  $CB_1^{-/-}/CB_2^{-/-}$  mice challenged with PR8 were modestly enhanced with respect to scores assessed for lung sections from  $CB_1^{-/-}/CB_2^{-/-}$  mice challenged with PR8 alone.  $CB_1^{-/-}/CB_2^{-/-}$  mice treated with  $\Delta^9$ -THC and infected with PR8 represented some of the most severely affected mice in the study and exhibited more vigorous inflammatory responses than  $CB_1^{-/-}/CB_2^{-/-}$  mice challenged with PR8 alone. Moreover the inflammatory response in  $\Delta^9$ -THC treated  $CB_1^{-/-}/CB_2^{-/-}$  mice infected with PR8 was more pronounced than the respective  $\Delta^9$ -THC treated wild type mice challenged with PR8. Also of interest, was the similarity between inflammation scores and concentrations of total BALF-associated protein and  $CD4^+$  T cells, suggesting that immune responses to PR8 in the  $CB_1^{-/-}/CB_2^{-/-}$  mouse are hypersensitive and include increased vascular permeability and a disproportionate number of  $CD4^+$  T cells.

#### **VIII. Effect of a single PR8 instillation on epithelial cell apoptosis and MCM in the presence or absence of $\Delta^9$ -THC in wild type and $CB_1^{-/-}/CB_2^{-/-}$ mice.**

Lastly, we examined epithelial cell changes in airways (e.g., apoptosis and MCM) that occurred during the immune response to PR8. CAS-3 is a well-known marker for committed activation of apoptosis (127). Apoptosis can be initiated either directly by the

virus in infected host cells (128, 129), or by effector cell functions of cytotoxic T cells or NK cells. PR8 treatment alone enhanced mRNA levels of CAS-3 and tissue staining as expected. There was a dose-related decrease in CAS-3 tissue staining, but not mRNA levels with  $\Delta^9$ -THC treatment. In the comparison of wild type and  $CB_1^{-/-}/CB_2^{-/-}$  mice, PR8 challenge led to increased CAS-3 staining as expected in both genotypes; however, there were no effects observed with  $\Delta^9$ -THC administration.

MCM is an adaptive response of the epithelium brought about by soluble mediators of inflammation. An early indicator of increased mucin production, and possibly MCM, is the expression of MUC5AC messenger RNA that encodes for the goblet cell-derived mucin MUC5AC. Mice challenged with PR8 in the absence of  $\Delta^9$ -THC exhibited an increase in both the levels of MUC5AC mRNA and alcian blue staining of tissue, as shown previously (115). Interestingly,  $\Delta^9$ -THC treatment at a dose of 25 mg/kg enhanced the levels of MUC5AC mRNA at 7 dpi, whereas the observed staining of mucosubstances was decreased with 75 mg/kg  $\Delta^9$ -THC at 10 dpi. Moreover, the dose-dependent effects of  $\Delta^9$ -THC treatment on MUC5AC mRNA at 7 dpi and mucosubstance staining at 10 dpi were similar in profile. It should be re-emphasized, that mRNA levels are reflective of whole lung homogenates, whereas quantification of morphologic changes in tissue sections (3 days later) is limited in scope to a single section of the lung. Therefore, the magnitude of the effect elicited by  $\Delta^9$ -THC is relative to the measurements made. It is presently unclear whether  $\Delta^9$ -THC treatment can directly interfere with upregulation of MUC5AC gene expression or whether the effect is mediated indirectly through the suppression of the inflammatory response, more specifically soluble mediators derived from macrophages and lymphocytes ( $CD4^+$  and

CD8<sup>+</sup> T cells). In the comparison of wild type and CB<sub>1</sub><sup>-/-</sup>/CB<sub>2</sub><sup>-/-</sup> mice, we surprisingly found that CB<sub>1</sub><sup>-/-</sup>/CB<sub>2</sub><sup>-/-</sup> mice had significantly greater numbers of goblet cells lining the airways at G5 when treated with Δ<sup>9</sup>-THC alone at 7 dpi, suggesting that Δ<sup>9</sup>-THC is potentially interacting directly with a signaling pathway tied with increased mucin production or mucous cell metaplasia in CB<sub>1</sub><sup>-/-</sup>/CB<sub>2</sub><sup>-/-</sup> mice.

### **VIII. Significance and relevance**

The body of work presented in this dissertation is a significant contribution to our understanding of Δ<sup>9</sup>-THC and host-immunity to influenza infection. The present project characterized time-dependent epithelial and leukocyte responses to a low titre PR8 infection of the pulmonary airways of mice. A rather unique finding in our characterization was time-dependent PR8-induced MCM of the bronchiolar epithelium. Although, MCM has been previously reported for adenovirus (23), respiratory syncytial virus (RSV) (24) and influenza virus (25) infection, the study conducted as a part of this project was the first to characterize the adaptive epithelial response using morphometric analysis of the epithelium and cytometric bead array technology to examine a panel of cytokines that have been implicated in its etiology.

A second unique contribution of these studies was the use of orally administered Δ<sup>9</sup>-THC. Typically, Δ<sup>9</sup>-THC has been administered either intraperitoneally or intravenously for host immunity studies. These routes of administration result in larger circulating concentrations of Δ<sup>9</sup>-THC, initially. The circulating levels of Δ<sup>9</sup>-THC measured in the present studies were in the ng/ml range for Δ<sup>9</sup>-THC and its metabolites. The concentrations of Δ<sup>9</sup>-THC measured were a reflection of the poor absorption of Δ<sup>9</sup>-

THC from the gastrointestinal tract following oral administration. Nevertheless, it was interesting that these low circulating levels of  $\Delta^9$ -THC were still capable of altering host-immunity, in particular leukocyte recruitment, to result in increased levels of viral H1 mRNA.

Another unique aspect of these studies was the analysis of viral burden by quantitative real-time RT-PCR of the H1 gene. Traditionally, viral burden is measured by the Madin-Darby Canine Kidney (MDCK) cell assay. The difficulty with the MDCK assay is that it is not practical for a large number of samples and is not sensitive enough to distinguish between small differences in burden brought about by the introduction of another variable, like  $\Delta^9$ -THC treatment. Quantitative PCR-based methods have been shown to have greater sensitivity and specificity as compared to conventional methods for quantifying influenza virus, such as hemagglutination assays (56, 117). Moreover, RT-PCR allows for the analysis of large numbers of samples in a rapid and sensitive manner. Accordingly, the detection of viral H1 message in these studies demonstrated that  $\Delta^9$ -THC administration influenced viral H1 mRNA levels in a dose-dependent manner.

Finally, these studies employed the use of  $CB_1^{-/-}/CB_2^{-/-}$  mice to elucidate the role of the cannabinoid receptors  $CB_1$  and  $CB_2$  in the modulation of immune and epithelial cell responses to PR8. Prior to the generation of  $CB_1^{-/-}/CB_2^{-/-}$  mice, the identification of  $CB_1$  and  $CB_2$  receptor-mediated events brought about by  $\Delta^9$ -THC treatment were assessed by utilizing cannabinoid receptor antagonists for  $CB_1$  and  $CB_2$  (e.g., SR141716 and SR144528, respectively). However, these cannabinoid receptor antagonists have also been shown to have partial and inverse agonist properties (130-132). Since the

generation of  $CB_1^{-/-}/CB_2^{-/-}$  mice, studies from our laboratory have begun to address the  $CB_1$  and  $CB_2$  receptor-independent actions for the suppression of the expression of cytokines IL-2 and IFN- $\gamma$  by the endocannabinoid 2-arachidonyl glycerol (83, 133). In the current studies, wild type and  $CB_1^{-/-}/CB_2^{-/-}$  mice infected with PR8 in the presence or absence of  $\Delta^9$ -THC demonstrate similarities in detectable levels of viral H1 mRNA and leukocyte recruitment, suggesting a  $CB_1/CB_2$  receptor-independent mechanism of increased viral H1 mRNA content. However, the magnitude of expression of viral H1 mRNA was reduced by several orders of magnitude in  $CB_1^{-/-}/CB_2^{-/-}$  mice and there were markedly greater numbers of  $CD4^+$  T cells in the receptor-null genotype, suggesting that the kinetics for immune-mediated viral clearance were altered due to the lack of  $CB_1/CB_2$  receptors. Therefore, the latter finding emphasized a  $CB_1/CB_2$  receptor-dependence for normal leukocyte recruitment and activation. In addition, another finding unique to the  $CB_1^{-/-}/CB_2^{-/-}$  mice was the increased numeric cell density of mucin-positive epithelial cells with  $\Delta^9$ -THC treatment alone. The induction of MCM by  $\Delta^9$ -THC in the absence of PR8 challenge and, more importantly, in the absence of  $CB_1/CB_2$  receptors indicates that there are, indeed, other  $CB_1/CB_2$  receptor-independent activities commenced by treatment with  $\Delta^9$ -THC.

This body of work is a relevant contribution to our understanding of the potential human health impacts of exposure to chemical agents that render individuals more susceptible to infection. In these studies we demonstrated that the use of an oral dose of  $\Delta^9$ -THC, that produced serum levels of the parent compound in mice comparable to those found in humans, decreased host-immunity (e.g.; decreased leukocyte recruitment) to influenza virus while leading to increased levels of H1 mRNA in the lungs. This finding

is important in light of recent concerns regarding the potential for pandemic influenza infections and the susceptibility to infection of individuals who lack competent immune systems.

In the last four years attention has been drawn to the newly emergent H5N1 influenza strain that has killed millions of birds in Asia. This virulent strain has jumped species by infecting and killing a small number of people in Asia. Currently, the H5N1 strain has not mutated enough to allow for the efficient human-to-human transmission. However, it is noteworthy that the influenza pandemic of 1918 similarly started as a bird flu. Unlike previous pandemics, the threat of spreading influenza virus globally with greater speed has been enhanced by our advances in travel. Therefore early detection has become a priority amongst health organizations like the Centers for Disease Control and the World Health Organization. In addition, people regarded as belonging to a group of individuals that are more “susceptible” to influenza have been encouraged to seek early vaccination. However the term “susceptible” is nebulous, and based on current guidelines, includes individuals with chemical-induced immune suppression.

Within the last two decades we have witnessed, or in some states voted on, legislation dealing with the use of marijuana for medicinal purposes. This issue has been brought to our attention by advocates of medical marijuana for persons suffering from the adverse wasting effects of acquired immune deficiency syndrome (AIDS) or from nausea resulting from AIDS or chemotherapy (for treatment of AIDS or cancer). In 1985, the Food and Drug Administration approved the drug Marinol, a synthetic  $\Delta^9$ -THC, for the treatment of these symptoms; however, patients have contested that the effects of this pure psychoactive drug rendered them incapacitated. Although patients suffering from

AIDS or cancer may claim a therapeutic benefit from marijuana or its components, little is known regarding increased susceptibility of AIDS or cancer patients consuming Marinol or marijuana to infection by respirable pathogens, in light of an already compromised immunity. This is an important point since one of the two known cannabinoid receptors (CB<sub>2</sub>) is found on immune cells, and cannabinoids have been shown in human and animal-derived immune cells to be immune suppressive. Therefore, even within the general population, recreational users of marijuana may be placing themselves at an added risk for a respiratory infection.

Given the increased viral burden resulting from treating PR8-infected mice with  $\Delta^9$ -THC, we explored the role of CB<sub>1</sub> and CB<sub>2</sub> receptors in regulating  $\Delta^9$ -THC-mediated immune suppression. The observations in these studies clearly point to the importance these receptors have in maintaining homeostatic immune responsiveness. These studies also provide evidence that there are other potential receptor targets for  $\Delta^9$ -THC. For example, the observation of increased MCM in CB<sub>1</sub><sup>-/-</sup>/CB<sub>2</sub><sup>-/-</sup> mice treated with  $\Delta^9$ -THC may provide a tool with which to evaluate signaling pathways linked with this metaplastic event in bronchiolar epithelium.

## LITERATURE CITED

1. Reznik, G. K. 1990. Comparative anatomy, physiology, and function of the upper respiratory tract. *Environ Health Perspect* 85:171.
2. Ward, H. E., and T. E. Nicholas. 1984. Alveolar type I and type II cells. *Aust N Z J Med* 14:731.
3. Castranova, V., J. Rabovsky, J. H. Tucker, and P. R. Miles. 1988. The alveolar type II epithelial cell: a multifunctional pneumocyte. *Toxicol Appl Pharmacol* 93:472.
4. Houtmeyers, E., R. Gosselink, G. Gayan-Ramirez, and M. Decramer. 1999. Regulation of mucociliary clearance in health and disease. *Eur Respir J* 13:1177.
5. Clarke, S. W. 1989. Rationale of airway clearance. *Eur Respir J Suppl* 7:599s.
6. Swain, S. L., J. N. Agrewala, D. M. Brown, D. M. Jelley-Gibbs, S. Golech, G. Huston, S. C. Jones, C. Kamperschroer, W. H. Lee, K. K. McKinstry, E. Roman, T. Strutt, and N. P. Weng. 2006. CD4+ T-cell memory: generation and multifaceted roles for CD4+ T cells in protective immunity to influenza. *Immunol Rev* 211:8.
7. Brown, D. M., A. M. Dilzer, D. L. Meents, and S. L. Swain. 2006. CD4 T cell-mediated protection from lethal influenza: perforin and antibody-mediated mechanisms give a one-two punch. *J Immunol* 177:2888.
8. Brown, D. M., E. Roman, and S. L. Swain. 2004. CD4 T cell responses to influenza infection. *Semin Immunol* 16:171.
9. Yagita, H., S. Hanabuchi, Y. Asano, T. Tamura, H. Nariuchi, and K. Okumura. 1995. Fas-mediated cytotoxicity--a new immunoregulatory and pathogenic function of Th1 CD4+ T cells. *Immunol Rev* 146:223.
10. Hahn, S., R. Gehri, and P. Erb. 1995. Mechanism and biological significance of CD4-mediated cytotoxicity. *Immunol Rev* 146:57.
11. Kumar, R. K., C. Herbert, and M. Kasper. 2004. Reversibility of airway inflammation and remodelling following cessation of antigenic challenge in a model of chronic asthma. *Clin Exp Allergy* 34:1796.
12. Reader, J. R., J. S. Tepper, E. S. Schelegle, M. C. Aldrich, L. F. Putney, J. W. Pfeiffer, and D. M. Hyde. 2003. Pathogenesis of mucous cell metaplasia in a murine asthma model. *Am J Pathol* 162:2069.

13. Tesfaigzi, Y. 2002. The role of apoptotic regulators in metaplastic mucous cells. *Novartis Found Symp* 248:221.
14. Fanucchi, M. V., J. A. Hotchkiss, and J. R. Harkema. 1998. Endotoxin potentiates ozone-induced mucous cell metaplasia in rat nasal epithelium. *Toxicol Appl Pharmacol* 152:1.
15. Harkema, J. R., and J. A. Hotchkiss. 1993. Ozone- and endotoxin-induced mucous cell metaplasias in rat airway epithelium: novel animal models to study toxicant-induced epithelial transformation in airways. *Toxicol Lett* 68:251.
16. Jamil, S., R. Breuer, and T. G. Christensen. 1997. Abnormal mucous cell phenotype induced by neutrophil elastase in hamster bronchi. *Exp Lung Res* 23:285.
17. Kawano, H., A. Haruta, Y. Tsuboi, Y. Kim, P. A. Schachern, M. M. Paparella, and J. Lin. 2002. Induction of mucous cell metaplasia by tumor necrosis factor alpha in rat middle ear: the pathological basis for mucin hyperproduction in mucoid otitis media. *Ann Otol Rhinol Laryngol* 111:415.
18. Dabbagh, K., K. Takeyama, H. M. Lee, I. F. Ueki, J. A. Lausier, and J. A. Nadel. 1999. IL-4 induces mucin gene expression and goblet cell metaplasia in vitro and in vivo. *J Immunol* 162:6233.
19. Justice, J. P., J. Crosby, M. T. Borchers, A. Tomkinson, J. J. Lee, and N. A. Lee. 2002. CD4(+) T cell-dependent airway mucus production occurs in response to IL-5 expression in lung. *Am J Physiol Lung Cell Mol Physiol* 282:L1066.
20. Reader, J. R., D. M. Hyde, E. S. Schelegle, M. C. Aldrich, A. M. Stoddard, M. P. McLane, R. C. Levitt, and J. S. Tepper. 2003. Interleukin-9 induces mucous cell metaplasia independent of inflammation. *Am J Respir Cell Mol Biol* 28:664.
21. Shim, J. J., K. Dabbagh, I. F. Ueki, T. Dao-Pick, P. R. Burgel, K. Takeyama, D. C. Tam, and J. A. Nadel. 2001. IL-13 induces mucin production by stimulating epidermal growth factor receptors and by activating neutrophils. *Am J Physiol Lung Cell Mol Physiol* 280:L134.
22. Holtzman, M. J., J. T. Battaile, and A. C. Patel. 2006. Immunogenetic programs for viral induction of mucous cell metaplasia. *Am J Respir Cell Mol Biol* 35:29.
23. Kajon, A. E., A. P. Gigliotti, and K. S. Harrod. 2003. Acute inflammatory response and remodeling of airway epithelium after subspecies B1 human adenovirus infection of the mouse lower respiratory tract. *J Med Virol* 71:233.
24. Harrod, K. S., R. J. Jaramillo, C. L. Rosenberger, S. Z. Wang, J. A. Berger, J. D. McDonald, and M. D. Reed. 2003. Increased susceptibility to RSV infection by

- exposure to inhaled diesel engine emissions. *Am J Respir Cell Mol Biol* 28:451.
25. Wohlleben, G., J. Muller, U. Tatsch, C. Hambrecht, U. Herz, H. Renz, E. Schmitt, H. Moll, and K. J. Erb. 2003. Influenza A virus infection inhibits the efficient recruitment of Th2 cells into the airways and the development of airway eosinophilia. *J Immunol* 170:4601.
  26. Uhal, B. D., K. M. Flowers, and D. E. Rannels. 1991. Type II pneumocyte proliferation in vitro: problems and future directions. *Am J Physiol* 261:110.
  27. Palese, P., and J. L. Schulman. 1976. Mapping of the influenza virus genome: identification of the hemagglutinin and the neuraminidase genes. *Proc Natl Acad Sci USA* 73:2142.
  28. Ronni, T., T. Sareneva, J. Pirhonen, and I. Julkunen. 1995. Activation of IFN-alpha, IFN-gamma, MxA, and IFN regulatory factor 1 genes in influenza A virus-infected human peripheral blood mononuclear cells. *J Immunol* 154:2764.
  29. Julkunen, I., K. Melen, M. Nyqvist, J. Pirhonen, T. Sareneva, and S. Matikainen. 2000. Inflammatory responses in influenza A virus infection. *Vaccine* 19 Suppl 1:S32.
  30. Chu, V. C., and G. R. Whittaker. 2004. Influenza virus entry and infection require host cell N-linked glycoprotein. *Proc Natl Acad Sci USA* 101:18153.
  31. Tsuru, S., H. Fujisawa, M. Taniguchi, Y. Zinnaka, and K. Nomoto. 1987. Mechanism of protection during the early phase of a generalized viral infection. II. Contribution of polymorphonuclear leukocytes to protection against intravenous infection with influenza virus. *J Gen Virol* 68 (Pt 2):419.
  32. Allan, W., Z. Tabi, A. Cleary, and P. C. Doherty. 1990. Cellular events in the lymph node and lung of mice with influenza. Consequences of depleting CD4+ T cells. *J Immunol* 144:3980.
  33. Graham, M. B., V. L. Braciale, and T. J. Braciale. 1994. Influenza virus-specific CD4+ T helper type 2 T lymphocytes do not promote recovery from experimental virus infection. *J Exp Med* 180:1273.
  34. Moran, T. M., H. Park, A. Fernandez-Sesma, and J. L. Schulman. 1999. Th2 responses to inactivated influenza virus can be converted to Th1 responses and facilitate recovery from heterosubtypic virus infection. *J Infect Dis* 180:579.
  35. Baumgarth, N., O. C. Herman, G. C. Jager, L. E. Brown, L. A. Herzenberg, and J. Chen. 2000. B-1 and B-2 cell-derived immunoglobulin M antibodies are nonredundant components of the protective response to influenza virus infection. *J Exp Med* 192:271.

36. Julkunen, I., T. Sareneva, J. Pirhonen, T. Ronni, K. Melen, and S. Matikainen. 2001. Molecular pathogenesis of influenza A virus infection and virus-induced regulation of cytokine gene expression. *Cytokine Growth Factor Rev* 12:171.
37. Zlotnik, A., and O. Yoshie. 2000. Chemokines: a new classification system and their role in immunity. *Immunity* 12:121.
38. Sprenger, H., R. G. Meyer, A. Kaufmann, D. Bussfeld, E. Rischkowsky, and D. Gemsa. 1996. Selective induction of monocyte and not neutrophil-attracting chemokines after influenza A virus infection. *J Exp Med* 184:1191.
39. Bussfeld, D., A. Kaufmann, R. G. Meyer, D. Gemsa, and H. Sprenger. 1998. Differential mononuclear leukocyte attracting chemokine production after stimulation with active and inactivated influenza A virus. *Cell Immunol* 186:1.
40. Matikainen, S., J. Pirhonen, M. Miettinen, A. Lehtonen, C. Govenius-Vintola, T. Sareneva, and I. Julkunen. 2000. Influenza A and sendai viruses induce differential chemokine gene expression and transcription factor activation in human macrophages. *Virology* 276:138.
41. Matsukura, S., F. Kokubu, H. Noda, H. Tokunaga, and M. Adachi. 1996. Expression of IL-6, IL-8, and RANTES on human bronchial epithelial cells, NCI-H292, induced by influenza virus A. *J Allergy Clin Immunol* 98:1080.
42. Adachi, M., S. Matsukura, H. Tokunaga, and F. Kokubu. 1997. Expression of cytokines on human bronchial epithelial cells induced by influenza virus A. *Int Arch Allergy Immunol* 113:307.
43. Sareneva, T., S. Matikainen, M. Kurimoto, and I. Julkunen. 1998. Influenza A virus-induced IFN-alpha/beta and IL-18 synergistically enhance IFN-gamma gene expression in human T cells. *J Immunol* 160:6032.
44. Nain, M., F. Hinder, J. H. Gong, A. Schmidt, A. Bender, H. Sprenger, and D. Gemsa. 1990. Tumor necrosis factor-alpha production of influenza A virus-infected macrophages and potentiating effect of lipopolysaccharides. *J Immunol* 145:1921.
45. Gong, J. H., H. Sprenger, F. Hinder, A. Bender, A. Schmidt, S. Horch, M. Nain, and D. Gemsa. 1991. Influenza A virus infection of macrophages. Enhanced tumor necrosis factor-alpha (TNF-alpha) gene expression and lipopolysaccharide-triggered TNF-alpha release. *J Immunol* 147:3507.
46. Ronni, T., S. Matikainen, T. Sareneva, K. Melen, J. Pirhonen, P. Keskinen, and I. Julkunen. 1997. Regulation of IFN-alpha/beta, MxA, 2',5'-oligoadenylate synthetase, and HLA gene expression in influenza A-infected human lung

- epithelial cells. *J Immunol* 158:2363.
47. Cella, M., M. Salio, Y. Sakakibara, H. Langen, I. Julkunen, and A. Lanzavecchia. 1999. Maturation, activation, and protection of dendritic cells induced by double-stranded RNA. *J Exp Med* 189:821.
  48. Baggiolini, M. 1998. Chemokines and leukocyte traffic. *Nature* 392:565.
  49. Stark, G. R. 1997. Genetic analysis of interferon and other mammalian signaling pathways. *Harvey Lect* 93:1.
  50. Marrack, P., J. Kappler, and T. Mitchell. 1999. Type I interferons keep activated T cells alive. *J Exp Med* 189:521.
  51. Choi, A. M., K. Knobil, S. L. Otterbein, D. A. Eastman, and D. B. Jacoby. 1996. Oxidant stress responses in influenza virus pneumonia: gene expression and transcription factor activation. *Am J Physiol* 271:L383.
  52. Hofmann, P., H. Sprenger, A. Kaufmann, A. Bender, C. Hasse, M. Nain, and D. Gemsa. 1997. Susceptibility of mononuclear phagocytes to influenza A virus infection and possible role in the antiviral response. *J Leukoc Biol* 61:408.
  53. Pahl, H. L., and P. A. Baeuerle. 1995. Expression of influenza virus hemagglutinin activates transcription factor NF-kappa B. *J Virol* 69:1480.
  54. Flory, E., M. Kunz, C. Scheller, C. Jassoy, R. Stauber, U. R. Rapp, and S. Ludwig. 2000. Influenza virus-induced NF-kappaB-dependent gene expression is mediated by overexpression of viral proteins and involves oxidative radicals and activation of IkappaB kinase. *J Biol Chem* 275:8307.
  55. Hahon, N., J. A. Booth, F. Green, and T. R. Lewis. 1985. Influenza virus infection in mice after exposure to coal dust and diesel engine emissions. *Environ Res* 37:44.
  56. Jaspers, I., J. M. Ciencewicki, W. Zhang, L. E. Brighton, J. L. Carson, M. A. Beck, and M. C. Madden. 2005. Diesel exhaust enhances influenza virus infections in respiratory epithelial cells. *Toxicol Sci* 85:990.
  57. Cai, J., Y. Chen, S. Seth, S. Furukawa, R. W. Compans, and D. P. Jones. 2003. Inhibition of influenza infection by glutathione. *Free Radic Biol Med* 34:928.
  58. Lippmann, M., and R. B. Schlesinger. 2000. Toxicological bases for the setting of health-related air pollution standards. *Annu Rev Public Health* 21:309.
  59. Graham, D. E., and H. S. Koren. 1990. Biomarkers of inflammation in ozone-exposed humans. Comparison of the nasal and bronchoalveolar lavage. *Am Rev*

*Respir Dis 142:152.*

60. Wolcott, J. A., Y. C. Zee, and J. W. Osebold. 1982. Exposure to ozone reduces influenza disease severity and alters distribution of influenza viral antigens in murine lungs. *Appl Environ Microbiol 44:723.*
61. Boatman, E. S., and R. Frank. 1974. Morphologic and ultrastructural changes in the lungs of animals during acute exposure to ozone. *Chest 65:Suppl:9S.*
62. Dungworth, D. L., W. L. Castleman, C. K. Chow, P. W. Mellick, M. G. Mustafa, B. Tarkington, and W. S. Tyler. 1975. Effect of ambient levels of ozone on monkeys. *Fed Proc 34:1670.*
63. Freeman, G., R. J. Stephens, D. L. Coffin, and J. F. Stara. 1973. Changes in dogs' lung after long-term exposure to ozone: light and electron microscopy. *Arch Environ Health 26:209.*
64. Dewey, W. L. 1986. Cannabinoid pharmacology. *Pharmacol Rev 38:151.*
65. Mechoulam, R., and Y. Gaoni. 1965. Hashish. IV. The isolation and structure of cannabinolic cannabidiolic and cannabigerolic acids. *Tetrahedron 21:1223.*
66. Turk, R. F., J. E. Manno, N. C. Jain, and R. B. Forney. 1971. The identification, isolation, and preservation of delta-9-tetrahydrocannabinol (delta-9-THC). *J Pharm Pharmacol 23:190.*
67. Coper, H. 1982. Chapter 8. Pharmacology and Toxicology of Cannabis. In *Handbook of Experimental Pharmacology*. Vol. 55/III. F. Hoffmeister, Stille, G., ed. Springer-Verlag, Berlin Heidelberg New York, p. 135.
68. Coper, H., Fernandes, M., Honecker, H., Kluwe, S. 1971. The influence of solvent agents on the effects of cannabis. *Acta Pharmacol. Toxicol. 29:89.*
69. Perez-Reyes, M., M. A. Lipton, M. C. Timmons, M. E. Wall, D. R. Brine, and K. H. Davis. 1973. Pharmacology of orally administered 9 -tetrahydrocannabinol. *Clin Pharmacol Ther 14:48.*
70. Klausner, H. A., and J. V. Dingell. 1971. The metabolism and excretion of delta 9-tetrahydrocannabinol in the rat. *Life Sci 10:49.*
71. Ho, B. T., Fritchie, G.E., Kralik, P.M., Englert, L.F., McIsaac, W.M., Idanpaan-Heikkila, J. 1970. Distribution of tritiated-1- $\Delta^9$ -tetrahydrocannabinol in rat tissue after inhalation. *Journal of Pharmacy and Pharmacology 22:538.*
72. Matsuda, L. A., S. J. Lolait, M. J. Brownstein, A. C. Young, and T. I. Bonner. 1990. Structure of a cannabinoid receptor and functional expression of the cloned

cDNA. *Nature* 346:561.

73. Munro, S., K. L. Thomas, and M. Abu-Shaar. 1993. Molecular characterization of a peripheral receptor for cannabinoids. *Nature* 365:61.
74. Pettit, D. A., D. L. Anders, M. P. Harrison, and G. A. Cabral. 1996. Cannabinoid receptor expression in immune cells. *Adv Exp Med Biol* 402:119.
75. Schatz, A. R., M. Lee, R. B. Condie, J. T. Pulaski, and N. E. Kaminski. 1997. Cannabinoid receptors CB1 and CB2: a characterization of expression and adenylate cyclase modulation within the immune system. *Toxicol Appl Pharmacol* 142:278.
76. McCoy, K. L., M. Matveyeva, S. J. Carlisle, and G. A. Cabral. 1999. Cannabinoid inhibition of the processing of intact lysozyme by macrophages: evidence for CB2 receptor participation. *J Pharmacol Exp Ther* 289:1620.
77. Buckley, N. E., K. L. McCoy, E. Mezey, T. Bonner, A. Zimmer, C. C. Felder, M. Glass, and A. Zimmer. 2000. Immunomodulation by cannabinoids is absent in mice deficient for the cannabinoid CB(2) receptor. *Eur J Pharmacol* 396:141.
78. Zhu, L. X., S. Sharma, M. Stolina, B. Gardner, M. D. Roth, D. P. Tashkin, and S. M. Dubinett. 2000. Delta-9-tetrahydrocannabinol inhibits antitumor immunity by a CB2 receptor-mediated, cytokine-dependent pathway. *J Immunol* 165:373.
79. Ruiz, L., A. Miguel, and I. Diaz-Laviada. 1999. Delta9-tetrahydrocannabinol induces apoptosis in human prostate PC-3 cells via a receptor-independent mechanism. *FEBS Lett* 458:400.
80. Chen, Y., and J. Buck. 2000. Cannabinoids protect cells from oxidative cell death: a receptor-independent mechanism. *J Pharmacol Exp Ther* 293:807.
81. Zygmunt, P. M., D. A. Andersson, and E. D. Hogestatt. 2002. Delta 9-tetrahydrocannabinol and cannabinol activate capsaicin-sensitive sensory nerves via a CB1 and CB2 cannabinoid receptor-independent mechanism. *J Neurosci* 22:4720.
82. Kaplan, B. L., C. E. Rockwell, and N. E. Kaminski. 2003. Evidence for cannabinoid receptor-dependent and -independent mechanisms of action in leukocytes. *J Pharmacol Exp Ther* 306:1077.
83. Kaplan, B. L., Y. Ouyang, C. E. Rockwell, G. K. Rao, and N. E. Kaminski. 2005. 2-Arachidonoyl-glycerol suppresses interferon-gamma production in phorbol ester/ionomycin-activated mouse splenocytes independent of CB1 or CB2. *J Leukoc Biol* 77:966.

84. Costa, B., M. Colleoni, S. Conti, D. Parolaro, C. Franke, A. E. Trovato, and G. Giagnoni. 2004. Oral anti-inflammatory activity of cannabidiol, a non-psychoactive constituent of cannabis, in acute carrageenan-induced inflammation in the rat paw. *Naunyn Schmiedebergs Arch Pharmacol* 369:294.
85. Watzl, B., P. Scuderi, and R. R. Watson. 1991. Influence of marijuana components (THC and CBD) on human mononuclear cell cytokine secretion in vitro. *Adv Exp Med Biol* 288:63.
86. Srivastava, M. D., B. I. Srivastava, and B. Brouhard. 1998. Delta9 tetrahydrocannabinol and cannabidiol alter cytokine production by human immune cells. *Immunopharmacology* 40:179.
87. Zimmer, A., A. M. Zimmer, A. G. Hohmann, M. Herkenham, and T. I. Bonner. 1999. Increased mortality, hypoactivity, and hypoalgesia in cannabinoid CB1 receptor knockout mice. *Proc Natl Acad Sci U S A* 96:5780.
88. Galiegue, S., S. Mary, J. Marchand, D. Dussossoy, D. Carriere, P. Carayon, M. Bouaboula, D. Shire, G. Le Fur, and P. Casellas. 1995. Expression of central and peripheral cannabinoid receptors in human immune tissues and leukocyte subpopulations. *Eur J Biochem* 232:54.
89. Specter, S., G. Lancz, G. Westrich, and H. Friedman. 1991. Delta-9-tetrahydrocannabinol augments murine retroviral induced immunosuppression and infection. *Int J Immunopharmacol* 13:411.
90. Zheng, Z. M., S. Specter, and H. Friedman. 1992. Inhibition by delta-9-tetrahydrocannabinol of tumor necrosis factor alpha production by mouse and human macrophages. *Int J Immunopharmacol* 14:1445.
91. Coffey, R. G., Y. Yamamoto, E. Snella, and S. Pross. 1996. Tetrahydrocannabinol inhibition of macrophage nitric oxide production. *Biochem Pharmacol* 52:743.
92. Zhu, W., C. Newton, Y. Daaka, H. Friedman, and T. W. Klein. 1994. delta 9-Tetrahydrocannabinol enhances the secretion of interleukin 1 from endotoxin-stimulated macrophages. *J Pharmacol Exp Ther* 270:1334.
93. McCoy, K. L., D. Gainey, and G. A. Cabral. 1995. delta 9-Tetrahydrocannabinol modulates antigen processing by macrophages. *J Pharmacol Exp Ther* 273:1216.
94. Smith, S. R., G. Denhardt, and C. Terminelli. 2001. The anti-inflammatory activities of cannabinoid receptor ligands in mouse peritonitis models. *Eur J Pharmacol* 432:107.
95. Kawakami, Y., T. W. Klein, C. Newton, J. Y. Djeu, G. Dennert, S. Specter, and H. Friedman. 1988. Suppression by cannabinoids of a cloned cell line with natural

- killer cell activity. *Proc Soc Exp Biol Med* 187:355.
96. Klein, T. W., C. A. Newton, R. Widen, and H. Friedman. 1985. The effect of delta-9-tetrahydrocannabinol and 11-hydroxy-delta-9-tetrahydrocannabinol on T-lymphocyte and B-lymphocyte mitogen responses. *J Immunopharmacol* 7:451.
  97. Kawakami, Y., T. W. Klein, C. Newton, J. Y. Djeu, S. Specter, and H. Friedman. 1988. Suppression by delta-9-tetrahydrocannabinol of interleukin 2-induced lymphocyte proliferation and lymphokine-activated killer cell activity. *Int J Immunopharmacol* 10:485.
  98. Zhu, W., T. Igarashi, Z. T. Qi, C. Newton, R. E. Widen, H. Friedman, and T. W. Klein. 1993. delta-9-Tetrahydrocannabinol (THC) decreases the number of high and intermediate affinity IL-2 receptors of the IL-2 dependent cell line NKB61A2. *Int J Immunopharmacol* 15:401.
  99. Klein, T. W., C. A. Newton, N. Nakachi, and H. Friedman. 2000. Delta 9-tetrahydrocannabinol treatment suppresses immunity and early IFN-gamma, IL-12, and IL-12 receptor beta 2 responses to Legionella pneumophila infection. *J Immunol* 164:6461.
  100. Fischer-Stenger, K., A. W. Updegrove, and G. A. Cabral. 1992. Delta 9-tetrahydrocannabinol decreases cytotoxic T lymphocyte activity to herpes simplex virus type 1-infected cells. *Proc Soc Exp Biol Med* 200:422.
  101. Berdyshev, E. V., E. Boichot, N. Germain, N. Allain, J. P. Anger, and V. Lagente. 1997. Influence of fatty acid ethanolamides and delta9-tetrahydrocannabinol on cytokine and arachidonate release by mononuclear cells. *Eur J Pharmacol* 330:231.
  102. Condie, R., A. Herring, W. S. Koh, M. Lee, and N. E. Kaminski. 1996. Cannabinoid inhibition of adenylate cyclase-mediated signal transduction and interleukin 2 (IL-2) expression in the murine T-cell line, EL4.IL-2. *J Biol Chem* 271:13175.
  103. Jeon, Y. J., K. H. Yang, J. T. Pulaski, and N. E. Kaminski. 1996. Attenuation of inducible nitric oxide synthase gene expression by delta 9-tetrahydrocannabinol is mediated through the inhibition of nuclear factor- kappa B/Rel activation. *Mol Pharmacol* 50:334.
  104. Zheng, Z. M., and S. Specter. 1996. Delta-9-tetrahydrocannabinol: an inhibitor of STAT1 alpha protein tyrosine phosphorylation. *Biochem Pharmacol* 51:967.
  105. Klein, T. W., C. Newton, R. Widen, and H. Friedman. 1993. Delta 9-tetrahydrocannabinol injection induces cytokine-mediated mortality of mice infected with Legionella pneumophila. *J Pharmacol Exp Ther* 267:635.

106. Morahan, P. S., P. C. Klykken, S. H. Smith, L. S. Harris, and A. E. Munson. 1979. Effects of cannabinoids on host resistance to *Listeria monocytogenes* and herpes simplex virus. *Infect Immun* 23:670.
107. Mishkin, E. M., and G. A. Cabral. 1985. delta-9-Tetrahydrocannabinol decreases host resistance to herpes simplex virus type 2 vaginal infection in the B6C3F1 mouse. *J Gen Virol* 66 (Pt 12):2539.
108. Lu, T., C. Newton, I. Perkins, H. Friedman, and T. W. Klein. 2006. Role of cannabinoid receptors in Delta-9-tetrahydrocannabinol suppression of IL-12p40 in mouse bone marrow-derived dendritic cells infected with *Legionella pneumophila*. *Eur J Pharmacol* 532:170.
109. Lu, T., C. Newton, I. Perkins, H. Friedman, and T. W. Klein. 2006. Cannabinoid treatment suppresses the T-helper cell-polarizing function of mouse dendritic cells stimulated with *Legionella pneumophila* infection. *J Pharmacol Exp Ther* 319:269.
110. Plopper, C. G., A. T. Mariassy, and L. O. Lollini. 1983. Structure as revealed by airway dissection. A comparison of mammalian lungs. *Am Rev Respir Dis* 128:S4.
111. Harkema, J. R., and J. A. Hotchkiss. 1992. In vivo effects of endotoxin on intraepithelial mucosubstances in rat pulmonary airways. Quantitative histochemistry. *Am J Pathol* 141:307.
112. Harkema, J. R., C. G. Plopper, D. M. Hyde, J. A. St George, and D. L. Dungworth. 1987. Effects of an ambient level of ozone on primate nasal epithelial mucosubstances. Quantitative histochemistry. *Am J Pathol* 127:90.
113. Buchweitz, J. P., P. W. F. Karmaus, K. J. Williams, J. R. Harkema, and N. E. Kaminski. 2007. Modulation of airway responses to influenza A/PR/8/34 by delta-9-tetrahydrocannabinol in C57BL/6 mice. *Submitted for publication*.
114. Topham, D. J., R. A. Tripp, and P. C. Doherty. 1997. CD8+ T cells clear influenza virus by perforin or Fas-dependent processes. *J Immunol* 159:5197.
115. Buchweitz, J. P., J. R. Harkema, and N. E. Kaminski. 2007. Time-dependent airway epithelial and inflammatory cell responses induced by influenza virus A/PR/8/34 in C57BL/6 mice. *Tox Path*.
116. Azorlosa, J. L., S. J. Heishman, M. L. Stitzer, and J. M. Mahaffey. 1992. Marijuana smoking: effect of varying delta 9-tetrahydrocannabinol content and number of puffs. *J Pharmacol Exp Ther* 261:114.
117. Spackman, E., D. A. Senne, T. J. Myers, L. L. Bulaga, L. P. Garber, M. L. Perdue,

- K. Lohman, L. T. Daum, and D. L. Suarez. 2002. Development of a real-time reverse transcriptase PCR assay for type A influenza virus and the avian H5 and H7 hemagglutinin subtypes. *J Clin Microbiol* 40:3256.
118. Hayden, F. G., R. Fritz, M. C. Lobo, W. Alvord, W. Strober, and S. E. Straus. 1998. Local and systemic cytokine responses during experimental human influenza A virus infection. Relation to symptom formation and host defense. *J Clin Invest* 101:643.
119. Berdyshev, E., E. Boichot, M. Corbel, N. Germain, and V. Lagente. 1998. Effects of cannabinoid receptor ligands on LPS-induced pulmonary inflammation in mice. *Life Sci* 63:PL125.
120. Joseph, J., B. Niggemann, K. S. Zaenker, and F. Entschladen. 2004. Anandamide is an endogenous inhibitor for the migration of tumor cells and T lymphocytes. *Cancer Immunol Immunother* 53:723.
121. Sacerdote, P., C. Martucci, A. Vaccani, F. Bariselli, A. E. Panerai, A. Colombo, D. Parolaro, and P. Massi. 2005. The nonpsychoactive component of marijuana cannabidiol modulates chemotaxis and IL-10 and IL-12 production of murine macrophages both in vivo and in vitro. *J Neuroimmunol* 159:97.
122. Sacerdote, P., P. Massi, A. E. Panerai, and D. Parolaro. 2000. In vivo and in vitro treatment with the synthetic cannabinoid CP55, 940 decreases the in vitro migration of macrophages in the rat: involvement of both CB1 and CB2 receptors. *J Neuroimmunol* 109:155.
123. Stefano, G. B., M. Salzet, C. M. Rialas, D. Mattocks, C. Fimiani, and T. V. Bilfinger. 1998. Macrophage behavior associated with acute and chronic exposure to HIV GP120, morphine and anandamide: endothelial implications. *Int J Cardiol* 64 Suppl 1:S3.
124. Molina-Holgado, F., E. Molina-Holgado, and C. Guaza. 1998. The endogenous cannabinoid anandamide potentiates interleukin-6 production by astrocytes infected with Theiler's murine encephalomyelitis virus by a receptor-mediated pathway. *FEBS Lett* 433:139.
125. Newton, C. A., T. W. Klein, and H. Friedman. 1994. Secondary immunity to *Legionella pneumophila* and Th1 activity are suppressed by delta-9-tetrahydrocannabinol injection. *Infect Immun* 62:4015.
126. Yuan, M., S. M. Kiertscher, Q. Cheng, R. Zoumalan, D. P. Tashkin, and M. D. Roth. 2002. Delta 9-Tetrahydrocannabinol regulates Th1/Th2 cytokine balance in activated human T cells. *J Neuroimmunol* 133:124.
127. Fischer, U., R. U. Janicke, and K. Schulze-Osthoff. 2003. Many cuts to ruin: a

comprehensive update of caspase substrates. *Cell Death Differ* 10:76.

128. Wurzer, W. J., O. Planz, C. Ehrhardt, M. Giner, T. Silberzahn, S. Pleschka, and S. Ludwig. 2003. Caspase 3 activation is essential for efficient influenza virus propagation. *Embo J* 22:2717.
129. Takizawa, T., C. Tatematsu, K. Ohashi, and Y. Nakanishi. 1999. Recruitment of apoptotic cysteine proteases (caspases) in influenza virus-induced cell death. *Microbiol Immunol* 43:245.
130. Krylatov, A. V., L. N. Maslov, O. V. Lasukova, and R. G. Pertwee. 2005. Cannabinoid receptor antagonists SR141716 and SR144528 exhibit properties of partial agonists in experiments on isolated perfused rat heart. *Bull Exp Biol Med* 139:558.
131. Landsman, R. S., T. H. Burkey, P. Consroe, W. R. Roeske, and H. I. Yamamura. 1997. SR141716A is an inverse agonist at the human cannabinoid CB1 receptor. *Eur J Pharmacol* 334:R1.
132. Rhee, M. H., and S. K. Kim. 2002. SR144528 as inverse agonist of CB2 cannabinoid receptor. *J Vet Sci* 3:179.
133. Rockwell, C. E., N. T. Snider, J. T. Thompson, J. P. Vanden Heuvel, and N. E. Kaminski. 2006. Interleukin-2 suppression by 2-arachidonyl glycerol is mediated through peroxisome proliferator-activated receptor gamma independently of cannabinoid receptors 1 and 2. *Mol Pharmacol* 70:101.

## APPENDIX

### 1. Experimental design for examining the magnitude and severity of inflammatory response in mouse left lung lobes.

<i>Concentration of PR8</i>	<i>Number of mice</i>
50 pfu	3
300 pfu	3
500 pfu	3

All animals were intranasally instilled with 50  $\mu$ l of PR8 at concentrations of 50, 300, or 500 pfu. Animals were sacrificed 13 dpi. Lungs were inflation fixed with formalin and microdissected according to the material and methods. Sections of G5 and G11 were stained with H&E for analysis.

### 2. Experimental Design for examining the blood concentrations of $\Delta^9$ -THC and its metabolites 11-hydroxy- $\Delta^9$ -THC and 9-carboxy- $\Delta^9$ -THC.

<i>Dose of THC</i>	<i>Number of mice</i>
0 mg/kg	4
5 mg/kg	4
75 mg/kg	4

All animals were orally gavaged with either corn oil or  $\Delta^9$ -THC for 5 consecutive days. On the fifth day, 4 h after the last dose of  $\Delta^9$ -THC, the animals were anesthetized with 4% isoflurane and blood was removed from the animals by cardiac puncture. Dr. Jim Klaunig's laboratory at IUPUI analyzed the blood samples for  $\Delta^9$ -THC and its metabolites.

**3. Experimental Design for examining the time-dependent changes in pulmonary responses to PR8.**

<i>Intranasal Treatment</i>	<i>Sacrificed (dpi)</i>	<i>Number of mice</i>
Saline	3	6
Influenza	3	6
Saline	7	6
Influenza	7	6
Saline	10	6
Influenza	10	6
Saline	15	6
Influenza	15	6
Saline	21	6
Influenza	21	6

All animals were intranasally instilled with 50  $\mu$ l of saline or PR8 at a concentration of 50 pfu. Animals were sacrificed at 3, 7, 10, 15, and 21 dpi. Lungs were lavaged with 2 ml of sterile saline and then inflation fixed with formalin and microdissected according to the material and methods. Sections of G5 and G11 were stained with H&E, AB/PAS, and PCNA for analysis. Lavage was quantified for total and differential cell counts, protein, elastase, and cytokines by cytometric bead array.

**4. Experimental design for examining the concentration-dependent effects of  $\Delta^9$ -THC on pulmonary responses to PR8 (3 studies).**

<i>Oral Treatment</i>	<i>Intranasal Treatment</i>	<i>Sacrificed (dpi)</i>	<i>Number of mice</i>
Corn oil	Saline	7	5
Corn oil	Influenza	7	5
THC 75 mg/kg	Saline	7	5
THC 25 mg/kg	Influenza	7	5
THC 50 mg/kg	Influenza	7	5
THC 75 mg/kg	Influenza	7	5
Corn oil	Saline	10	5
Corn oil	Influenza	10	5
THC 75 mg/kg	Saline	10	5
THC 25 mg/kg	Influenza	10	5
THC 50 mg/kg	Influenza	10	5
THC 75 mg/kg	Influenza	10	5

Three separate experiments with this design were conducted. All animals were orally gavaged with corn oil or  $\Delta^9$ -THC (25, 50, or 75 mg/kg) and intranasally instilled with 50  $\mu$ l of saline or PR8 at a concentration of 50 pfu on the third day of gavage 4h prior to gavage. Animals were sacrificed at 7 and 10 dpi. In one experiment, lungs were lavaged with 2 ml of sterile saline. Lavage was quantified for total and differential cell counts, protein, elastase, and cytokines by cytometric bead array. In the second experiment, the lungs were inflation fixed with formalin and microdissected according to the material and methods. Sections of R1-4, G5 and G11 were stained with H&E, AB/H for analysis. In the third experiment, the entire lung was immersed in TRI reagent and total RNA was isolated for H1, MUC5AC, and CAS-3 analysis.

**5. Experimental design for examining the role of cannabinoid receptors in mediating the effects of  $\Delta^9$ -THC on immune cells and mediators following PR8 challenge (1<sup>st</sup> study).**

<i>Oral Treatment</i>	<i>Intranasal Treatment</i>	<i>C57Bl/6 genotype</i>	<i>Sacrificed (dpi)</i>	<i>Number of mice</i>
Corn oil	Saline	wild-type	7	8
Corn oil	Influenza	wild-type	7	8
THC 75 mg/kg	Saline	wild-type	7	8
THC 75 mg/kg	Influenza	wild-type	7	8
Corn oil	Saline	CB1(-)/CB2(-)	7	8
Corn oil	Influenza	CB1(-)/CB2(-)	7	8
THC 75 mg/kg	Saline	CB1(-)/CB2(-)	7	8
THC 75 mg/kg	Influenza	CB1(-)/CB2(-)	7	8

**Experimental design for examining the role of cannabinoid receptors in mediating the effects of  $\Delta^9$ -THC on immune cells and mediators following PR8 challenge (2<sup>nd</sup> study).**

<i>Oral Treatment</i>	<i>Intranasal Treatment</i>	<i>C57Bl/6 genotype</i>	<i>Sacrificed (dpi)</i>	<i>Number of mice</i>
Corn oil	Saline	wild-type	7	5
Corn oil	Influenza	wild-type	7	10
THC 75 mg/kg	Saline	wild-type	7	5
THC 75 mg/kg	Influenza	wild-type	7	10
Corn oil	Saline	CB1(-)/CB2(-)	7	5
Corn oil	Influenza	CB1(-)/CB2(-)	7	10
THC 75 mg/kg	Saline	CB1(-)/CB2(-)	7	5
THC 75 mg/kg	Influenza	CB1(-)/CB2(-)	7	14

Using the first experimental design, all animals were orally gavaged with corn oil or  $\Delta^9$ -THC (75 mg/kg) and intranasally instilled with 50  $\mu$ l of saline or PR8 at a concentration of 50 pfu on the third day of gavage 4h prior to gavage. Animals were sacrificed at 7 dpi. In the first experiment, right lung lobes were tied off and immersed in TRI reagent for the isolation of total RNA and the measurement of H1 mRNA. The left lung lobe was

lavaged with 1 ml of sterile saline and then inflation fixed with formalin and microdissected according to the material and methods. Lavage was quantified for total and differential cell counts, protein, elastase, and cytokines by cytometric bead array. The left lung lobe was sectioned at G5 and G11 and stained with H&E, AB/PAS for analysis. Using the second experimental design, the entire lung was immersed in TRI reagent and total RNA was isolated for H1 analysis.

MICHIGAN STATE UNIVERSITY LIBRARIES



3 1293 02956 1903